ΕΘΝΙΚΟ ΜΕΤΣΟΒΙΟ ΠΟΛΥΤΕΧΝΕΙΟ
ΣΧΟΛΗ ΕΦΑΡΜΟΣΜΕΝΩΝ
ΜΑΘΗΜΑΤΙΚΩΝ &
ΦΥΣΙΚΩΝ ΕΠΙΣΤΗΜΩΝ
ΣΧΟΛΗ ΜΗΧΑΝΟΛΟΓΩΝ
ΜΗΧΑΝΙΚΩΝ

ΕΘΝΙΚΟ ΚΕΝΤΡΟ ΕΡΕΥΝΑΣ
ΦΥΣΙΚΩΝ ΕΠΙΣΤΗΜΩΝ
¨ΔΗΜΟΚΡΙΤΟΣ¨
ΙΝΣΤΙΤΟΥΤΟ
ΝΑΝΟΕΠΙΣΤΗΜΗΣ &
ΝΑΝΟΤΕΧΝΟΛΟΓΙΑΣ
ΙΝΣΤΙΤΟΥΤΟ ΠΥΡΗΝΙΚΗΣ &
ΣΩΜΑΤΙΔΙΑΚΗΣ ΦΥΣΙΚΗΣ

Διατμηματικό Πρόγραμμα Μεταπτυχιακών Σπουδών
Φυσική και Τεχνολογικές Εφαρμογές

Τομέας Φυσικής
Εργαστήριο Πειραματικής Φυσικής Υψηλών Ενεργειών
& Συναφούς Οργανολογίας-Τεχνολογίας

Ανάπτυξη συστημάτων αυτομάτου ελέγχου για το New Small Wheel Upgrade του πειράματος ATLAS στο CERN

Μεταπτυχιακή Εργασία
του
Πολυνείκη Τζανή

Επιβλέπων:
Αλεξόπουλος Θεόδωρος
Καθηγητής Ε.Μ.Π.

Αθήνα, Απρίλιος 2020

ΕΘΝΙΚΟ ΜΕΤΣΟΒΙΟ ΠΟΛΥΤΕΧΝΕΙΟΛ
ΣΧΟΛΗ ΕΦΑΡΜΟΣΜΕΝΩΝ ΜΑΘΗΜΑΤΙΚΩΝ ΚΑΙ ΦΥΣΙΚΩΝ ΕΠΙΣΤΗΜΩΝ
ΤΟΜΕΑΣ ΦΥΣΙΚΗΣ
Εργαστήριο Πειραματικής Φυσικής Υψηλών Ενεργειών
& Συναφούς Οργανολογίας-Τεχνολογίας

Ανάπτυξη συστημάτων αυτομάτου ελέγχου για το New Small Wheel Upgrade του πειράματος ATLAS στο CERN

Μεταπτυχιακή εργασία

του

Πολυνείκη Τζανή

Επιβλέπων: Θεόδωρος Αλεξόπουλος
Καθηγητής Ε.Μ.Π.

Εξεταστική Επιτροπή:

....	....	....
Θ. Αλεξόπουλος	Ε. Γαζής	Σ. Μαλτέζος
Καθηγητής Ε.Μ.Π.	Καθηγητής Ε.Μ.Π.	Καθηγητής Ε.Μ.Π.

Αθήνα, 13 Απριλίου 2020

Περίληψη

Αυτή η μεταπτυχιακή εργασία αναφέρεται κυρίως στο σχεδιασμό και την ανάπτυξη συστημάτων ελέγχου που χρησιμοποιούνται για το New Small Wheel Upgrade που θα πραγματοποιηθεί το 2020 στο πείραμα ATLAS του Large Hadron Collider (LHC) στον Ευρωπαϊκό Οργανισμό Πυρηνικών Ερευνών, γνωστό όπως το CERN. Ως εκ τούτου, η εργασία αυτή στοχεύει στο σχεδιασμό και την εφαρμογή συστημάτων ελέγχου για την (α) High Voltage Validation, β) Gas Leak Validation των ανιχνευτών Micromegas, (γ) Integration του Micromegas Sector και (δ) Electronics Monitoring και των δύο ανιχνευτών Micromegas και sTGC πριν από την εγκατάσταση στο New Small Wheel. Οι διάφοροι σταθμοί ελέγχου αναπτύσσονται μέσω της εφαρμογής WinCC Open Architecture, η οποία είναι ένα σύστημα εποπτείας ελέγχου και απόκτησης δεδομένων (SCADA) και ένα σύστημα διεπαφής ανθρώπου-μηχανής (HMI) από τη Siemens. Βασική πρόκληση αυτής της εργασίας ήταν η ανάπτυξη συστημάτων συλλογής, ελέγχου και παρακολούθησης δεδομένων για διάφορα υλικά, το σύστημα τροφοδοσίας CAEN για εφαρμογές χαμηλής/υψηλής τάσης, ηλεκτρονικές πλακέτες/chips, μικροεπεξεργαστή Arduino και μικρο-υπολογιστή Raspberry-Pi, αισθητήρες πολλαπλών χρήσεων. Αυτές οι εφαρμογές μπορεί να έχουν διάφορες λειτουργίες και μπορούν να χρησιμοποιηθούν σε οποιοδήποτε πλαίσιο, όπως στην πειραματική φυσική υψηλής ενέργειας ή στη βιομηχανία υψηλής τεχνολογίας λόγω της επεκτασιμότητάς τους και της ευελιξίας τους, η οποία είναι η τέλεια επιλογή για τη δημιουργία λύσεων, συμπεριλαμβανομένων των κεντρικών σταθμών ελέγχου και γεωγραφικά ευρέως κατανεμημένων συστημάτων.

Ευχαριστίες

Στα πλαίσια της εργασίας αυτής θα ήθελα να ευχαριστήσω τον κύριο Θεόδωρο Αλεξόπουλο ή αλλιώς ¨Αρχηγό¨ για την ανάθεση αυτής της διπλωματικής και την ευκαιρία να εργαστώ σε ένα τόσο ενδιαφέρον θέμα. Επιπλέον, θα ήθελα να τον ευχαριστήσω για την εμπιστοσύνη και την καθοδήγηση του, την υπομονή στα ερωτήματα μου καθώς και το πάθος του για την φυσική και τα ηλεκτρονικά που με ενέπνευσε ώστε να ασχοληθώ με την πειραματική φυσική υψηλών ενεργειών. Επιπρόσθετα, θα ήθελα να ευχαριστήσω τον κύριο Σταύρο Μαλτέζο για την καθοδήγηση, βοήθεια και τις γνώσεις του που μου πρόσφερε πάνω στην φυσική και τους νόμους των αερίων για τον σχεδιασμό του συστήματος διαρροής αερίου μέσα από συζητήσεις και πολλές ώρες στο εργαστήριο. Επίσης, θα ήθελα να ευχαριστήσω των κύριο Γαζή, όπου μαζί με τον κ. Αλεξόπουλο και κ. Μαλτέζο μου έδωσαν την δυνατότητα να γίνω μέλος της αξιοθαύμαστης ομάδας όπου αναδεικνύει το ΕΜΠ και την ΣΕΜΦΕ στο CERN.Επιπλέον, θα ήθελα να ευχαριστήσω τον κύριο Βενέτη Πολυχρονάκο και τον Γιώργο Ιακωβίδη από το Brookhaven National Laboratory για την δυνατότητα που μου έδωσαν να βρίσκομαι στο CERN και να υλοποιήσω την μεταπτυχιακή μου εργασία καθώς και για την πολύτιμη βοήθεια τους και συμβουλές τους για την υλοποίηση της. Δεν παραβλέπω να ευχαριστήσω και τα υπόλοιπα μέλη της ομάδας Πάρη, Χρήστο Π., Στάθη, Αιμίλιο, Χρήστο Β., Πάνο, Γιώργο, Κώστα, Σταμάτη, Χαρά, Μάριο, Μαρία, Γιάννη, Αντρέα, Ίκαρο και άλλους πολλούς που μπορεί να ξεχνάω. Επιπλέον, θα ήθελα να ευχαριστώ την Έφη που μου στάθηκε, μου έδωσε πολλές ωραίες ιδέες και όρεξη και με παρότρυνε να συνεχίσω να γράφω αυτή την διπλωματική εργασία που δίχως την αγάπη της και στήριξη της θα έπαιρνε και άλλο χρόνο να την ολοκληρώσω. Επιπρόσθετα, θα ήθελα να ευχαριστήσω τους φίλους μου για την εμπιστοσύνη και την στήριξη τους καθ όλη την διάρκεια της μεταπτυχιακής εργασίας. Και εννοείται πάνω από όλα θα ήθελα να ευχαριστήσω τους γονείς μου Ιωάννη και Αλκμήνη και την αδερφή μου Ασπασία που δίχως την στήριξη και αγάπη τους δεν θα είχα φτάσει σε αυτό το σημείο.

Τέλος, θα ήθελα να σημειωθεί αυτή η μεταπτυχιακή εργασία πήρε πολλούς μήνες να γραφτεί, μέρος της γράφτηκε σε διαφορετικές χώρες του κόσμου όπως Γαλλία, Ελβετία, Μεξικό, Ρωσία, Ελλάδα, Κούβα, Ιταλία κλπ και τελικά πήρε την τελική της μορφή κατά την διάρκεια του εγκλεισμού λόγω της καραντίνας ελέω COVID19.

National Technical University of Athens
School of Applied Mathematical &
Physical Sciences
School of Mechanical Engineering

National Centre of Research
"Demokritos"
Institute of Nanoscience and
Nanotechnology
Institute of Nuclear and
Particle Physics

Postgraduate Program
Physics and Technological Applications

Department of Physics
Laboratory of Experimental High Energy Physics
& Related Technology-Instrumentation

Development of detector control systems for the New Small Wheel Upgrade of ATLAS experiment at CERN

Master Thesis
of
Polyneikis Tzanis

Advisor:
Theodoros Alexopoulos
Professor, N.T.U.A

Athens
13 April 2020

National Technical University of Athens
School of Applied Mathematical and Physical Sciences
Department of Physics
Laboratory of Experimental High Energy Physics
& Related Technology-Instrumentation

Development of detector control systems for the New Small Wheel Upgrade of ATLAS experiment at CERN

Master Thesis

of

Polyneikis Tzanis

Advisor: Theodoros Alexopoulos
Professor, N.T.U.A

Exam committee.

....	....	....
T. Alexopoulos	E. Gazis	S. Maltezos
Professor, N.T.U.A	Professor, N.T.U.A	Professor, N.T.U.A

Athens, 13 April 2020

....
Polyneikis Tzanis
Applied Physicist N.T.U.A.

Abstract

This master thesis mainly refers to the design and development of control systems that are being used for the New Small Wheel Upgrade which will take place in 2020 in the ATLAS experiment of the Large Hadron Collider (LHC) at the European Organization for Nuclear Research, known as CERN. Therefore, this thesis aims to the design and the implementation of slow control systems for the (a) High Voltage validation; (b) Gas Leak validation of the Micromegas detectors; (c) the integration of the Micromegas Sector and (d) the Electronics Monitoring of both Micromegas and sTGC detectors prior to the installation in the New Small Wheel. The various control stations are developed via the WinCC Open Architecture application, which is a supervisory control and data acquisition (SCADA) and human-machine interface (HMI) system from Siemens. Main challenge of this thesis was the development of data acquisition, control and monitoring systems for several hardware, CAEN power system for low/high voltage applications, electronics boards/chips, Arduino micro-controller and Raspberry-Pi single-board computer, and for multipurpose sensors. These implementations may have various functionalities and can be used in any context, such as in experimental high energy physics or the high tech industry due to their scalability and flexibility which is the perfect choice to create solutions, including centralized control stations and geographically widely distributed systems.

Acknowledgments

Contents

Chapter 1

The Large Hadron Collider and the ATLAS Experiment

This chapter is an introduction to the Large Hadron Collider (LHC) with emphasis on the ATLAS experiment conducted at the European Center for Nuclear Research (CERN). In the coming years the LHC will be upgraded to greater luminosity, as a result the ATLAS muon spectrometer needs to be remodeled so that it can handle the high particle rate. The Micromegas detector was selected for the upgrade of the New Small Wheel, which is the essential motivation for this theses.

1.1 The Large Hadron Collider

The Large Hadron Collider (LHC) [1], the largest and most powerful accelerator in the world, started operating in September 2008 and remains the latest addition to the CERN accelerator complex. This experimental device, located hundreds of meters below the Earth and the Swiss-French border, is a two-pack superconducting accelerator and collider where ultraviolet proton beams accelerate close to the speed of light until they eventually collide with each other. An image of the LHC superconducting magnets is shown in Fig. 1.1 In addition, the LHC is installed in the 26.7 km perimeter tunnel where it was built between 1984 and 1989 for the needs of the CERN LEP [2] accelerator where it stopped operating in 2000. The purpose of the LHC is to reveal physics beyond the Standard with center of mass energies for proton-proton collisions above 14 TeV.
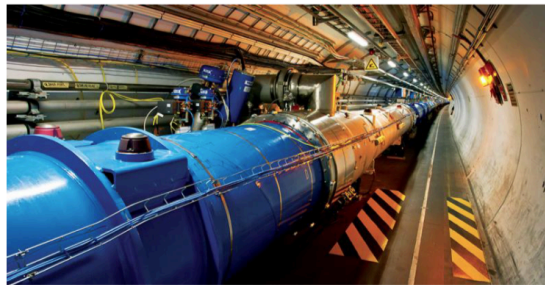
Figure 1.1: The LHC superconducting magnets in the 27 km LEP tunnel at CERN.

1.2 Accelerator Complex and Experiments

Before the particles reach the ring of the LHC, they undergo a process through a set of accelerators. These are a series of machines that accelerate the particles to increasingly higher energies. Each machine enhances the energy of the particle packs before they are injected into the next series machine. Initially, a simple hydrogen bottle feeds the source chamber of a linear accelerator with hydrogen atoms, by applying an electric field the hydrogen cores strip their electrons and the protons move on to the next step of their acceleration path. The beam is then injected into the Proton Synchrotron Booster (PSB), where the proton energy is increased to 1.4 GeV, before they go through the Proton Synchrotron (PS) reaching the energy of 25GeV. The last step before the LHC is the Super Proton Synchrotron (SPS), where the protons reach the energy of 450 GeV and the LHC then accelerates the particles at the design energy of 7 TeV. Finally,

the injector and pre-accelerators feed the 27 km ring with particle clusters that collide into 4 experimental input regions corresponding to the underground experiments (ATLAS [3], CMS [4], ALICE [5], LHCb [6]). The accelerators of this chain were originally designed for use in the LEP machine. They were later upgraded to meet the very stringent LHC requirements that require high intensity proton beams with small transverse and well defined longitudinal emissions. The task of upgrading the injectors included increasing the power of Linac 2, new RF systems in PS Booster and PS, increasing PS Booster energy from 1 GeV to 1.4 GeV with two phases of PS filling and installation of profile meters high resolution beam. A graphical representation of the full accelerator-injector assembly is shown in Fig. 1.2.
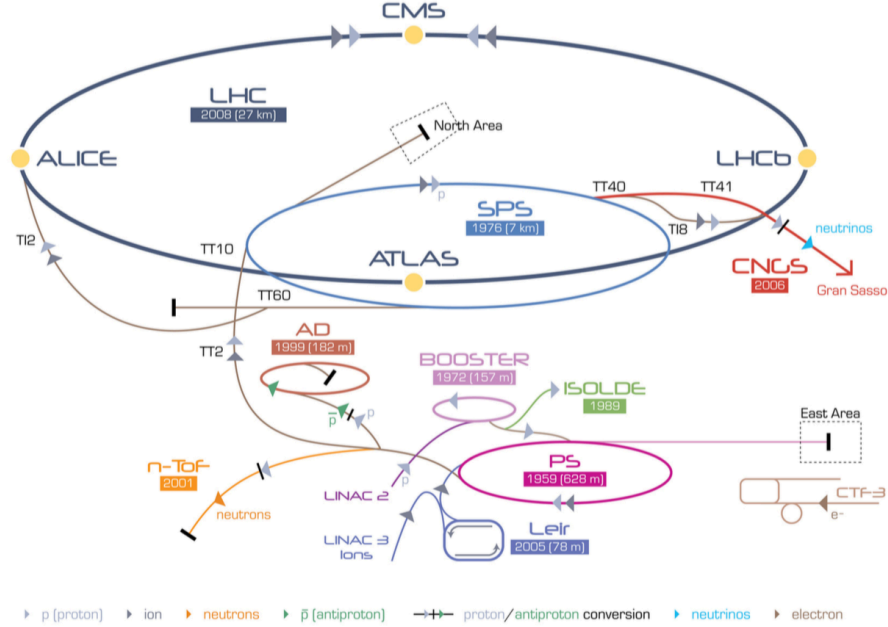

Figure 1.2: Schematic representation of its accelerators-injectors LHC. Above is the injector and pre-accelerators that supply the 27 km ring with particle beams. The beams collide into 4 experimental input regions corresponding to the underground experiments (ATLAS, CMS, ALICE, LHCb).

The LHC during Run-1 worked mainly with proton packets divided every 25 $mathrmns$, with this gap equal to $\sim$ 1404 packets per batch . The instantaneous LHC luminosity for pp conflicts $\mathcal{L}$, is proportional to the ratio R of the pp processes and equals $\mathcal{L} = R/\sigma$, where σ is the active cross section of the process pp. The absolute brightness depends on the beam parameters and can be written in the form of Eq. 1.1 [7], where f_r is the rotation frequency of LHC, n_b packets colliding at the point of interaction, n_1 and n_2 are the particle numbers in 2 colliding packets and Σ_x and Σ_y the horizontal and vertical profiles of the bond profiles, respectively.

$$\mathcal{L} = \frac{n_b \, f_r \, n_1 \, n_2}{2 \, \pi \, \Sigma_x \, \Sigma_y} \tag{1.1}$$

The brightness of the LHC does not remain constant during a natural course but deteriorates due to the depletion of circular beams and emissions. The main cause of the deterioration of brightness during LHC operation is the loss of the beam from collisions. Other contributions to beam losses stem from Touchek scattering and particle losses due to slow particle emission.

The LHC consists of 4 main experiments. Specifically, the ATLAS and CMS general luminosity experiments are designed to detect luminosity in the order of $\mathcal{L} = 10^{34} \, \mathrm{cm}^{-2}\mathrm{s}^{-1}$. It also consists of two low-brightness experiments, LHCb for B-physics designed for luminance of $\mathcal{L} = 10^{32} \, \mathrm{cm}^{-2}\mathrm{s}^{-1}$ and TOTEM cite totem, for detecting protons derived from elastic scattering at low angles in brightness of $\mathcal{L} = 2 \times 10^{29} \, \mathrm{cm}^{-2}\mathrm{s}^{-1}$. Unlike p-p beams, LHC also works with Pb-Pb and p-Pb beams. Finally, the ALICE experiment studies ion beams in the luminosity of $\mathcal{L} = 10^{27} \, \mathrm{cm}^{-2}\mathrm{s}^{-1}$.

1.3 LHC Performance

The year 2012 marked the end of a successful first run of LHC (Run-1) with $\sqrt{s} = 7 \, \mathrm{TeV}$ conflict actions in 2010 and 2012 as well and increase to $\sqrt{s} = 8 \, \mathrm{TeV}$ in 2012. The discovery of the Higgs particle was announced by the experiments ATLAS and CMS in the summer of 2012 , where search was one of the primary goals for the first run of LHC. Subsequently LHC was shut down for upgrades

in 2013 and 2014 and conflicts pp returned in 2015 to greater conflict energy $\sqrt{s} = 13\,\text{TeV}$. An overview of the beam parameters, the brightness in the 4 years of operation of LHC is illustrated in Fig. 1.3.

Beam Parameters	Design	2010	2011	2012	2015
Centre-of-mass energy, $\sqrt{s}$ [TeV]	14	7	7	8	13
Peak luminosity, L [10^{33} cm^{-2}s^{-1}]	10	0.21	3.65	7.73	5.02
Integrated luminosity, delivered, $\mathcal{L}$ [fb^{-1}/y]	80-120	0.048	5.46	22.8	4.2
Integrated luminosity, recorded, $\mathcal{L}$ [fb^{-1}/y]	–	0.045	5.08	21.3	3.9
Maximum number of colliding bunches	2880	348	1331[1]	1380	2232
Maximum number of protons per bunch [10^{11}]	1.15	1.2	1.4	1.6	1.2
Minimum bunch spacing [ns]	25	150	50	50	25
Average pile-up $\langle \mu \rangle$	19.02	< 3	9.1	20.7	13.7

Figure 1.3: Projected beam and brightness values as well as actual values during the 4 years of operation of the LHC.

1.4 ATLAS Experiment

The ATLAS [3] detector, is a general-purpose detector designed to meet the needs of many LHC experiments, such as Higgs particle searching, ultrasymmetry study, answering dark matter questions, and any extraneous matter. dimensional. Its overall shape is cylindrical, with a length of 45 $mathrmm$, diameter 25 m and weighs 7000 tons, in addition it is approximately symmetrical in length with respect to the IP interaction point and is up to today the largest volume detector ever built. A graphical representation of the ATLAS experiment is shown in Fig. 1.4. It is divided into the barrel region, where the modules are cylindrical layers and two endcaps regions, where the probes form discs to increase the probe coverage. The different parts of the detector are visible in the same shape with the design of the detector mainly due to the need to meet the general requirements for the LHC detectors.
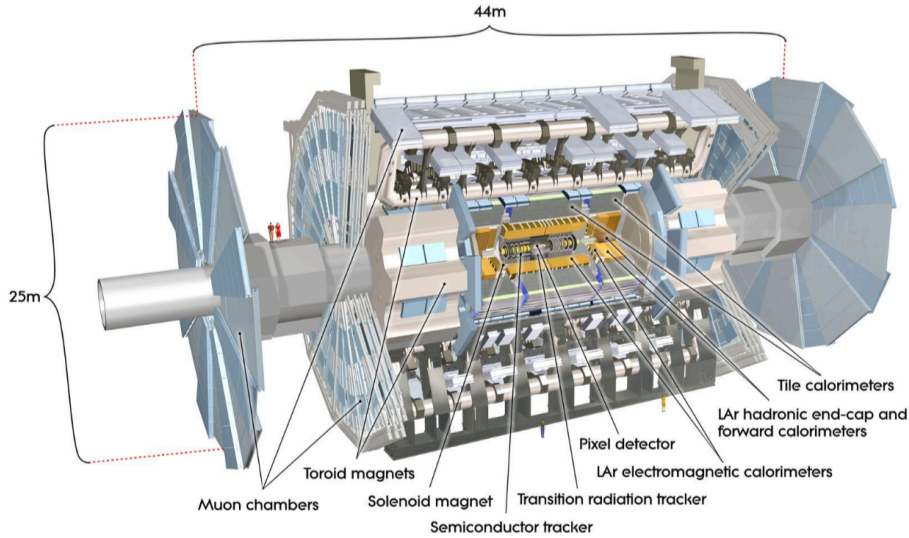

Figure 1.4: Graphical representation of the ATLAS experiment. The different parts of the experiment are marked on the figure.

The bunches of particles pass through the probe's cylindrical axis of symmetry and collide in the center producing new particles. The different ATLAS subsystems, layered, record the trajectory, momentum, and energy of the particles produced. A powerful magnet bends the orbits of the charged particles allowing them to measure their momentum, while the data is collected by the detector's electronic systems.

In order to clarify the details of the following ATLAS detection systems, it is good at this point to define the concept of pseudorapidity (η). If the angle with respect to the beam axis equals θ, then the pseudorapidity η [8] is defined as:

$$\eta = -ln\left[\tan\left(\frac{\theta}{2}\right)\right] \tag{1.2}$$

A particle with a high value of η is likely to escape the detector, since it will move almost synchronously with the beam of $90^0 - 45^0$. As a result, the end-caps of the detector correspond to large values of η, while the barrel cylinder housing at lower values of η.

The main ATLAS subsystems are:

- Magnet System

- Inner Detector

- Calorimeters

- Muon Spectometer

- Trigger and Data Acquisition System (TDAQ)

1.4.1   Magnet System

The ATLAS detector comprises 3 types of superconducting magnet systems to provide the force required to bend the charged particle orbits and then to measure their momentum around the point of interaction (IP):

- The Central Solenoid [9] responsible for the magnetic field in the internal detector.

- The air-core Barrel Torroid [10].

- The 2 air-cored End-Cap Toroids [11], which provide the necessary toroidal field for the muon spectrometer

The overall dimensions of the magnetic system are determined by the structure of Barrel Torroid where it extends to 26 m length and outer diameter of 20 m. The ATLAS superconducting magnetic system is cooled with liquid helium at 4.8 K, in energy terms the toroidal magnets are electrically connected in series and operate at a current of 20 kA while the central solenoid operates at a lower rated operation of 7.6 kA. Photos of the 3 different parts of the magnetic system of the experiment ATLAS are shown below in Fig. 1.5.
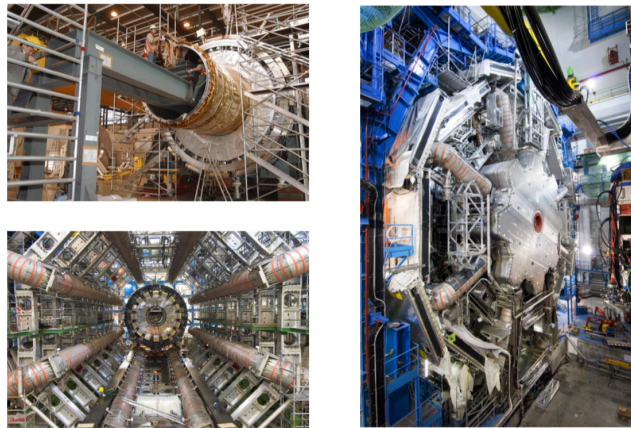

Figure 1.5: Photos of the 3 different parts of the experimental magnetic system ATLAS. In the top left image, the cylindrical tubular magnet is inserted into the liquid argon caliper on the surface. In the figure below, 8 barrel coils inside ATLAS and to the right one of the 2 end-cap toroidal magnets in their final position surrounded by barrel toroid coils.

The central superconducting solenoid is aligned with the beam axis and is designed to provide magnetic pitch at 2 T along the beam to measure the momentum in Inner Detector, minimizing it its emitted thickness in front of the electromagnetic calorimeter located at barrel. The inner and outer diameters are 2.46 m and 2.56 m, respectively, and their length is 5.8 m. It is mounted on a cryostat that shares it with the calorimeter to minimize hardware usage and operates at 4.8 K.

The toroidal magnet system provides a magnetic field for measuring momentum in the muon spectrometer and has an average intensity value of about 0.5 T. The magnetic field, which is toroidal and perpendicular to that of the solenoid, is created by eight superconducting coils in the barrel, and by 2 rotors with 8 coils each in endcaps.

The magnitude of the magnetic field varies according to pseudorapidity for the region of barrel with a maximum value of 3.9 T, while for endcaps the maximum value touches 4.1 T. A schematic representation of the magnetic system of ATLAS comprising the 3 parts mentioned above is shown in Fig. 1.6.
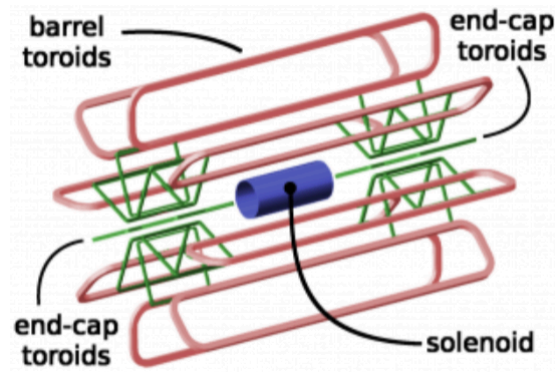
Figure 1.6: Schematic representation of the magnetic system of ATLAS. The central solenoid is installed within the liquid slow calorimeter (blue), surrounded by barrel (red) and end-cap toroid coils (green).

1.4.2 Inner Detector

The internal trajectory detector of ATLAS (ID) [12] [13], totaling $6.2\,\mathrm{m}$, covers the pseudorapidity range of $|\eta| \leq 2.5$ and analyzes the orbits of the particles that have escaped from the interaction point (IP). It is located inside a cylinder of length $7\,\mathrm{m}$ and radius $1.15\,\mathrm{m}$ and consists of three sub-detectors. Inside it we find the Pixel Detector, then the SemiConductor Tracker and finally the Transition Radiation Tracker. The inner track detector combines the high-resolution detectors inside it with the detectors in its outer radius. All are included in the central solenoid, which provides a magnetic field of $2\,\mathrm{T}$. Higher resolution is achieved around the peak region (vertex region) using semiconductor pixel detectors (Silicon Pixel Detectors). Typically, for each route, the semiconductor pixel detector contributes to 3 while the silicon microfluidic detector contributes to 4 track points. On the outside of the inner detector is the Transition Radiation Tracker which provides information at 36 points per orbit and helps identify the experiment's electrons by detecting the photon transition radiation using its drift tubes. The schematic representation of the ATLAS internal trajectory detector is shown in Fig. 1.7.
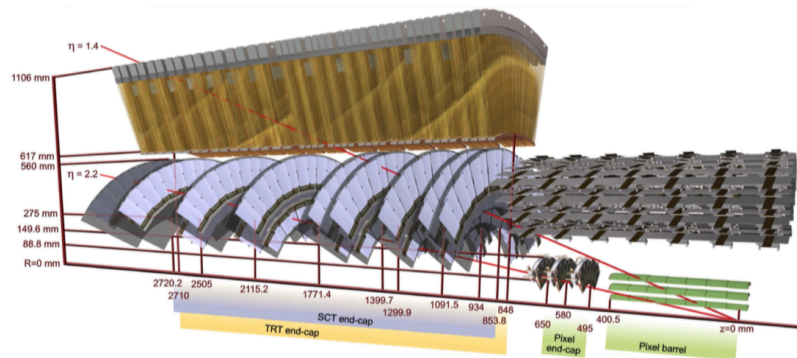

Figure 1.7: Schematic representation of the different subsystems of the ATLAS internal trajectory detector. Inside is Pixel Detector, then SemiConductor Tracker and finally Transition Radiation Tracker.

The relative accuracy of the measurement is well combined so that no measurement overrides the momentum sharpness. In the barrel area the Pixel Detector and SemiConductor Tracker are mounted in concentric cylinders around the beam axis, while the end-caps of the probe are mounted in trays perpendicular to the axis of the beam. The sensors are mounted in a very strong magnetic field, created by a cylindrical superconducting coil, which curves the particle orbits. By measuring the parameters of the orbit, we can find the momentum, direction, load sign and the point of origin of the particle.

1.4.3 Calorimeters

Around the inner track detector are the [14] calorimeters, devices designed to fully absorb the energy of some type of particle crashing on them. Usually, calorimeters are either adrenal, that is, they detect mesons or baryons, or electromagnetic, that is, they detect electrons, positrons and photons. The calorimeters of the experiment ATLAS are responsible for accurately measuring the energy and

position direction of electrons and photons or jets, also evaluating the lack of momentum p_T each event. In addition, they are able to identify particles and contribute to the reconstruction of the muon track. Due to the high energy center of mass provided by LHC, the calorimeters used in the experiments should be able to meet demanding performance requirements over an unprecedented energy range extending from a few GeV up to the scale. of TeV.

A graphical representation of ATLAS calorimeters is shown in Fig. 1.8, where the various parts of the calorimeter are visible. The electromagnetic calorimeter (EM) covers the pseudorapidity region $|\eta| < 3.2$. It is a liquid argon detector (LAr) [15] with electrodes Kapton in accordion shape and lead absorption plates over its full coverage, divided into barrel and end-caps. LAr is complemented by an adrenal calorimeter designed with the tile scintigraphy technique (Tile) [16], which covers the pseudorapidity region $|\eta| < 1.7$ and the region even closer to the beam end-cap $3.1 < |\eta| < 4.9$ completing the experiment calibrator system ATLAS.

The level of the electromagnetic calorimeter, which is located closest to the beam conductor, is capable of providing very accurate measurements of the position of the incoming particles and the deposited energy, based on their electromagnetic interaction with the material. The energy absorption materials of the electromagnetic calorimeter in the area of barrel are lead and stainless steel with liquid argon as a sampling material. The adrenal calorie absorbs energy from the particles through strong interaction (mainly hadrons) and passes through the electromagnetic calorimeter and is less accurate both in their energy size and in their detection. The energy-absorbing material is steel, with spark-plated tiles accepting energy deposition. Many of the calorimeter features are chosen because of their high cost because the machine is quite large and consists of huge amounts of building material.
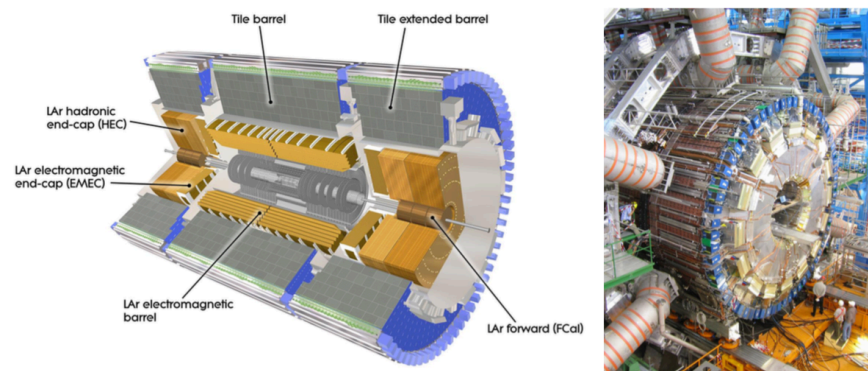

Figure 1.8: Left: Schematic representation of the cross section of ATLAS calorimeters. LAr and Tile are illustrated along with their segmentation in barre and end-cap calorimeters. Right: Photograph of the barrel calorimeter mounted on the detector ATLAS. The rotating coils of the end-cap surrounding the calorimeter layout are also visible.

1.4.4 Muon Spectometer

The role of the muon spectrometer (MS) [17] is to identify, measure and trigger muons. It encompasses monomer spectrometer systems and systems, incorporating state-of-the-art technologies for triggering and reconstruction of muon tracks (tracking) . Fig. 1.9 shows the layout of the ATLAS muon detection system.
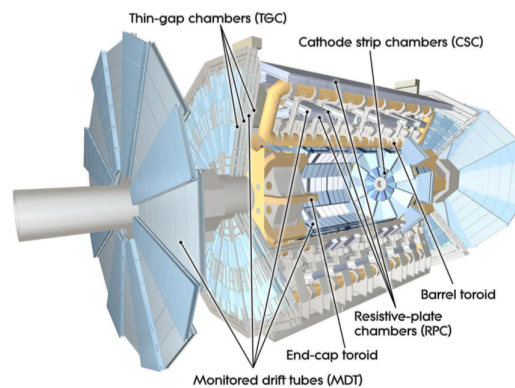

Figure 1.9: Schematic representation of the ATLAS muon spectrometer. The various technologies of the probe's masonry chambers are visible.

The muon spectrometer of ATLAS consists of two sub-detectors [17] for precision measurements:

- Monitored Drift Tubes (MDT)
- Cathode Strip Chambers (CSC)

And two triggering technologies:

- Resistive Plate Chambers (RPC)
- Thin Gap Chambers (TGC)

The following table Fig. 1.10 depicts the region of pseudorapidity $|\eta|$ and analyzes each subsystem of the muon spectrometer:

System	Function	$|\eta|$ coverage	Resolution (mm)
MDT	tracking	< 2.7	$z = 0.035$
CSC	tracking	$2.0 - 2.7$	$r = 0.04$, $\phi = 5$
RPC	trigger	< 1.05	$z = 10$, $\phi = 10$
TGC	trigger	$1.05 - 2.4$	$r = 2 - 6$, $\phi = 3 - 7$

Figure 1.10: Area of e pseudorapidity $|\eta|$ and analysis of each subsystem of the muon spectrometer.

Monitored Drift Tubes (MDT)

Sliding chambers (drift chambers) are a gas-filled enclosure containing electrons that bind electrons from the gas ionisations of the mixture gas Ar-CO$_2$ $(93 - 7\%)$ containing and carrying the electrical signal. They can accurately calculate the bending of particle orbits at the $r - z$ plane of the toroidal magnet and provide measurements of the momentum of the particles at the momentum of the particles. In the experiment ATLAS MDT covers the whole region the high pseudorapity of $|\eta| < 2.7$. The basic structure of a MDT is illustrated in Fig. 1.11 (left). It consists of two multi-level sliding chambers separated by a support frame. Each multi-layer comprises three levels of tubes with the exception of the internal structures of the muon spectrometer (small beam) where a floating tube frame is used in each multi-layer to improve pattern recognition in areas with a high background. A photo of MDT is shown in Fig. 1.11 (right) during the manufacturing process and their inspection process. The spatial resolution of a MDT tube after the calibration process and the correction for the electric field of the magnetic field can be as high as $80\,\mu$m. By combining ionization electron measurements in each slide tube in each tube, a 6-point segment can be reconstructed by improving the spatial resolution to $40\,\mu$m.

Cross plate
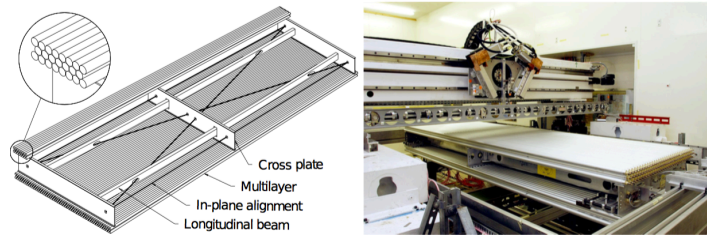Multilayer
In-plane alignment
Longitudinal beam

Figure 1.11: Left: Schematic representation of a MDT cell of the region barrel consisting of two multilevel three-level tubes each. Right: Photograph of a MDT chamber during its construction and inspection process.

Cathode Strip Chambers (CSC)

The Cathode Strip Chambers (CSC) are analog chambers where the descent is the readout strip and a symmetric cell within which the gap between the anode and the cathode is equal to the thickness of the anode pitch. The precision of its coordinate position is measured by measuring the charge induced on the partial cathode strips by the electron avalanche formed on the anode wire. They essentially cover areas where particle flow is high and replace MDTs and at the same time combine high spatial and temporal accuracy at high rates. They are filled with a gas mixture Ar-CO$_2$ $(80 - 20\%)$ and the cables have a voltage equal to $1800\,$V. Their spatial precision is $60\,$mum for the coordinates of strips and $5\,$mm for that of the cables. In addition they consist of 4 levels in each region end-cap and cover values pseudorapidity $|\eta| < 2.7$. The CSCs measure the set of events using an almost rectangular arrangement of ascending wires and cantilevers (strips). The cathode strips move radially from the beam and are used to measure the location of

events while the anode wires for the radial position. The signal generated on both the strips and the cables can be used to determine the time of an event with similar resolution. Fig. 1.12 illustrates the structure and function of CSC as well as its internal structure. As a particle passes through the gaseous medium of CSC it ionises it resulting in electrons created to move to the anode wires.
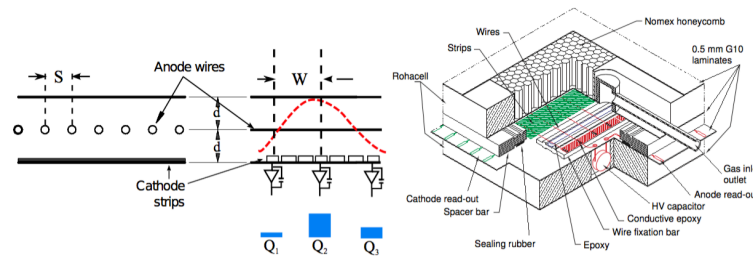

Figure 1.12: Left: Schematic representation of how a CSC detector operates. Right: The internal structure of a CSC.

Resistive Plate Chambers (RPC)

In the barrel area of ATLAS, the Resistive Plate Chambers (RPC) system is responsible for providing the trigger signals. The RPCs are parallel-plate gas detectors capable of providing particle time measurements with an accuracy of 1 ns wherever they meet the requirements of the ATLAS trigger system. Multi-component gas mixture $C_2H_2F_2$:4.5%-C_4H_{10} : 0.3%SF_6. In addition, fast and coarse track measurement can be used to identify events from precision detectors related to the detection of muon track. There are three layers of these chambers in each end-cap of the detector and cover the area of pseudorapidity $|\eta| < 1.05$. The structure of RPCs is illustrated in Fig. 1.13.
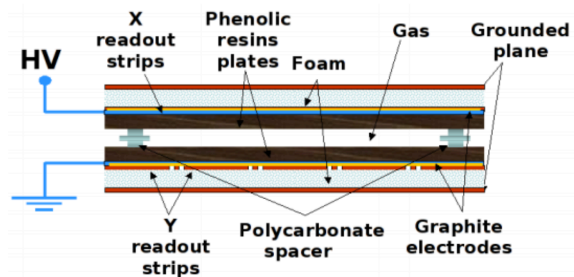

Figure 1.13: Internal structure of a RPC detector.

Thin Gap Chambers (TGC)

Information on the trigger in the muon region end-cap is provided by TGCs. In addition they are able to provide a measurement of the azimuthal coordinate to complete the bending coordinate from the cells MDT of end-cap. The middle end-cap area from MDTs is complemented by 7 levels TGCs, which provide both measurements for triggering and azimuthal coordinate, while the two layers are from the inner muon end-cap Small Wheel measures the azimuthal coordinate. The TGCs are similar in technology to the multi-channel analogue chambers with anode wires MWPC enclosed by two levels of cathode and two levels of reading strands perpendicular to the cables. For time, momentum and azimuthal coordinate measurements, they operate with high damping gas $CO_2 + 45\%n-C_5H_{12}$ and a high electric field 3200 V. There are four layers of TGCs in each end-cap of the detector ATLAS and the internal structure of the detector is shown in Fig. 1.14.

Trigger and Data Acquisition System (TDAQ)

Reading the data collected from the interactions that occur during the experiment on ATLAS requires a triggering and data acquisition (TDAQ)) [18]. The trigger system consists of three separate levels: Level-1 (L1), Level-2 (L2) and Event Filter (EF). Each level of trigger improves previous level decisions and constantly sets new dynamic selection criteria. On the other hand, the data collection system temporarily receives and saves data from these events from the special electronic detector reading systems at the selection rates permitted by (L1). The first level of triggering, using the data from the muon chamber detectors and triggering systems, makes the first
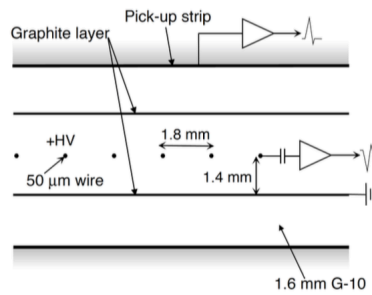
Figure 1.14: Internal structure of a TGC detector.

decision in less than $2\,\mu$s. This procedure reduces the initial particle collision rate to $20\,\text{MHz}$, to $75\,\text{kHz}$. Next, the data is ready to supply the Level-2 (L2) level with data in the region of Interest (ROI). The triggering 2 layer is software-based and uses the data derived
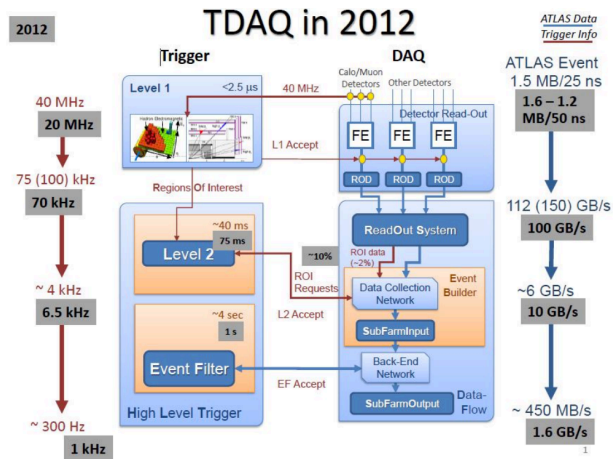

Figure 1.15: Schematic representation of the triggering and data collection system of ATLAS experiment.

from L1 and in combination with the Inner Detector data optimizes the data selection. This procedure improves the data selection and the rate of events is $3.5\,\text{kHz}$.

Once the data is ready from the Level-2 (L2) [19] layer it reaches the final level of the Event Filter where it is based on software and has access to all the previous information. The rate is now reduced to $0.4\,\text{kHz}$ and the data is ready for final analysis. The schematic representation of the triggering and data collection system of experiment ATLAS described above is illustrated in Fig. 1.15.

After the level of Event Filter the data is ready for analysis. The particle trajectory is being reconstructed, the particle is identified by measurement and momentum, and we now have all the data to discover new particles and theories even beyond the Standard Model. Fig. 1.16 shows the trajectories as well as the energy deposited by the particles resulting from the interaction p-p at the interaction point.
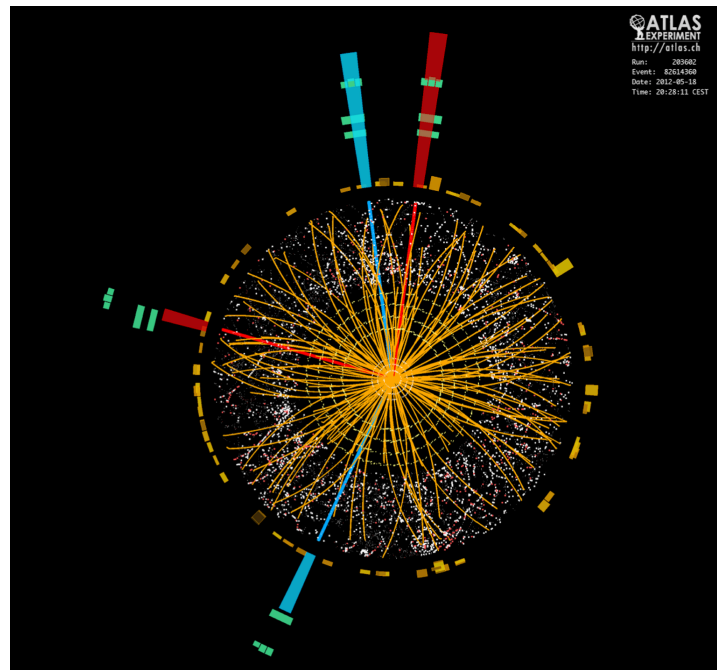
Figure 1.16: Event from data obtained from the ATLAS experiment.

Chapter 2

New Small Wheel Upgrade Project

This chapter will provide an extensive description of the New Small Wheel Upgrade experiment ATLAS of CERN. Increasing the brightness of LHC it is necessary to upgrade Small Wheel with two new types of detectors, sTGC and Micromegas, which will be used with a new electronic system able to process large numbers of particles. Finally, the layout and principle of New Small Wheel, the electronics responsible for data collection and distribution, as well as the VMM chip type ASIC which will constitute a cornerstone for collecting data from detectors.

2.1   High Luminosity LHC (HL-LHC)

During Run-1 (2010-2012), LHC could distribute a total of $\int \mathcal{L} \, dt = 28.26 \, \text{fb}^{-1}$ from pp data conflicts leading to remarkable physical results from experiments such as the discovery of the boson Higgs [20].
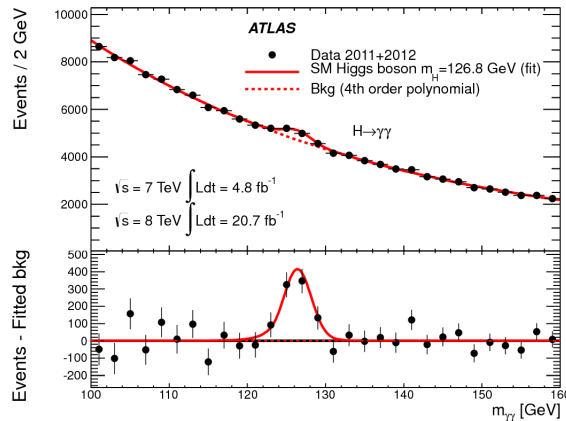
Figure 2.1: The discovery of the boson Higgs during Run-1 using experiment data from ATLAS [21].

The very successful first LHC run came to an end in December 2012, followed by a major shutdown of LHC (Long Shutdown 1 (LS1)). During the 2-year period of shutdown, the accelerators as well as the experiments went through a series of upgrades and maintenance activities to address the LHC program. During Run-2 launched in early 2015, LHC is projected to run at twice the mass center energy (14 TeV) and smaller bunch crossing (BC) of the order of 25 ns and will result in an increased brightness equal to $\mathcal{L} \approx 10^{34} \, \text{cm}^{-2}\text{s}^{-1}$.

The current timetable of LHC, as shown in Fig. 2.2, provides for 2 additional periods shutdown LS2 (2019) and LS3 (2024). Upgraded injector chain and LHC after LS2, will lead to a further increase in brightness wherever it reaches $\mathcal{L} = 2 \times 10^{34} \, \text{cm}^{-2}\text{s}^{-1}$. The transition from LHC to HL-LHC will take place during LS3, with more than 3000 fb^{-1} data being delivered during Run-3. The severe HL-LHC environment will be particularly demanding for experiments due to the predicted maximum brightness in the order of $\mathcal{L} = 7 \times 10^{34} \, \text{cm}^{-2}\text{s}^{-1}$ for experiments ATLAS and CMS. In order to cope with the experiments with the predicted high particle rate, a series of upgrades have been proposed for the LHC experiments to maintain their operation during the HL-LHC period.
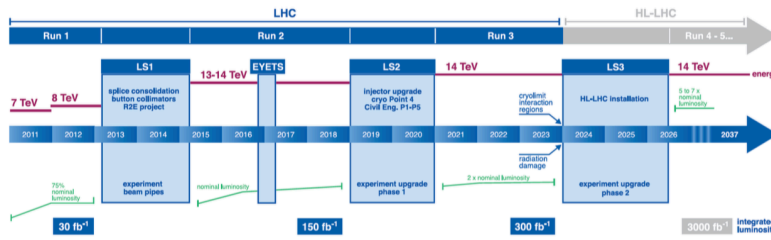
Figure 2.2: The time schedule of LHC.

2.2   New Small Wheel Upgrade

For experiment ATLAS, such an increase in brightness means an increase in the particle rate. The following Fig. 2.3 depicts the maximum mean number per junction of the beam over time for p-p events during 2010-12.
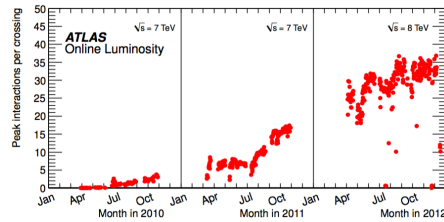

Figure 2.3: The maximum average number per beam junction over time for p-p events during 2010-12 [22].

In the period between Long Shutdown 1 (LS1) and Long Shutdown 2 (LS2) the number of inelastic scattering for each junction packet junction (bunch-crossing) is expected to increase from 35 to 60-70 and thereafter (Long Shutdown 3 (LS3)) this number will exceed 140. Most of the experimenter ATLAS muon systems have enough room to handle them particle rates, but the "front" system of the muon spectrometer, called Small Wheel, is unable to handle this number based on the detectors currently installed (MDTs, TGCs) where they are provided in pseudorapidity $|\eta| = 2.7$, rate of $15\,\text{kHz/cm}^2$. However, the end-cap area covers about 63 % of the ATLAS muon system, so it is necessary to upgrade this area to meet the needs of HL-LHC [23].

The Phase-I [24] upgrade of the ATLAS muon spectrometer focuses on the endcaps region. The barrel sub-probe system covers the region of pseudorapidity for $|\eta| < 1.0$ while the endcaps system covers $1.0 < |\eta| < 2.7$ for muon detection and $1.0 < |\eta| < 2.4$ for Level-1 trigger. The areas above are plotted in Fig.2.4 where it shows a transverse cross-section of the detector ATLAS at the plane $z - y$. So in high luminosity the following 2 points are of particular importance:

- Muon triggering of end-cap

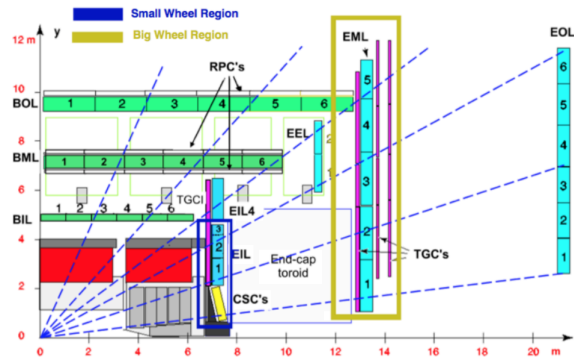- Detector Tracking Performance & Efficiency

Figure 2.4: Cross-section of the ATLAS on the plane $z - y$ [25].

2.2.1   End-cap Muon Trigger

The Level-1 muon triggering of the end-cap region is based on orbital imprints on the chambers TGC at the midsize station (Big Wheel) located behind the torus magnet of end-cap. The transverse momentum of the muons, p_T, is determined by the angle of the signal segment with respect to the direction pointing to the point of interaction (IP). Low-energy particles, such as protons, produced in the material located between the Small Wheel and the electromagnetic calorimeter (EM), produce false triggers as they pass through the chambers of the end-cap region at an angle similar to the really high transverse momentum p_T muons. These fake triggers constitute 90% of total triggers, and thus the muon Level-1 trigger rate at end-caps is projected to be 8 to 9 times higher in the region of barrel. This situation is shown in Fig. 2.5, where it shows that a large fraction of remanufactured muons do not match the candidate muons from the internal probe.
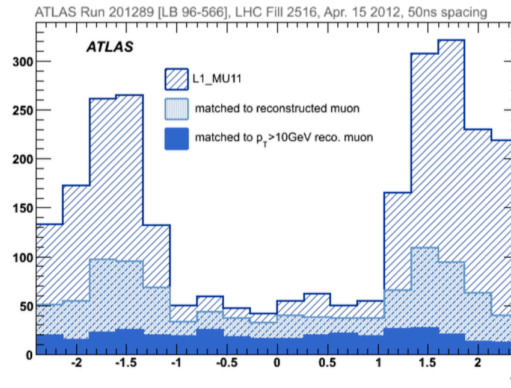
Figure 2.5: The pseudorapidity distribution of Level-1 trigger rate in 3 levels [25].

In Fig. 2.5, the intermittent distribution of the ionic trigger Level-1 with transverse momentum $p_T > 10$ GeV (L1 _MU11) is plotted, with the light blue distribution depicts the subset of the candidate muons resulting from the offline remanufactured muons by combining the information from the inner probe track and the muon spectrometer with $p_T > 3$ GeV. In addition, the blue distribution reflects the remanufactured muons with a threshold at the transverse momentum equal to $p_T > 10$ GeV. This analysis conducted in 2012 showed us that 90% of total scandal in end-cap is due to fake triggers.

2.2.2   Tracking Performance & Efficiency

In the Small Wheel region the brightness will increase the particle rate to 15 kHz/cm², resulting in the present detection devices (MDTs, CSCs, TGCs) will not be able to cope with such high particle flow rates. This can be seen from the dependency of the efficiency of a single MDT pipe on the rate of events. The efficiency shows a rapidly decreasing trend as opposed to increasing the event rate, already reaching the level of 70% for the event rate predicted for the high brightness of LHC (≈ 300 kHz/$Tube$). The above conclusion is drawn from Fig. 2.6.
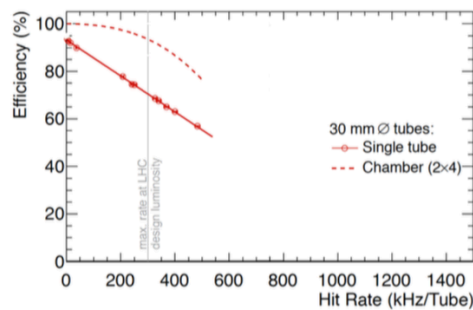

Figure 2.6: The efficiency of a single MDT tube and a MDT chamber, 2X4 tube levels, as a function of events from beam experiment data to luminosity $\mathcal{L} = 3 \times 10^{34}$ cm^{-2}s^{-1} [25].

2.3 The concept of the New Small Wheel Upgrade

To solve the above two problems that limit the performance of ATLAS during HL-LHC, ATLAS proposes to replace the existing muon Small Wheels with the new New Small Wheels (NSW) during LS2. NSW is a set of precision orbital tracking and trigger detectors capable of working at high particle flow rates with excellent spatial and temporal resolution in real time.

An explanation of the principle of particle trajectory estimation is illustrated in Fig. 2.7. The existing Big Wheel trigger system accepts all three tracks shown (A, B, C). With the introduction of the new New Small Wheel [25] trigger system, the trigger logic of the end-cap region will only accept the track (A), where the desired track will be confirmed both from Big Wheel and New Small Wheel. Track (B) will be discarded because NSW will not find any part coming from the interaction point that fits into Big Wheel. The trajectory (C) will be rejected because the part of the trajectory from NSW does not match the point of interaction (IP).
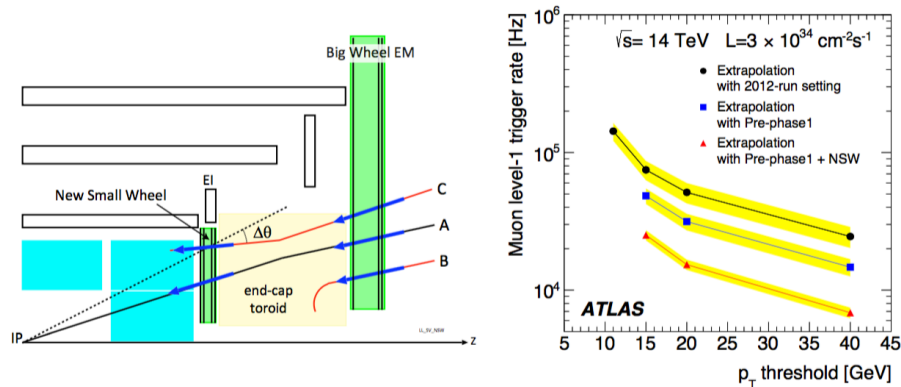
Figure 2.7: Left: Description of an event of trigger system of New Small Wheel [26].

After upgrading the triggering system by adding the NSW system only the real muon track A, where it will be confirmed by BW at the same time, will be accepted by NSW reducing thus the false triggers based on the paths B, C. The simulations were done to fully understand the effect of the increase in brightness on the overall rate of triggering. In Fig. The estimation of the rate of Level-1 trigger for pp collisions in energy $\sqrt{s} = 14\,\text{TeV}$ with instantaneous brightness $\mathcal{L} = 3 \times 10^{34}\,\text{cm}^{-2}\text{s}^{-1}$ is plotted as a function of the threshold threshold p_T for three different configurations. The forecasts of the trigger rate, assuming the current configuration of the trigger system, are shown in black, while the blue curve illustrates the expected reduced trigger rate using data from the chambers EI4-TGC with Tile area $1 < |\eta| < 1.3$. Finally, the red curve represents the expected trigger rate given by NSW where it shows a significant decrease in the rate $\approx 15\,\text{kHz}$ for a threshold of p_T equal to $20\,\text{GeV}$.

The design of NSW meets the specifications for a very good angular trajectory resolution of 1 mrad at Level-1 trigger. Background signals in the high density orbital environment of NSW can be suppressed using this angular resolution. For the Phase-II [27] upgrade of the Level-1 system triggering for even higher yet higher brightness, the reaction time will be reduced to more selective triggering than calorimeters and new Level-1 trigger trigger system as well as the muon system can be implemented. Upgrading Phase-II will dramatically improve the resolution of p_T of the ion trigger system Level-1, lowering the activation threshold and reducing the contribution from lower p_T muons, less than nominal threshold.

Essentially, this will be achieved by using the data from the Precision Detector (Monitured Drift Tubes) as part of the muon firing system at endcaps and combining it with the angle of the corresponding activated segment provided from New Small Wheel. In addition, following the principles of the current muon system, NSW should consist of multiple levels of detection to improve the pattern recognition performance of track reconstruction, rejecting the multiple background events expected in the environment of Small Wheel. An excessive number of detection levels will also ensure the efficient operation of the detector, which will offset any failures of a detection level.

2.4 Layout of the New Small Wheel

The proposed New Small Wheel [25] detection system is designed to meet all the specifications presented in the previous subsection. The detection technologies to be used come from the family of gas detectors (gaseous detectors), the first being a multi-channel microchannel technology called small-strip Thin Gap Chambers (sTGCs) [28], and the second comes from the category of Micro-Pattern gas detectors and is named Micromesh Gaseous Structure (MicroMeGas) [29]. The new experimental layout will consist of 16 detection levels in 2 layers of 4 levels per detection technology (4 levels sTGC and 4 levels Micromegas). The Micromegas and sTGC probes will fully cover NSW in a 1200 m² detection range. NSW will follow the dimensions of the existing SW and the same

segmentation into 16 sections per wheel (wheel) will be followed to match existing Big Wheel and muon station end-cap. Fig.2.8 Shows the current Small Wheel on the surface of the earth prior to its installation in ATLAS as well as an overview of the overall layout of the New Small Wheel.
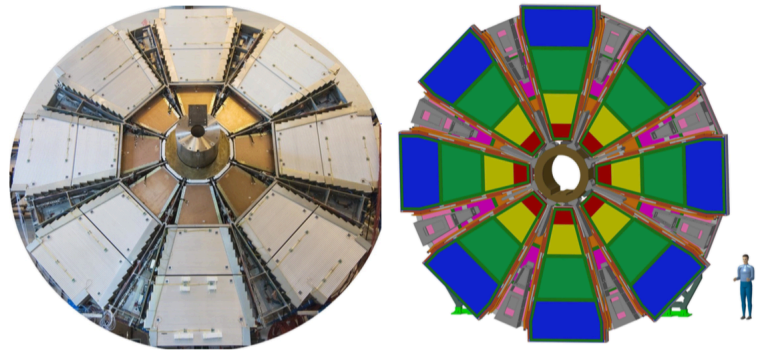

Figure 2.8: Left: The current Small Wheel on the surface of the earth before installing it in ATLAS. Right: Illustration of the New Small Wheel layout.

The layout of NSW will be provided with 8 levels of each technology separated by a frame of $50\,\text{mm}$. The inner part will consist of micromegas detectors while the outer part will consist of sTGCs detectors forming an area of $400\,\text{mm}$. Each section will consist of 2 wedges (a set of modules of a single technology in the direction z, covering an entire sector (sector), at the level $r - \phi$, oriented as shown in the schematic representation in Fig. 2.9 (left). The detectors sTGC will be radially divided into 3 modules, (a set of multiplets in the direction of r which is a single independent object), while micromegas in two. An overall representation of a segment is shown in Fig. 2.9 (right).
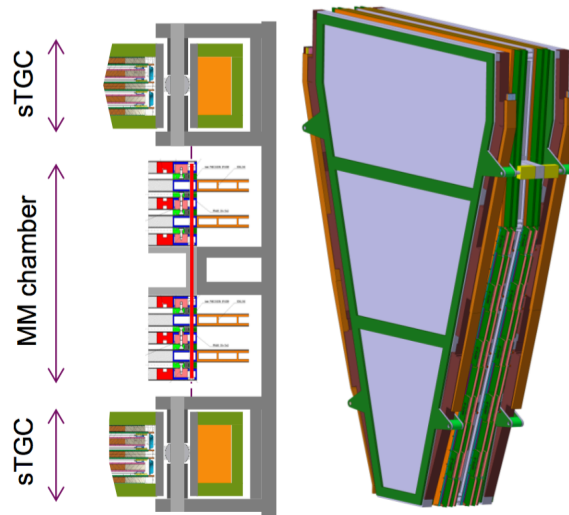
Figure 2.9: Left: Layout detectors inside a sector. Right: Illustration of a sector of New Small Wheel.

The sTGC detectors have been mainly developed for triggering, given the lack of recognition capability they have to trigger recordings. Detection technologies will be arranged in such a way (sTGC-MM-MM-sTGC) to maximize the distance between the two sTGC layers. As the online track is rebuilt, this distance between the sTGC layers allows for improved resolution for the online track, given the angle provided by the the first layer of detectors. On the other hand, MM detectors are used for track analysis due to their excellent track tracking accuracy, due to the small vacuum ($5\,\text{mm}$) and the small strip pitch (strip pitch $0.5\,\text{mm}$), more on the Micromegas detector mounted on NSW will be given in the next chapter. In addition, NSW is expected to run throughout the life of the experiment ATLAS, as a result the high number of levels will ensure a proper detector performance and in case any of the levels fails to function properly. of. Finally, the two probe technologies to be used also complement each other in their main functions. The sTGC can contribute to offline track tracking accuracy as they are able to measure track collisions with a resolution of approximately $150\,\text{m}$. The MM probes will assist sTGC to provide improved particle track results as they act as a trigger mechanism.

Detection technology of sTGC

Requirements for the NSW trigger system require the detectors to provide the ability to identify and separate the pulses passing through it, also require good time resolution and good angular resolution for online track segment reconstructions, that is, good online spatial resolution. The small-strip Thin Gap Chambers (sTGC) will be the main trigger mechanism providing the right angular resolution for online track reconstruction. In addition, these detectors are characterized by good discretion for offline track detection using the best precision coordinates (from readout strips), compared to current TGC and detector's strip pitch equal to 3.2 mm, as a result of these detectors helping to accurately track the particle trajectory during HL-LHC. The internal structure of the detectors sTGC is illustrated in Fig. 2.10. The signal due to the drift of the ionization loads and their multiplication by the snowball effect is induced on the anode cables, the readouts strips and pads are below the downstream levels.
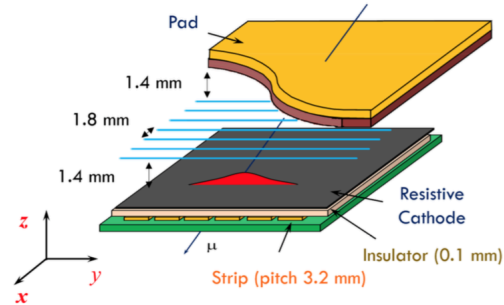
Figure 2.10: The internal structure of the small-strip Thin Gap Chamber (sTGC) detector.

The MicroMeGas detector

The resistive-strip MicroMeGas used in the upgrade of New Small Wheel will be the main track detection mechanism, featuring excellent spatial resolution ($\sigma < 100\,\mu$) irrespective of the particle incidence angle, high detection efficiency even at the highest background noise values, and good two-track separation to reject the delta electron angles accompanying the muons. The very thin segmentation of the MM readouts (readout-strips), together with sufficiently good time resolution, can also be exploited to complement the TGC trigger system. , adding to system stability and verification even as backups. In the next chapter, a more detailed analysis of the gas detectors and their physical properties, as well as the MicroMeGas detector used to upgrade the New Small Wheel will be provided.

2.5 Overview of the Electronic System of the NSW

With the increase in luminosity, or the increase in the rate of interactions due to successive upgrades, the spatial resolution of the Small Wheel detectors will be degraded, while the muon trigger system will be considered useless. As a result, in addition to upgrading NSW detectors, a sophisticated [25] [26] electronic system is required where it will first collect triggering data and send it to the trigger processing department of CERN quickly and save the energy deposited by the particles in the detection system as well as the time it occurred.

The key axes of the electronic system on top of the detectors, Front-End Electronics (FE) [30], are fast trigger system data collection, accurate power and time measurement, and distribution of this data in the electronic system that is inserted between the detector and the computer center of CERN, Back-End Electronics. In addition, they should receive commands to modify their operation from the ATLAS control center and send back data to external agents. While these electronics have to cope with the harsh conditions of irradiation, their primary purpose is to quickly and accurately calculate the trigger and to reconstruct the particle trajectory.

The system of front-ent boards of NSW electronics consists of the following three electronic boards (Printed Circuit Boards, PCB):

MicroMeGas Front-Ent Board (MMFE8)

This electronic board [30] will be located on the detectors MicroMeGas and its primary goal is to collect the original signals from the sensors. Each MMFE8 card contains eight ASIC [31] responsible for read-out, called VMM [32]. Each VMM ASIC has 64 channels, each corresponding to a strip of the detector and in total each MMFE will read 512 readout-strips of a MicroMeGas. In addition to VMM on this board there is another ASIC, GBT-SCA (Slow Control Adapter) [33] and Read-Out Controller (ROC) [34] responsible for distributing monitoring/control signals from 8 VMM and digital data at a e-link output. A schematic representation of the board is illustrated in Fig. 2.11. In addition, the prototypes of MMFE8 will not have these two utilities ASIC but a FPGA [35] which will replace the

functions of both ASIC chip. In addition, these cards will be fitted with external access protection against sparks and ensure entry to 8 VMM. Flexible high frequency links Zebra will be used to connect the signals from the detectors Micromegas to the channels of VMM.
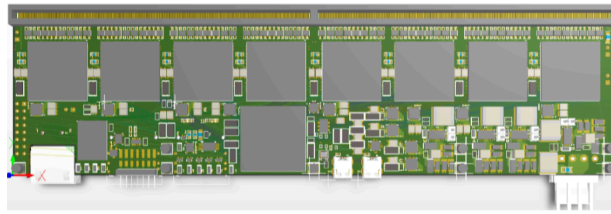

Figure 2.11: Schematic representation of the board MMFE8.

Level-1 Data Driver Card (L1DDC)

The L1DDC [36] card will serve as an intermediate stage between the front-end boards and the Felix system and is designed for the needs of upgrading NSW from the NTUA high-energy experimental physics team. ROC chip from MMFE collects data from 8 VMM and sends it via 80 Mb/s e-link to a ASIC chip, the GBTx [33] located on L1DDC. Subsequently, GigaBit Tranceiver (GBTx) collapses the data into a link optical fiber that ends up in the back-end electronics system and the FELIX (Front End Link) network eXchange) [37]. A schematic representation of the board is shown in Fig. 2.12 below. Also, L1DDC and GBTx send MMFE8 data TTC (Timing and Trigger Control), such as timing (BC Clock) in ASIC of MMFE8. In addition to this data, it also provides commands that address changes in the functionality of VMM ASIC.
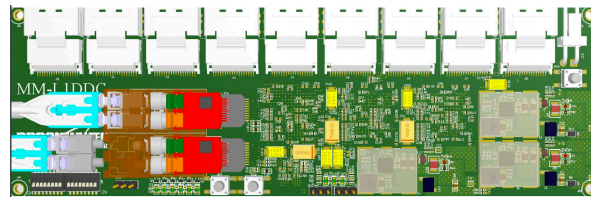
Figure 2.12: Schematic representation of the board L1DDC.

ART Data Driver Card (ADDC)

The ADDC [38] card will be used for the detectors Micromegas and will receive data Adress in Real Time (ART), the first data above the threshold from 8 MMFE. Two GBTx ASIC will collect the data ART and send it in two steps via a link optical fiber to back-end electronics and specifically to USA15 where and is the host of trigger. For Micromegas detectors, the primary signal trigger is ART, which is generated from the 64 channels of VMM in each bunch crossing and corresponds to 5 - bit geographical address at strip for each event. This board communicates with a L1DDC, which sends the configuration data from the control center and provides timing signals. A schematic representation of the board is shown in Fig. 2.13.

Figure 2.13: Schematic representation of the board ADDC.

The front-end electronics will be installed on the wedges of Micromegas axially along both sides to offset the load on both sides of the detector as well as the wiring. The following figure illustrates the schematic representation of the connection between the front-end electronics of NSW (left) and its location along the wedges of a Micromegas sector (right).

The communication between the cards is done serially by 3 pairs of different lines which are the clock signal (Clk +, Clk-), the data transmission (Dout +, Dout-) and the data reception (Din +, Din-). All of these pairs of differential signals are called e-link, follow the LVDS standard and can be programmed at three different data transmission rates (80, 160, 320 Mbps). The connections between
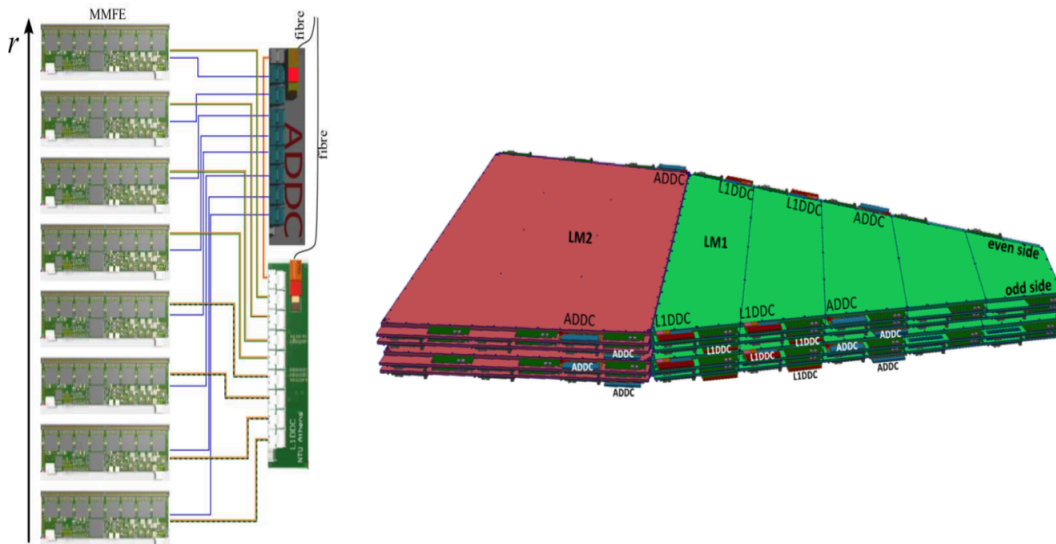
Figure 2.14: Schematic representation of the wiring between front-end electronics of NSW (left) and its location along the wedges of a Micromegas sector (right)

.

MMFE8 and ADDC are uniform along the radial direction of the detector at a rate of 160 MHz. The L1DDC card implements the e-link configuration links, which are along the radial direction with a transmission rate of $80/$, Mbps, while readout e-links with flow rate 160 Mbps for the four outer MMFE and 320 Mbps for the inner four in number. This is due to the higher particle rate requiring greater bandwidth in the inner radius of the detector.

2.6   VMM ASIC

The VMM [32] [39] is a front-end readout ASIC designed by Brookhaven National Laboratory (BNL) for the needs of upgrading New Small Wheel of the experiment ATLAS at CERN. Manufactured using the 180 nm Global Fountries 8RF-DM process and with dimensions of 13.5×8.4 mm² contains about five million transistors with technology CMOS. Each of its 64 channels is connected to a read-out strip and implements a load amplifier (charge amplifier), a configuration amplifier shaping amplifier, a clarifier discriminator with lower threshold and peak detection and a Timitng to Amplitude Converter (TAC). The analog signals produced by these electronic subsystems are digitized by 3 Ananog-to-Digital Converters (ADC), with outputs 6, 8 and 10 bit. The resulting digital data is then stored in a FIFO which sends the data to ROC ASIC of MMFE8. VMM3 will be manufactured using Ball Grid Array (BGA) technology at 400 ball with pitch 1 mm and the device size will be 21×21mm² in accordance with pitch of detectors Micromegas. The surface size (layout size) of VMM3 will be 15.308×8.384mm² and the package size (die size) will be 15.308×8.464mm², which is also illustrated in Fig. 2.15 below:
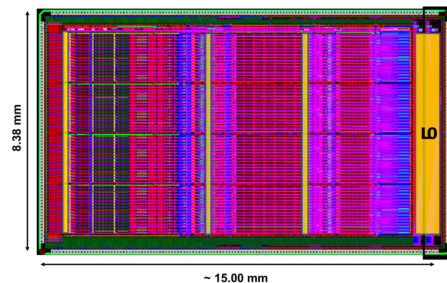
Figure 2.15: VMM3 die layout

Inside the VMM [40] when a pulse enters, the preamplifier converts it into an analog voltage pulse, and then the shaper forms the final form of the input voltage. The (shaper) filter is 3rd degree designed in retrospective delay feedback (delayed dissipative feedback (DDF)), and can be set to 4 load end times (peaking time), $25, 50, 100, 200$ ns. In addition, it is possible to increase the electronic

pulse to 0.5, 1, 3, 4.5, 6, 12, 16 mV/fC. The modulated signal then enters the discriminator, where when a pulse exceeds the threshold (threshold) set, the pulse peak detection method is activated.
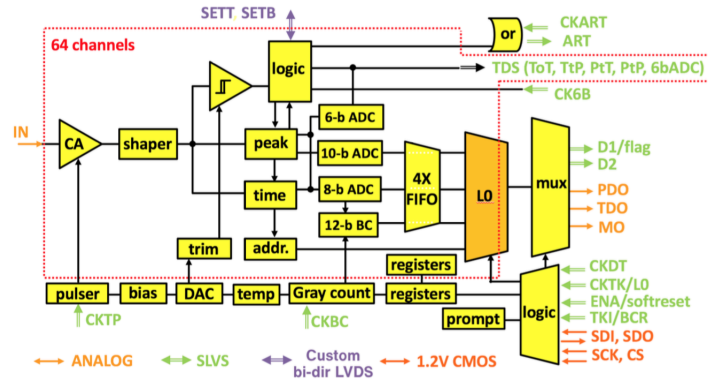
Figure 2.16: Schematic representation of a VMM architecture.

Once the pulse tip is detected TAC is activated and the capacitor discharge process is started. This process stops with the next falling-edge of BC clock (CKBC) where the charger ceases to discharge. Finally, we are able to calculate the height of the pulse, ie its load, and the time of occurrence of the pulse in relation to BC clock (BCID). The following Fig. 2.17 illustrates the procedure described for calculating the pulse height as well as the time of occurrence.
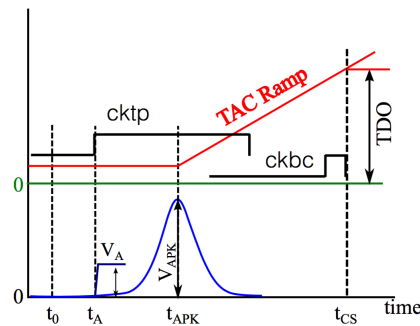
Figure 2.17: Schematic representation of the process of calculating the pulse height as well as the time of pulse occurrence.

Three different analog to digital conversion (ADC) systems accept the results of signal analysis and digitize them. The time is measured by the 8-bit ADC via the output of TAC, the energy is measured by the 10-bit ADC which receives the signal bearing the maximum height information of the pulse from the peak detector, and finally the 6-bit ADC also converts this signal to the peak detector but less accurately. The choice of ADC to build the package depends on the needs of the user.

Chapter 3

Introduction to WinCC-Open Architecture

This chapter introduces the reader to the central automated experiment control system ATLAS. The central system DCS of ATLAS checks the status of all detectors, sub-detectors and system to achieve optimum operation of the experiment. In addition, an introduction is made to the WinCC-OA program and principles of Siemens for the development of automated control systems.

3.1 Introduction

Due to its complexity and long-term operation, the ATLAS detector requires the development of a sophisticated detector control system or otherwise Detector Control System (DCS). The use of such a system is necessary to allow the detector to function consistently and safely as well as to function as a seamless interface to all sub-detectors and the technical infrastructure of the experiment. The central system handles the transition between the probe's possible operating states while ensuring continuous monitoring and archiving of the system's operating parameters. Any abnormality in any subsystem of the detector triggers a signal or alert (alarm), which alerts the user and either adapts to automatic processes or allows manual actions to reset the system to function properly. In fact, it is a SCADA (Supervisory Control and Data Acquisition) system that describes a class of industrial automatic control and telemetry systems.

3.2 Central Control System of ATLAS

The ATLAS DCS [41] [42] was designed and implemented in the framework of the joint project Joint COntrols Project (JCOP) [43], a collaboration of the CERN and DCS groups of LHC experiments. JCOP combines common standards for the use of DCS hardware based on SCADA system Siemens, WinCC Open Architecture [44], also known as PVSS with its older name, where it serves as the basis for all DCS applications. Fig. 3.1 depicts the architecture of DCS [45] [29] which can be divided into Front-End (FE) equipment and a system Back -End (BE). FE includes equipment DCS, including customized electronic systems and related services such as high voltage power supplies and cooling circuits. The BE system uses the software WinCC, integrating front-end control systems into the JCOP framework components to facilitate the integration of standard hardware devices and the implementation of homogeneous control applications. The two ends of DCS communicate mainly through the industrial protocol bus CAN, while the communication standard OPC is used inter alia as a communication software protocol. The system BE is organized hierarchically on three levels, the Local Control Stations (Local Control Stations (LCS), the Sub-detector Control Stations (SCS)) and the Central Control Stations (Global Control Stations (GCS)). In total, BE consists of more than a hundred computer stations connected to a distributed system. Communication between subsystems of the system is handled by WinCC via a local area network. A distributed finite state machine, Finite State Machine (FSM), represents the complete hierarchy of the BE system as it integrates more than 10 million data elements into a single tree structure and ensures proper operation and efficient handling errors in each operating layer. The most important element of this system is the structure datapoint (DP), which plays the role of the global variable network. Each element (element) of this structure has a unique name and configurability, and special DPs are used to read data from the hardware components updated by the interface OPC [46] client-server communication.

Each node FSM has a unique name based on the subsystem name and its functionality following the conventions of ATLAS DCS and the state in which they are specified by a corresponding internal DP. The type of object FSM which defines the basic functionality of the node and its components, depends on the functional purpose and position of the element in the DCS architecture hierarchy. The main graphical user interface of ATLAS DCS with all subsystems integrated into a hierarchical structure FSM is illustrated in Fig. 3.2. The FSM is based on a strict hierarchical structure that constitutes parent-child relationships, where in tree construction commands are passed from parents to children, and situations from children to parents. This way, when some action is required on all children it is extremely efficient to command a higher node and correspondingly the status of the higher node summarizes the status of all nodes
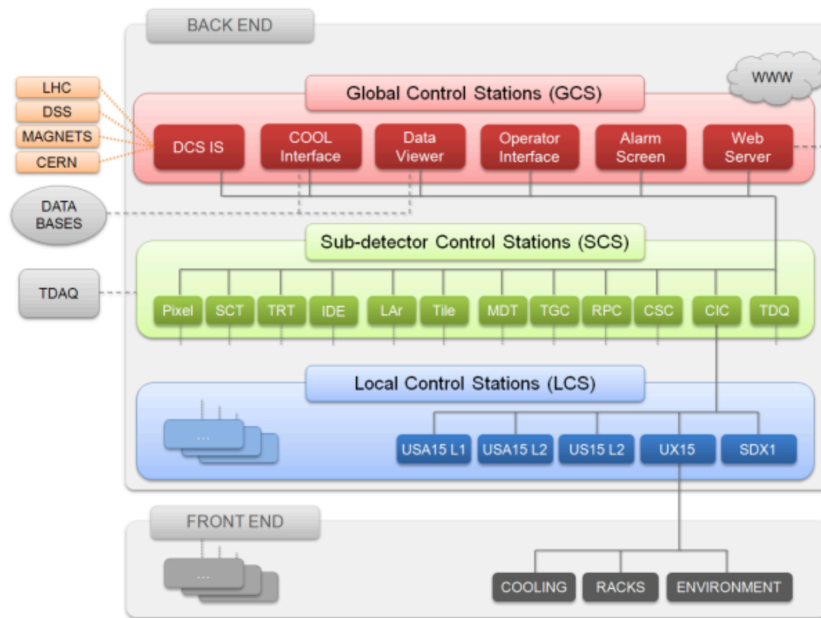
Figure 3.1: Graphical representation of the DCS architecture of the experiment ATLAS divided into 3 levels: GCS, SCS and LCS.

of any generation. All nodes are in a predefined state and only accept predefined commands as defined in the FSM type to which they belong.

3.3 WinCC Open Architecture

WinCC is a software package with a main application area handling and controlling technical installations using a complete graphical interface to visualize and simulate the various modules. Implementing these processes requires an interactive communication environment with hardware to monitor, transmit commands, use alarms, and store history. It was eventually selected by the JCOP committee due to the widespread use of the tool for building automated control systems in the developers and experiments of CERN.

3.3.1 Architecture

The philosophy of a WinCC-OA system is based on its core components being managers, which communicate through a specific protocol of WinCC, TCP/IP. Administrators contribute to the data and then only send it for change to the Event Manager (Event Manager), which is the heart of the system. In addition, guides can be configured to send data to the event handler when a significant change appears. Thus, in a properly configured system, there is virtually no data traffic impediment in steady state, that is, when the process variables are not changed.

A typical application WinCC consists of several managers, which are illustrated below and a graphical representation of them.

- Event Manager - EVM: It is the processing center of WinCC and is responsible for all communications. It sends or receives data from Drivers, transfers it to Database Managers to be stored in the database, and further distributes it to the Managers who need to manage it. In addition, it maintains the process image in memory, that is, the current value of all data, as it is stored in datapoints and ensures the distribution of all data, manages system alerts and alarms.

- Drivers : This manager implements the communication protocol with hardware where it provides connection to external devices via connection templates such as OPC, ModBus, etc. Allows editing instantly and during operation by streamlining data flow, undertaking value conversion and communicating with drivers and finally providing application programming interface to create new interface.

- DataBase Manager-DBM : Provides a link to the database, where it records the latest system values and alerts, historical price data and alerts. The database is accessed via the SQL language and WinCC supports an optimized version of RAIMA as well as Oracle.
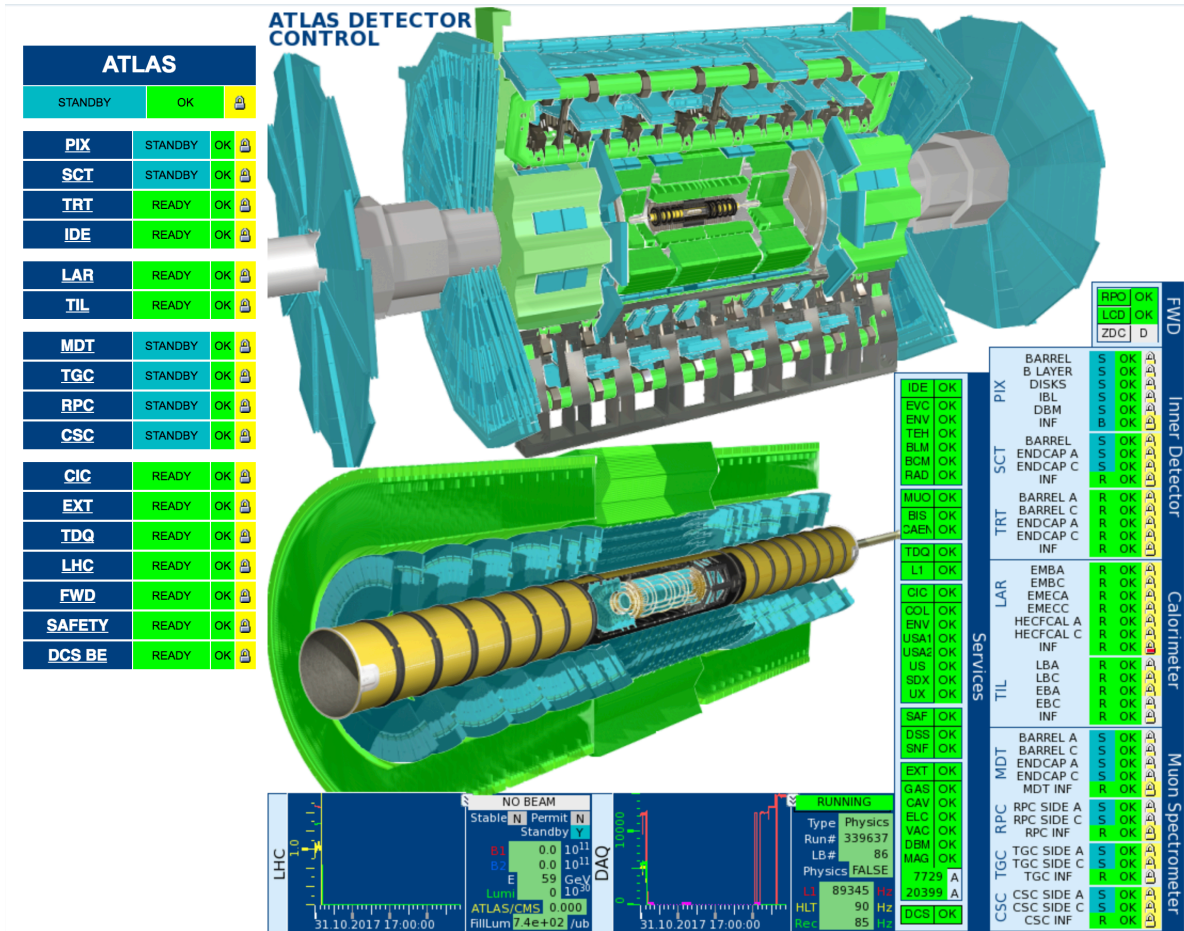
Figure 3.2: The main user interface of ATLAS DCS with all subsystems integrated into a hierarchical structure FSM.

- User Interface Managers-UIM : They are responsible for visualizing messages received from Event Manager. They can retrieve hardware data from the database or send the data to the database to be sent to hardware. In addition, UIM can also run in a deployable state, PARA to configure DPTs/DPs and GEDI for the graphic editor, where the user can to design his own panels. In addition, it includes a multitude of libraries and allows the user to add additional plugins and panels and finally provides the script editor for writing code.

- Control Manager (CTRL): WinCC provides the ability to develop algorithms for graphic design panels, decision making, command generation and further data processing. The programming language it uses is called CTRL and is based on its ANSI-C syntax with additional modifications, such as non-existence of pointers, special processing strings, and dynamic tables, as well as it has a very large library of algorithms and functions to allow the introduction of algorithms to execute program functions.

- API managers : It allows the user to build their own library of algorithms in CTRL and integrate them into the existing system.

- Archive Managers) : These managers allow the user to archive the data for later retrieval and examination as well as the ability to configure whom to store the corresponding data.

- ASCII Managers : Allows the user to export / import the configuration of a project (DPTs/DPs) from/to a file ASCII. Allows users to choose which items to export to make it easier for the user to integrate parts of their work into a ready project.

In WinCC a system is an application containing a Event Manager, a Data Manager as well as a number of other managers, user interfaces and other things that run only when they are called. This allows the system to be easily adapted to each user's needs and managers to open or close without having to restart the entire software. This specific structure and communication through a common protocol TCP/IP enables distributed systems to be created on a single computer network by sharing the burden on multiple computers and separating functions by creating a distributed system.
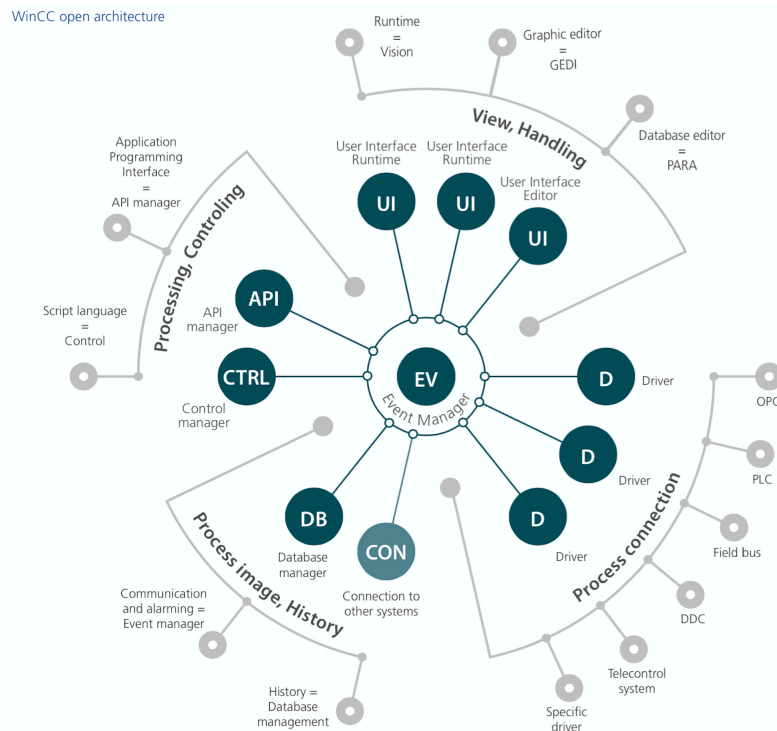
Figure 3.3: The architecture of a typical WinCC-OA system and the set of managers it consists of.

3.4 Basic tools of WinCC-OA

Database

Data processing and communication between managers is an object-oriented process. The structure of WinCC-OA is based on datapoints. Highest in the hierarchy are the so-called Datapoint Types (DPT), which have the role of classes in radial terminology and correspond to a mechanical system or an integrated set of their sub-units. Objects have Datapoints (DP) objects that refer to a set of properties or devices of the control system. All of Datapoint information is located in Datapoints Elements (DPE). Each DPE corresponds to a value or state of DPE while through Datapoint Attributes (DPA) we can obtain information to change a state or change various variables. The entire structure is user-defined and modified and created through PARA Database Editor of WinCC. In addition, the user is allowed to specify various settings for notifications or connectivity to various devices or archives, by adding configuration files (configs) to the various DPEs. Fig. 3.4 depicts an image of the tool PARA as well as an example of the structure of a DPT.
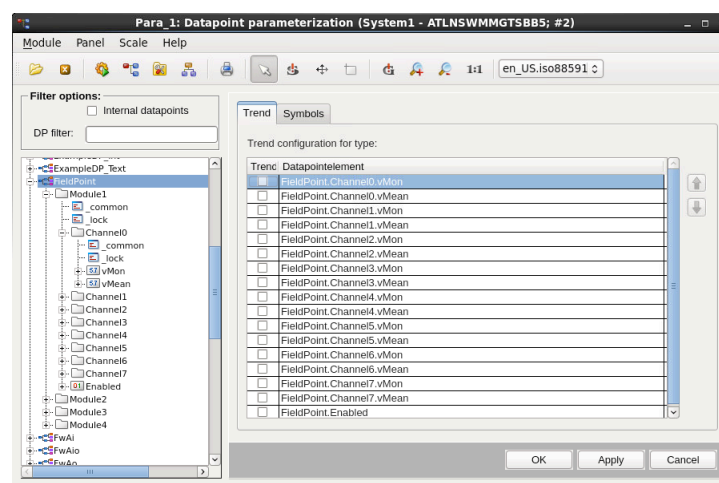
Figure 3.4: The too PARA Database Editor of WinCC and an example of a DPT's structure.

The FieldPoint is Datapoint Type (DPT), which consists of 4 Structure Elements (Modules). Each of the Modules consists of 8 Structure Elements (Channels), which then include each of the 2 Datapoint Elements type float, as well as a DPE where type boolean. In addition, each DPE may contain some configuration files (configs).

Graphical Editor Environment

WinCC allows the user to create their own panels through a special User Interface Manager, GEDI (Graphical EDItor). The user can build their own user interfaces, namely panels, with the object user as it is enabled in various objects such as buttons, tables, text fields, lists etc. In them developer can adjust through scripts the various processes of the object, such as what action to implement as it is called (initialize), what to do as it is pressed (clicked), what action to implement as it closes (Close), and many more at the discretion of the developer. Some very basic commands are provided by the software through dialogs but to model a complex process, it is necessary to create various scripts where the various algorithms will run. Fig. 3.5 depicts Graphical Editor of WinCC, as well as the various toolbars, panel and Properly Editor where the developer will match the various functions of its objects with Datapoint Elements.
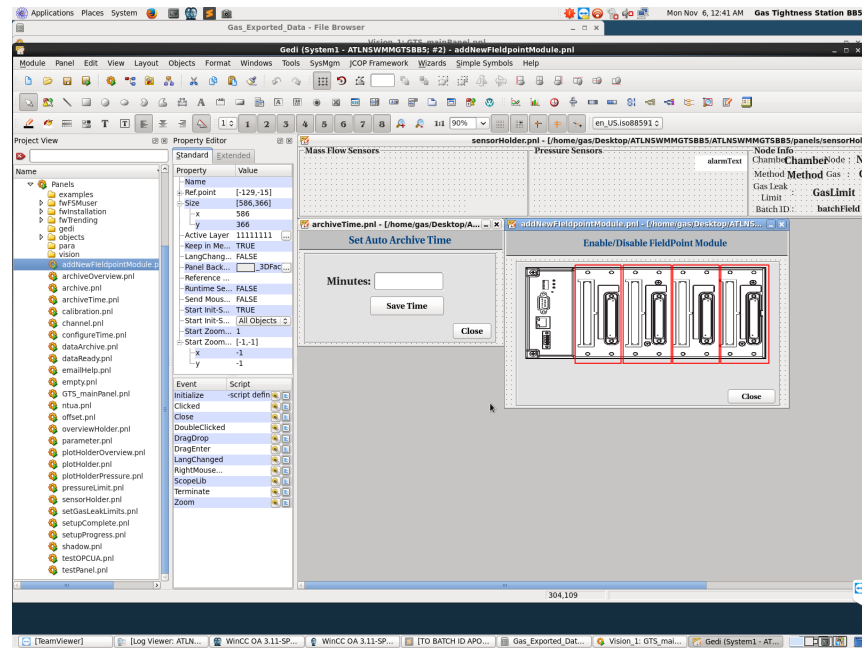
Figure 3.5: Graphical Editor Environment tool of WinCC.

Programming in Control

As mentioned earlier, the programmer has the ability to create his own algorithms to determine the behavior of his objects and panel as well as the dynamic manipulation of graphical objects and technical processing. WinCC provides a complete library of methods and functions that facilitate data management, graphics and external communications. The programming language is Control, a language based on C but introduces some variations with the introduction of new types of variables and dynamic size tables.

Hardware Connectivity

The connection of Event Manager to hardware is done through drivers and therefore WinCC has several drivers with separate communication protocols such as OPC, ProfiBus, CanBus, DIM etc.

Archiving

The database is automatically archived to the various values of DPEs so that it can be retrieved later from the different user interfaces for display, editing and whatever the user wishes.

Alarm generation and handling

Through the Alert Screen of WinCC the user can investigate the various alarms created as well as the reason and location from which they were triggered. These alarms are stored in a database and can be displayed selectively from an alert presentation.

3.5 Joint COntrols Project Framework (JCOP)

The incentive to create the JCOP Framework package was to facilitate the development of the control system in CERN experiments. It consists of a set of instructions, parts and tools designed to facilitate the user in the implementation of automatic control applications. The Framework instructions define a convention-based name for Datapoints, the functions and files of WinCC, and also cover the look and feel of the control system's graphical interfaces. Therefore, JCOP provides the user with an easy-to-use interface for composing their system and offering common features across a range of time and labor saving systems. As shown in Fig. 3.6 JCOPFw occupies the first level of the hierarchy associated with hardware.
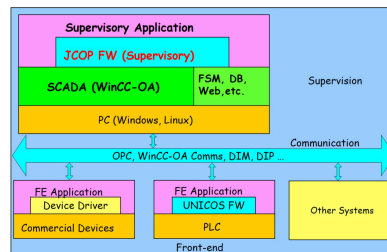
Figure 3.6: The system architecture and the location of JCOPFw in the core of DCS.

Some of the key tools of the JCOP Framework are:

- Installation Component: Necessary for the installation of the various components, the removal or renewal of the existing components and the supervision of the operation of the various components. Installation of this component is required to install the various components.

- Core Component: It provides the basic functions of various components such as configuration, hierarchy, hardware connectivity and alerts.

- Access Control Component: Necessary tool for controlling and accessing users.

- CAEN Power Supplies Component: Allows WinCC to connect to CAEN high-voltage power supplies via an OPC server and their supply channels.

- Configuration Database: Required for storing and retrieving control system data in an Oracle external database to automate the handling of configuration data required at runtime.

- Trending Tool: It allows the graphical representation of DPEs value differences by generating graphs.

The Fig. 3.7 depicts panel for managing components. The partial approach followed by the Framework promotes standardization within control applications and allows code reuse, significantly reducing development and maintenance efforts.

3.6 Finite State Machine (FSM)

Representation of all probe controls by a finite state machine (FSM) is essential for homogeneous control of a heterogeneous collection of FE probe systems. Proposals for a system behavior model consisting of a number of finite states, transitions between states, and actions. The mechanism adopted to model subsystem detectors in LHC is to use a parent/child hierarchical structure. The structure consists of three types of nodes:

- Device Units
- Logical Units
- Control Units
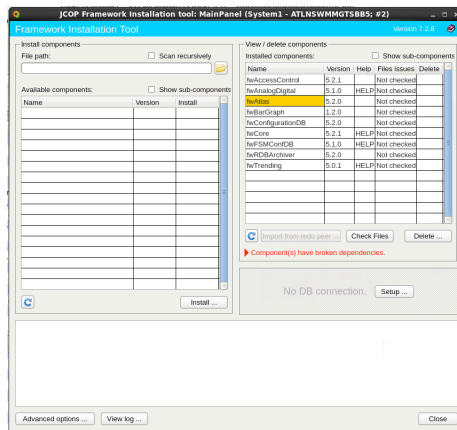
Figure 3.7: The panel to install components of the JCOPFw.

Device units (DU) model specific pieces of equipment that correspond to them and allow monitoring and control of situations derived from hardware values. The values derived from their parents are translated into values for setting the device and determine the status of the devices. Control Units (CU) control all elements that are lower in the hierarchy than these and may not be device interfaces but can contain device units as children and control them. Finally, logic units (LU) control DU and have CU as parents. The summary of the hierarchical structure of FSM is illustrated in Fig. 3.8, where an example of the FSM hierarchy is given.
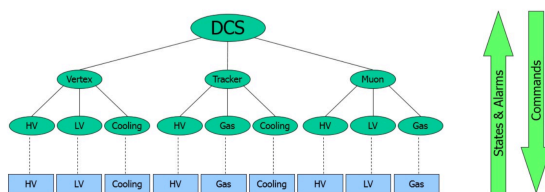
Figure 3.8: Modeling control system using FSM.

Chapter 4

Gas Tightness Station

This chapter describes the experimental setup and develops the automated Gas Tightness Station system to measure gas leakage and QA/QC detectors Micromegas quadruplets which will be performed in the BB5 laboratory of CERN. Experimental reference is made to the experimental device for measuring gas leakage using the Flow Rate Loss (FRL) and Pressure Decay Rate (PDR) methods as well as to the sensors and devices used to operate it. In addition, the design and implementation of the system is analyzed and finally the communication with the sensors is reported through the communication protocol OPC.

4.1 Introduction

The mass production of Micromegas Modules (MM) to upgrade the New Small Wheel (NSW) of the ionic spectrometer of the experiment ATLAS requires the existence of independent quality assurance and quality control Q_A/Q_C. One of the most critical issues of control is to ensure chamber leakage (gas tightness), so gas leakage control is crucial to the smooth operation and maximum performance of Micromegas detectors. As mentioned in the previous chapters, Micromegas detectors are gas detectors whose basic principle is the ionization of the gas when the charged particle passes through the probe's interior and the collection of electrons produced in the amplification region and as a result pulse shaping in reading electronics. In the presence of a gas leak, the Micromegas detector loses its maximum electron propagation capacity in the amplification region due to the presence of air oxygen inside the detector capable of binding the transducer electrons to the generating region of the detector. According to the specifications of NSW, the general rule for the gas leakage rate of the various Micromegas Modules is the leakage rate to be equal to $10^{-5} \times V$ per minute, where V is the volume of each module, so different leakage limits vary due to different volumes.

Figure 4.1: The BB5 building at CERN.

During the production of Micromegas Modules (MM) from January 2018 until the end of 2019, the Q_A/Q_C checks of MM will take place at the specially designed workshop site BB5 of CERN, as shown in Fig. 4.1. At the arrival of the detectors, the primary task is to control the high voltage (HV Test) as well as the gas tightness (Gas Tightness Test). If both checks are successful MM MPs will proceed to the next checks such as checking electronics, link placement, downloading cosmic data and aligning them.

The gas leakage will be examined using two methods, the pressure drop method (PDR) and the flow loss method (FRL) as mentioned in the previous chapter. The complexity of the experimental leakage controller of the two methods requires the creation of an automated control system that enables the processing, control, and recording of data collected by the experimental device sensors. The automatic gas leakage control system was designed in WinCC-OA software, which will be analyzed in detail in the following sections, providing the possibility to measure the gas leakage of gas detectors through a simplified user interface for automation, efficiency and optimization of measurements to determine the gas leakage of MM QPs.

4.2 Experimental Setup at BB5

To perform the gas leakage control of MM QPs an experimental setup is proposed as illustrated in Fig. 4.2, for simultaneous measurement of 4 MM QPs using either the FRL method or the method PDR. The proposed method is that of mass flow loss (Flow Rate Loss (FRL)) where its advantages as outlined in the preceding chapter lie in the simplicity, speed and direct measurement of gas leakage with the only critical factor being pressure internally of the chamber under investigation. According to the method PDR, it is necessary to record the temperature as well as the atmospheric pressure throughout the measurement to re-determine the final result. An important advantage of the method FRL over PDR is that it results in the speed of the method as in less than 1 hour a sufficient conclusion can be drawn for the leakage of the chamber, in contrast to the method PDR. The measurement takes several hours to reach the conclusion, the time at which the final can be underestimated or overestimated by changes in both temperature and atmospheric pressure occurring in that time period.
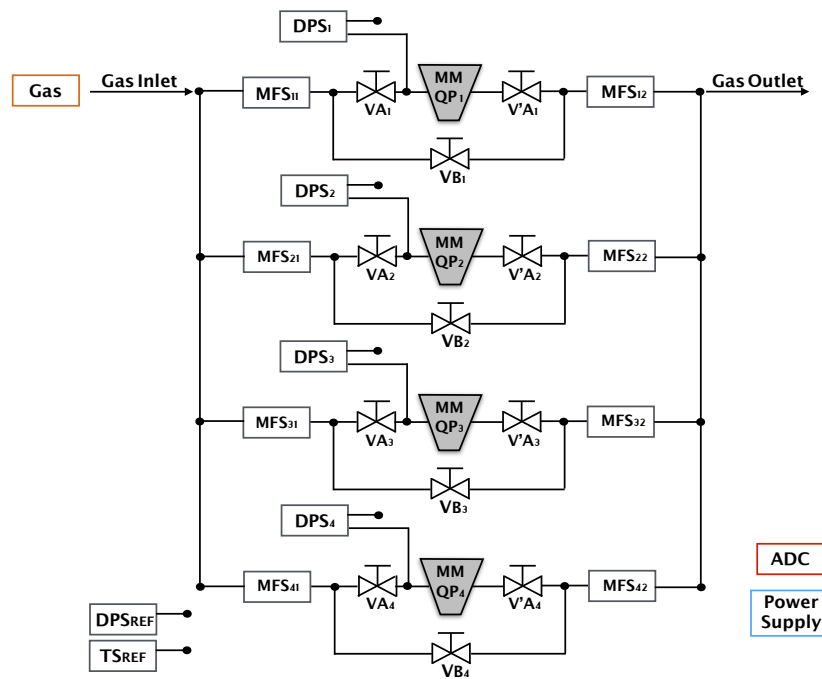
Figure 4.2: The experimental gauge for measuring gas leakage 4 Micromegas QPs in the laboratory BB5 of CERN.

The experimental device for measuring the gas leakage of 4-QPs consists of 4 nodes or else 4 nodes. The layout is an overlay of a node and for simplicity and description can be represented in the layout of Fig. 4.3 in the form of a node where $1 \leq n \leq 4$.
The setup consists of the following items:

- Gas bottle (air or mixture Ar : CO_2)
- 3 high tightness valves, V_{An}, V'_{An} and V_{Bn}
- 2 mass flow sensors, MFS_{n1} and MFS_{n2}
- 2 differential pressure sensors , DPS_n, DPS_{ref}
- 1 temperature sensor, TS_{ref}
- 1 Analog-to-Digital Converter (ADC)
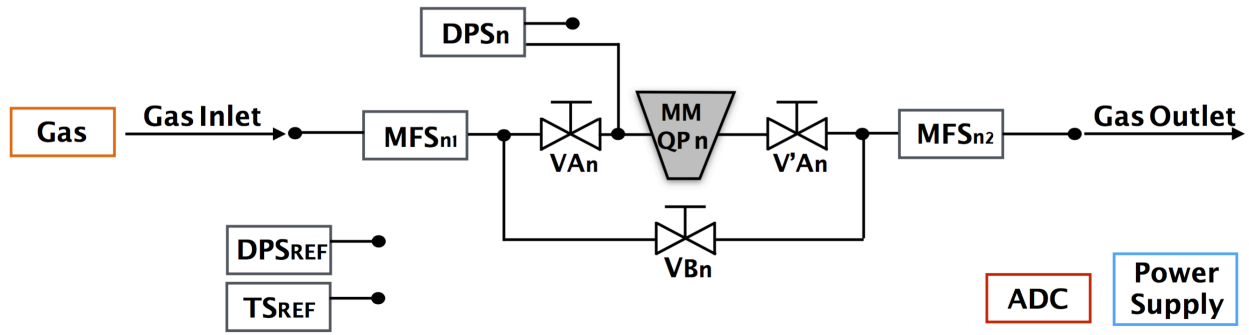
Figure 4.3: The simplified form of the experimental gas leakage measuring device 4 MM QPs in the BB5 laboratory of CERN.

- 1 power Supply

- Micromegas quadruplet

This system can support the measurement of the gas leakage of the detectors MM QP using both methods FRL and PDR with the support of the appropriate sensors respectively. As the gas flows through the device, the various sensors will produce an analog output voltage V_{out} which will be converted by the appropriate coefficient into a mass flow Q or the differential pressure P, this analog the voltage V_{out} will be recorded via a ADC connected to a computer. In the following subsections we will analyze the measurement process with the two methods and how to utilize the device.

4.2.1 Gas leak measurement with FRL method

In the flow loss method FRL [47], the gas leakage rate from the detector MM QP is expressed by the difference in flow loss between the inlet and outlet chamber gas pressure equals 3 mbar from the following relation:

$$Q_L = \frac{1}{b}\left(\Delta V_0^A - \Delta V_0^B\right) \tag{4.1}$$

where b is the conversion factor of the analogue output signal of the probe to mass flow, ΔV_0^A is the differential analog signal of class A and ΔV_0^B is the class B differential analog signal. Branch A is the gauge of the gas leakage of the chamber while Branch B is the gauge of ter/offset of the two sensors. The method of measuring the proportional voltage of branches A and B will then be analyzed.

Measurement of ΔV_0^B

The primary step before measuring the ter of the sensors is to check the flow pressure equal to 3 mbar using the differential pressure sensor DPS_n.

The sensors ter are measured by bypassing the chamber MM QP n and passing the gas only through the two mass flow sensors, MFS_{n1} and MFS_{n2}, by closing the valves V_{An}, V'_{An}, and opening the valve V_{Bn}. As illustrated in Fig. 4.15, this procedure allows the gas to pass through the sensors and bypass the chamber MM QP n. By stabilizing the flow, the differential signal ΔV_0^B is recorded.
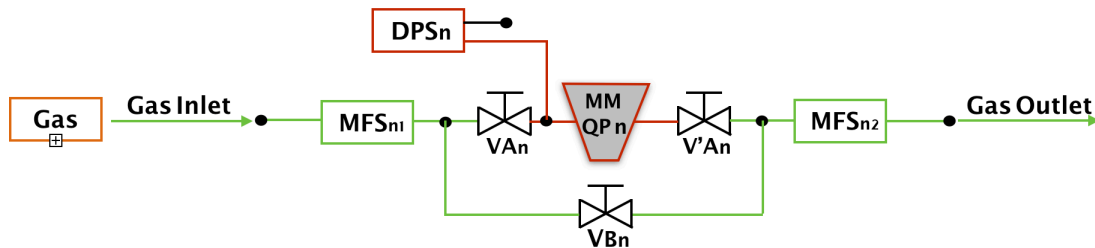
Figure 4.4: The measurement of the tare branch of the device sensors.

Measurement of ΔV_0^A

The leakage of the chamber MM QP n is measured by bypassing Class B and passing the gas only through the two mass flow sensors, MFS_{n1} and MFS_{n2}, and the chamber by opening the valves V_{An}, V'_{An}, and closing the valve V_{Bn}. As illustrated in Fig. 4.24, this procedure allows the gas to pass through the sensors and the chamber MM QP n. By stabilizing the flow, the differential signal ΔV_0^A is recorded.
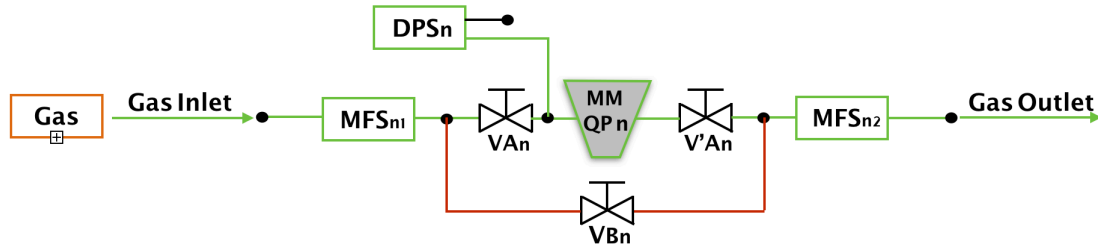
Figure 4.5: The leakage measurement of MM QP n of the device.

4.2.2   Gas leak measurement with PDR method

Measuring the leakage rate using the PDR method first requires the chamber MM QP n to be supplied with a pressure gas such as 5 mbar, by activating the valves V_{An}, V'_{An} and valve closure V_{Bn} that does not affect our layout, as illustrated in Fig. 4.6. It then takes time for the so-called flashing of the detector and its complete filling with gas. The achievement of flushing is reflected in the stabilization of the output flow signal by the sensor MFS_{n2}.
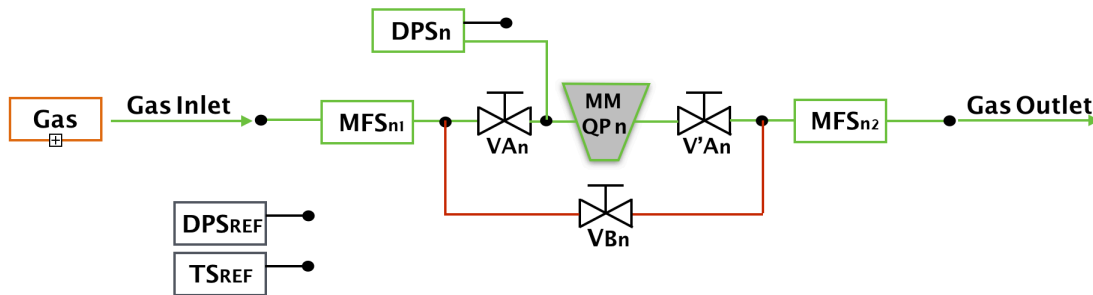
Figure 4.6: Filling of MM QP n with a specified pressure gas.

From the moment of stabilization, the next step is to isolate the chamber MM QP n by closing the valves V_{An}, V'_{An} and recording the pressure drop through the sensor DPS_n as well as atmospheric pressure through the sensor DPS_{ref} and ambient temperature TS_{ref}, as illustrated in Fig. ??.
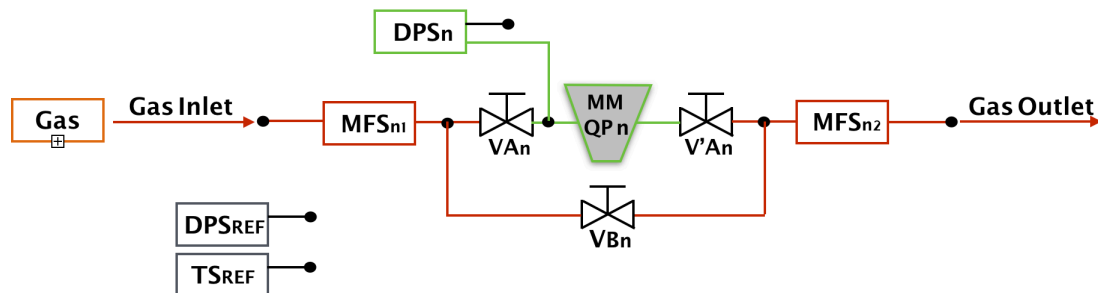
Figure 4.7: Isolation of MM QP n to measure pressure drop.

4.3   Gas Tightness Station at BB5

The design of the Gas Tightness Station has completed the experimental gauge of gas leakage in the BB5 laboratory of CERN. The final layout of the measurements will take the form of Fig. 4.8, where the gas flow through the gas mixture bottle Ar : CO7 is traced through a flow regulator and then enters 4 branches (nodes). Inside a node it enters the input flow sensor MFS_{in}. The gas is then branched into the leakage and bypass branches which are regulated by high-tightness valves. On entering the leakage branch, the gas enters the pressure sensor and then into MM QP where it exits, ending in the outlet flow sensor MFS_{out}. At the same time, atmospheric pressure and temperature values are recorded through the sensors DPS_{ref} and TS_{ref}. All sensors generate an analog voltage that ends in FieldPoint and digitizes the data. Finally, the data is transferred to the computer via Ethernet and through the communication protocol OPC the data is checked, recorded and analyzed through the Gas Tightness Station.
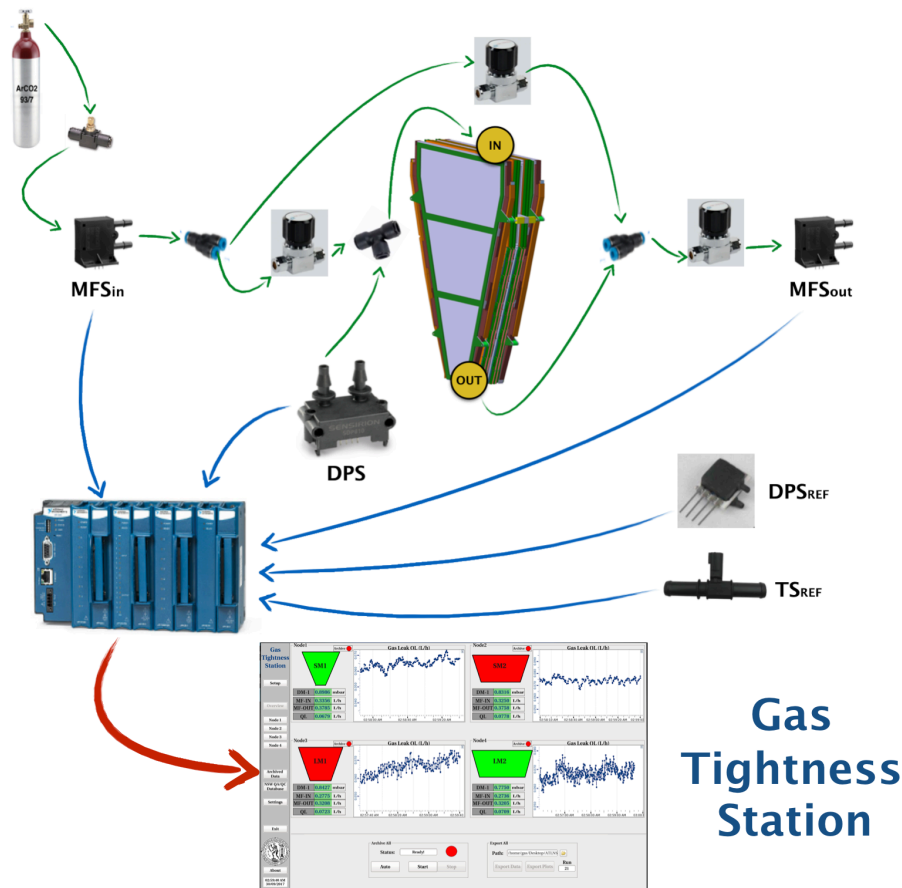
Figure 4.8: The final version of the MM QP gas leakage control system in BB5.

4.4   Gas Tightness Station operation principles

This section is the step-by-step guide to measuring gas leakage using Gas Tightness Station. Extensive reference is made to the steps that the user must perform to measure the MM QP leakage using the FRL and PDR methods using Gas Tightness Station.

4.4.1   Start

The user starts project ATLNSWMMGTSBB5 through the Project Administrator of WinCC by selecting the project and pressing the Start Project button. At the start of the project it will open the Console with all the Managers necessary for its proper operation as well as the logviewer to investigate various errors. It will automatically launch the manager which includes the User Interface of Gas Tightness Station and the UI of GTS displayed as depicted in Fig. 4.9. It is the first contact of the user with GTS the possibilities of the various options he observes will be described in detail in the following subsections.
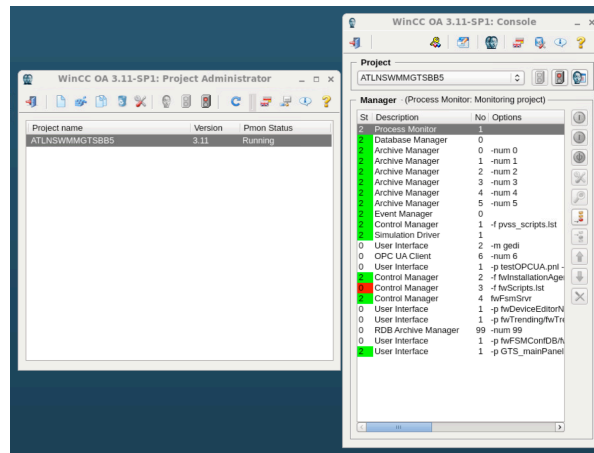
Figure 4.9: Starting Gas Tightness Station via Project Administrator of WinCC.

4.4.2 Check connectivity of FieldPoint and sensors

The primary step in performing gas leakage measurements of the detectors MM QP is the proper operation of the sensors and their connectivity to FieldPoint and then to the computer and system GTS. Therefore, it was designed through GTS to allow connectivity to be controlled by the Settings button in the left column of the original panel, as shown in Fig. 4.9. By pressing the Settings button the user enters a new environment that includes a multitude of options. To check the connectivity of the sensors and FieldPoint the FieldPoint Settings box is designed with 2 buttons, Enable/Disable Module and OPC DA Client Communication.
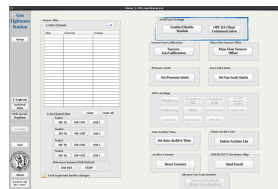
Figure 4.10: Check for connectivity between FieldPoint, sensor and GTS.

Initially, the user presses the button marked Enable/Disable Module in order to enable the Module cFP-CB-1 that he has connected to FieldPoint. A new window opens, as illustrated in Fig. 4.11, where the user switches Modules on specific FieldPoint locations with the On/Off switch. In our case, we activated the 2 Modules we had connected to the FieldPoint module. After completing the Modules
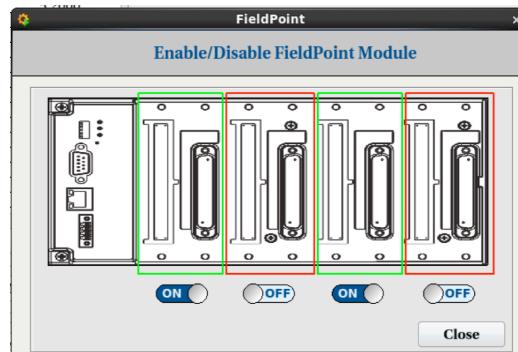
Figure 4.11: Enable or disable Modules cFP-CB-1 mounted on FieldPoint via the Enable/Disable Module button of Settings Tab.

activation, the user presses the Close button and returns to the previous area, in particular to Tab Settings of Fig. 4.10.
Then the connectivity of the sensors to the respective Module must be checked. This is done by selecting the OPC DA Client Communication button where a new window opens as shown in Fig. 4.12. In this window (Fig. 4.12), the user controls the analog input
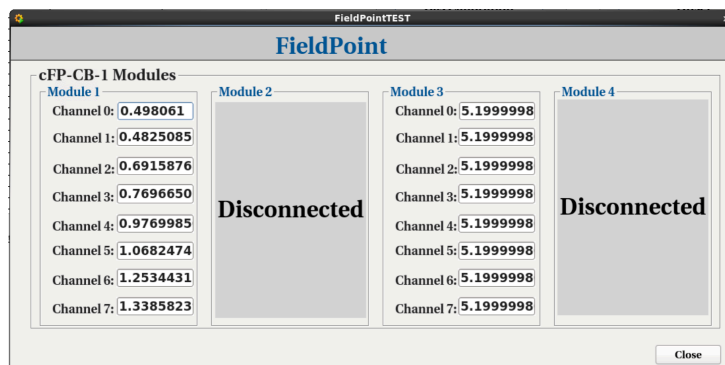
Figure 4.12: Checking the connectivity of Modules cFP-CB-1 with FieldPoint.

voltage of the 8 channels of modules that are connected to FieldPoint. By controlling the voltage in each channel it can check the correct connectivity to the corresponding Module channel as values are updated in real time.

If there is no connectivity and all Modules appear as Disconnected , this is due to incorrect connection to OPC DA Client. The user should check 3 things if the correct connection is not achieved:

- Checking the correct power supply of the FieldPoint
- Check the connection status of FiedPoint to the computer via Ethernet cable
- Check the status of the OPCFIELDPOINT project which is install inside the Windows Virtual Machine

If all 3 queries have been properly verified then communication with FieldPoint will be achieved and channel voltage values of Modules will be automatically updated. If the voltage values are not as expected, the user should check the sensor supply as well as the correct connection of the sensors to the FieldPoint channels as discussed in the previous chapter.

4.4.3 Mapping FieldPoint's channels with sensors

After successfully connecting the sensors to FieldPoint and communicating properly with GTS, a second step is to pair the Modules channels with the sensors. This is achieved through the Sensor Alias box in the Settings Tab area as shown in Fig. 4.13. In addition, the user with the Refresh button is now able to see in the table all available channels of the Refresh button he has activated. The first column is the alias of the channel, which is the sensor assignment to the second column channel, and the third column shows the voltage value of the corresponding channel. The user first selects the lock to enable the system with the buttons below the panel the
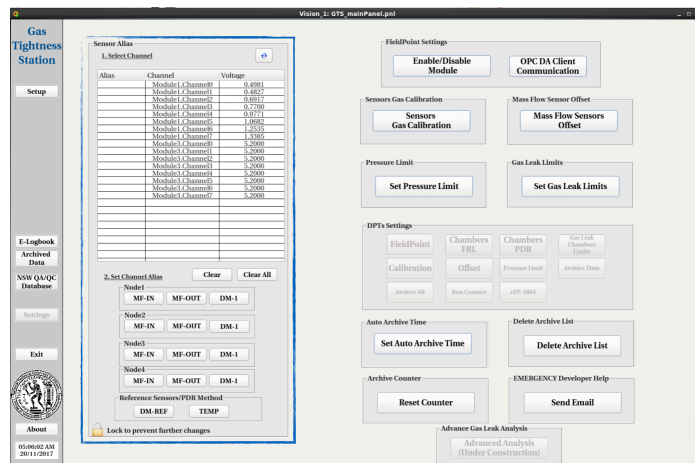
Figure 4.13: Assign the sensors to the FieldPoint's channels.

ability to match the inlet and outlet mass flow sensors (MFS), the pressure sensors (DM -1) for each node of the experimental device as well as the channels corresponding to the barometric pressure sensor (DM-REF) and the ambient temperature sensor (TEMP). Upon completion of the assignment, as shown in Fig. 4.14, the user presses the lock to lock their options and not alter the course of use of

the program. In addition, the system is designed in such a way as to memorize this assignment and not need this setting whenever the user wishes to make a measurement. In addition, this assignment is not foreseen to be reset by the user as the experimental setup's sensors in BB5 will determine both their location and their correspondence with the FieldPoint channels.
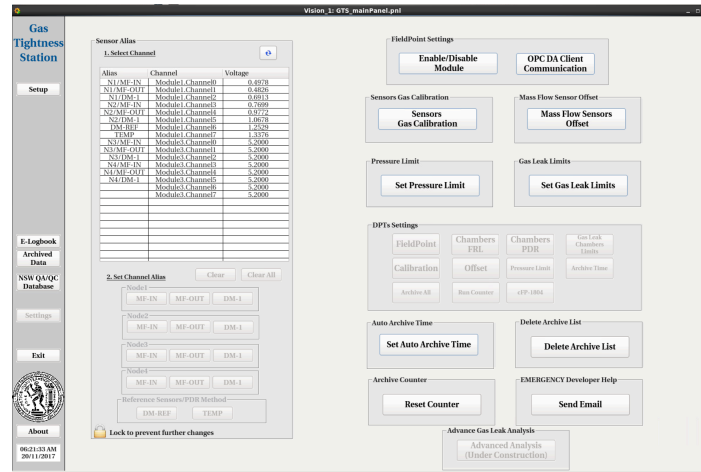
Figure 4.14: Complete the sensor assignment to the FieldPoint channels.

4.4.4 Specifying the offset of the sensors

As mentioned in this chapter, the input and output mass flow sensors, MFS_{IN} and MFS_{OUT}, show some variation of some mV for this it is necessary to measure the offset/tare of the sensor pairs of each node. To perform the measurement of the offset of the sensors we adjust the valves so that the gas bypasses the chamber MM QP as shown in Fig. 4.15. The offset can be measured via the GTS, in
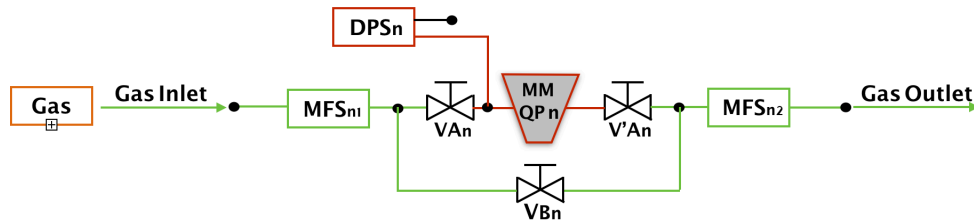
Figure 4.15: Measurement of offset of the input and output mass flow sensors, MFS_{IN} and MFS_{OUT} of the experimental device.

particular the Mass Flow Sensors Offset button in the Tab Settings area and in the Mass Flow Sensor Offset as shown in Fig. 4.16. Selecting this button gives the user a new window as shown in Fig. 4.17. Through it, the user in real time can control the proportional voltage of the input and output flow sensors for each node and their difference through the DV frame. In the available boxes on the right, the user specifies offset in units of mV for each node. It should be noted that the voltages reported for the sensors for each node are the statistical average of 60 measurements per second. The determination of offset can be performed for the first time when measuring the experimental device. However, it should be noted that if the test MM QP has a very low leakage therefore some tens of mV voltage differential signal, the offset should be set equal to 0 and study the behavior of offset in order to be removed after the result of the leak. Once the offset setting for each node is set, the user presses the Save Offsets button to save their settings. It should be emphasized again that if the user wants to measure or restart the system there is no need to reset the offset because the values are stored permanently until the user is reset.

4.4.5 Sensors Calibration

One of the most important steps is to calibrate all the sensors of the experimental device. That is, the transformation of the proportional output order of the flow, pressure and temperature sensors must be determined for each node separately and for each type of gas to be used as air and mixture Ar : CO_2. The calibration of the sensors will be done by the specifications set by the manufacturers as well as by artificial leakage using a medical needle as described in Chapter 5 as depicted in Fig. 4.18. Without the proper calibration of the
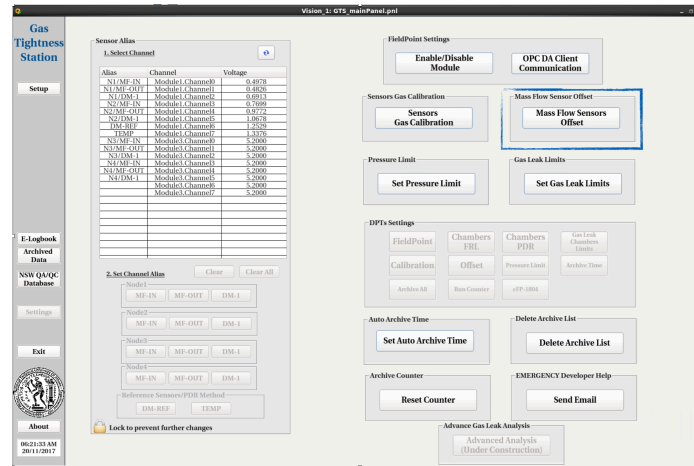
Figure 4.16: Measurement of offset of the input and output mass flow sensors, MFS$_{IN}$ and MFS$_{OUT}$ of the experimental device.
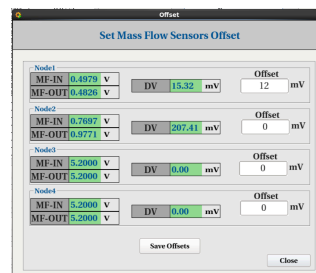
Figure 4.17: Measurement of offset of the input and output mass flow sensors, MFS$_{IN}$ and MFS$_{OUT}$ of the experimental device.

sensors, the flow or pressure values we produce will be incorrect as a result of the MM QP leakage effect.

Through the GTS it is possible to calibrate the sensors by introducing the proportional output voltage conversion ratio to the correct value of the flow sensor measurement in L/h, pressure in mbar and temperature in C. This adjustment is made via theSensors Gas Calibration button located in the Tab Settings area as shown in Fig. 4.19 below. When you press the button, a new window appears as shown in Fig. 4.20. The user through this window has the ability to calibrate the sensors. It consists of 4 frames, each for a node of the layout. The user first determines the conversion ratio of the mass flow sensors for 3 gas types, which are air, argon and mixture Ar : CO2. On the right it has the ability to introduce the primary equations resulting from the calibration of the pressure sensor, barometric pressure and temperature. By entering the formulas, the user is ready to press the Save Calibration button to save the settings he has made. It should be noted that calibration of the system and parameter setting can only be done before or after some measurement, and calibration is required the first time the sensors are installed in the experimental setup of BB5.
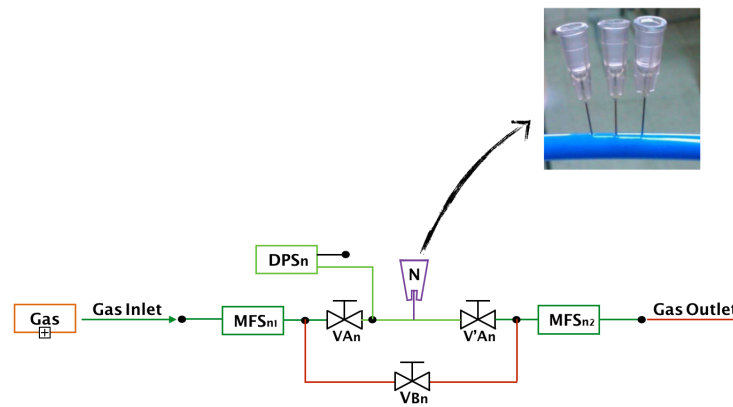
Figure 4.18: Experimental device for mass flow sensor calibration using hypodermic medical needles.
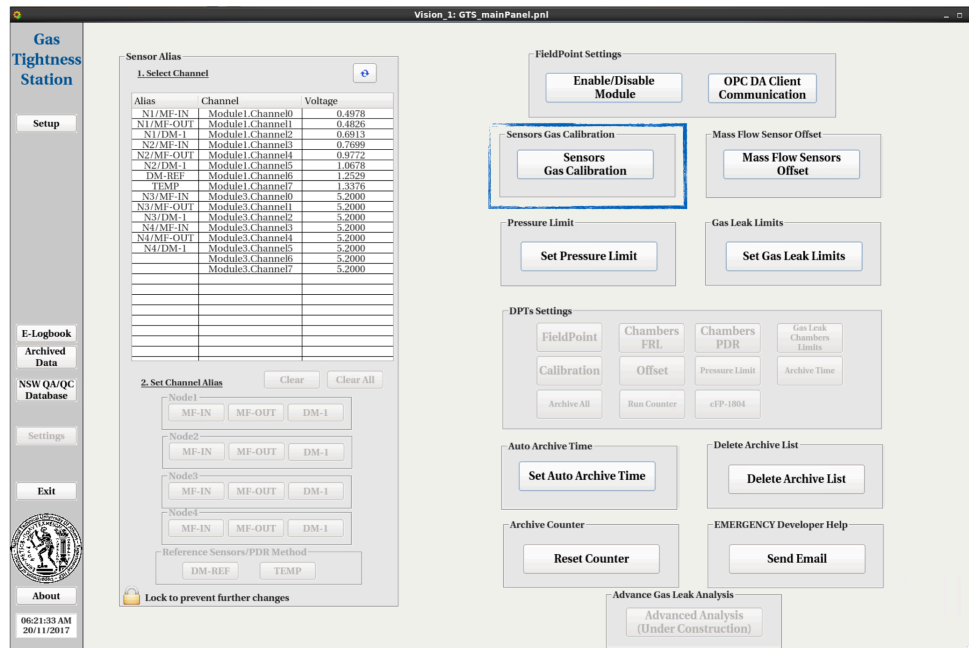
Figure 4.19: Calibration of the sensors

4.4.6   Determination of gas leak limits of the MM QPs

From the previous chapter, the detectors MM QP to be examined in BB5 must meet specific gas leakage limits set for each type MM QP (LM1, LM2 , SM1, SM2). The GTS enables real-time monitoring of the gas leakage of the detectors so that the user can determine the state of the detector directly by alerting him through a special alarm. For control, the user via GTS has the option to enter the MM QP gas leakage limits through the Set Gas Leak Limits button in the Gas Leak Limits in Tab Settings, as shown in Fig. 4.21 below.

At the push of a button, a new window appears to the user as illustrated in Fig. 4.22. Through the window, the user sets the gas leak limits to L/h for each type of detector MM QP where the Save Limits button saves the settings. Additionally, the Default button automatically fills in the suggested leakage limits.
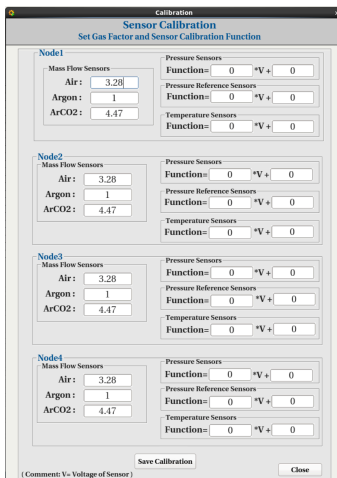
Figure 4.20: Experimental calibration calibration window with the introduction of coefficients and conversion relationships for the different sensors for different gases.
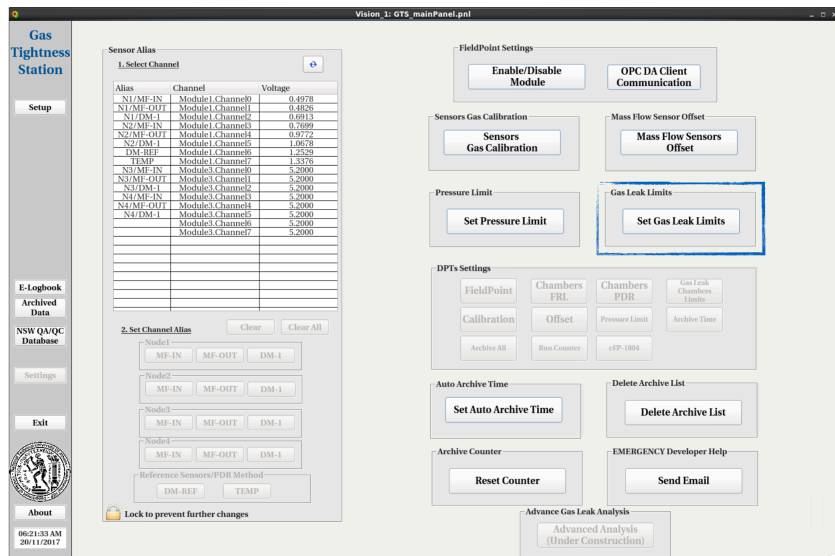
Figure 4.21: Determination of gas leakage limits for each type of detector MM QP through Tab Settings of GTS.

4.4.7 Determination of the gas pressure

To measure gas leakage using the method FRL it is necessary to adjust the pressure to the specified limit of 3 mbar, a different pressure value would lead to an underestimation or overstatement of the gas leak. Thus, for the proper measurement of gas leakage, it is essential to stabilize the pressure of the sensor DMS at the specified value as well as to control this value in real time by alerting the user alarm in case change the pressure beyond this value. The user can adjust the pressure limit of all node of the device with some delay by entering the value through the Set Pressure Limit button located in the Pressure Limit box of Settings Tab as shown in Fig. 4.23.
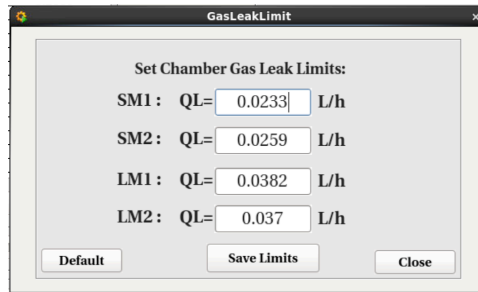
Figure 4.22: Determination of gas leakage limits for each type of detector MM QP.
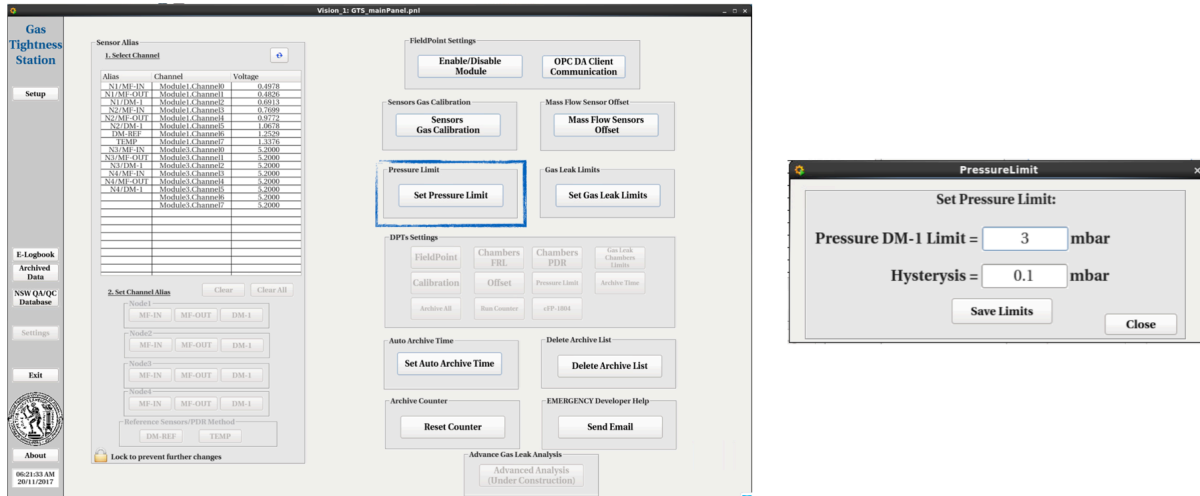
Figure 4.23: Determination of pressure limits through Tab Settings of GTS.

4.4.8   Gas leak measurement with FRL method

By completing the steps mentioned in the previous sections, the user is now able to measure the gas leak using the FRL method. The first step is to adjust the valves so that the gas enters the leakage branch and yes it passes through the detector MM QP for each node as shown in Fig. 4.24. The next step is to set up the experimental layout through the GTS panel. The user prepares
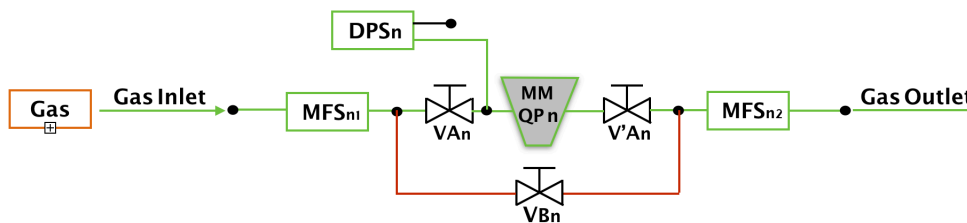
Figure 4.24: Valve adjustment to measure gas leakage of MM QP.

the system through the Tab Setup where he/she is given the choice between FRL and PDR method. Pressing the FRL method makes it possible to select the gas to be used for the measurement, the options given are for air, argon and Ar : CO2 as shown in Fig. 4.25. By selecting the gas, the user FRL is made visible to the user comprising 4 subframes each for a node of the ex-
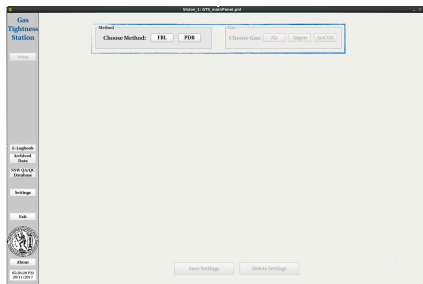
Figure 4.25: Choice of method and gas to be used to measure leakage of MM QP.

perimental layout, which include the information of each node respectively.
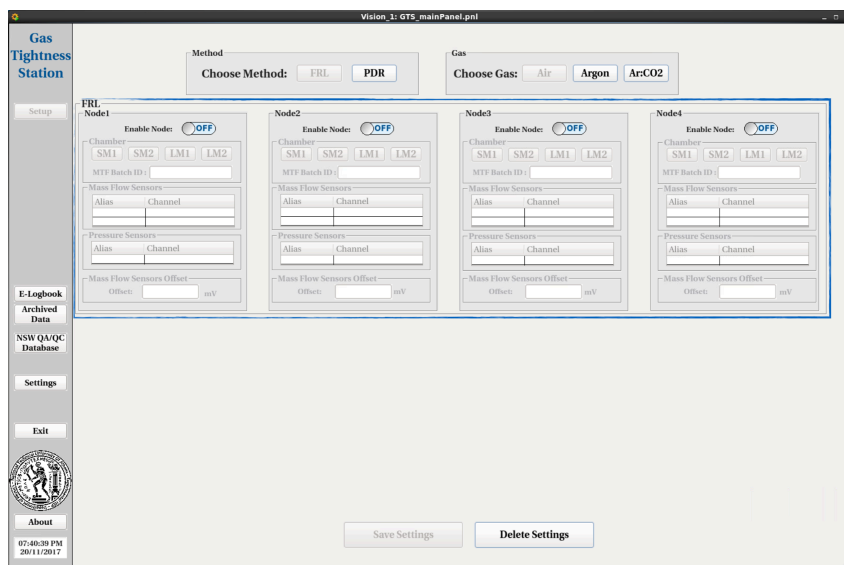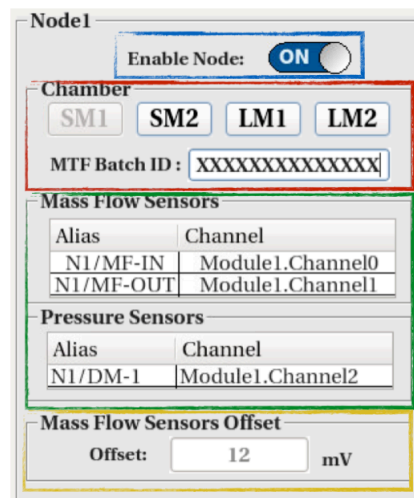
Figure 4.26: Configure the settings for each node to measure gas leakage using the FRL method.

The configuration of a node method FRL is divided into the following frames:

- Blue frame: Enable the corresponding node.

- Red frame: Select the type of MM QP found in the corresponding node and enter the 14-digit code MTF Batch ID that is the identifier of the detector.

- Green frame: Includes information on mass flow sensors MFS and pressure DPS for channels with FieldPoint. Sensor panels are automatically completed by activating each node once the mapping described in previous subsection has been completed.

- Yellow frame: Returns the value of offset/tare of the 2 sensors MFS of the corresponding node, a value that was set by the procedure described in previous section.

After completing the nodes setting for the available detectors MM QP under review, the user is ready to press the Save Settings button to start the final setting of the automatic control system for the number of nodes selected, as shown in Fig. 4.27. It should be noted that the fact that GTS enables the measurement of 1 to 4 node simultaneously and depends on the user activating nodes. The Delete Settings button deletes the settings from a pre-set setting to restart the creation of a new experimental layout.
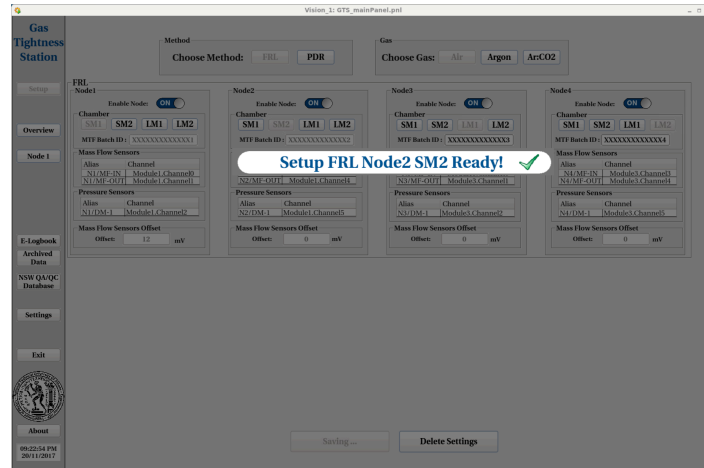
Figure 4.27: Automatically configure each node by pressing the Save Settings button and saving user-set settings.

Upon completion of the nodes setup, the user will notice that the Overview and Node 1-Node 4 buttons on the right side of the gray bar (depending on the number of nodes selected). Through these buttons the user can have a general overview of the experimental layout with simultaneous control of the 4 4-Node Mode he has selected (Overview button) as well as detailed control of each node (1-Node Mode) and hence each MM QP separately (Node X button, where X = 1-4), as shown in Fig. 4.28. The functions of the 2 types of buttons will be discussed in greater detail in the following subsections.
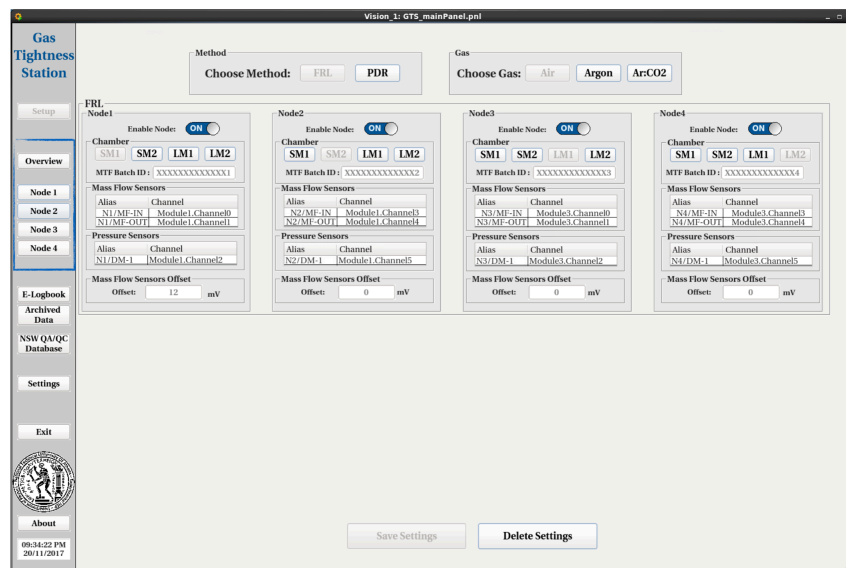
Figure 4.28: The control options of nodes, 1-Node Mode and 4-Node Overview Mode.

4.4.9   1-Node Mode

The user by pressing one of the Node X buttons enters the 1-Node control, that is, the control and recording of the data of all the sensors of a Node. At the moment the button is pressed, a new user interface appears, as shown in Fig. 4.29, which contains all the information for each node and is divided into 4 information boxes:

- Checking the values of node sensors and checking leakage directly through alarm

- Information on the leak limit, BatchID of MM QP and the method and gas of the measurement

- Graphical representation of sensor behavior and leakage over time

- Recording and storing sensor values in data or graph formats
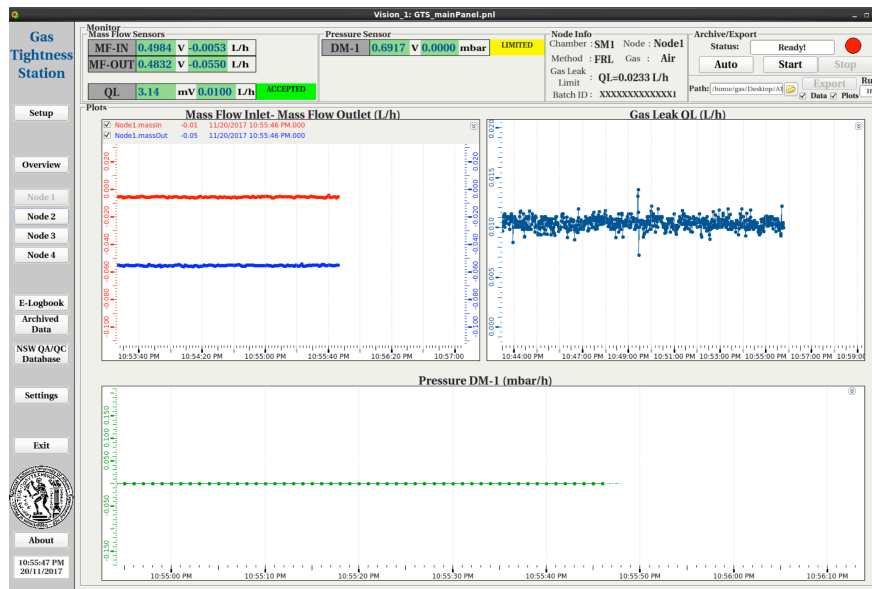
Figure 4.29: Check the sensors and MM QP of each node with 1-Node Mode.

Monitor

Through the Monitor box, as shown in Fig. 4.30, the user can monitor in real time the value of the mass flow sensor (MFS) in and out of units V and L/h, as well as the leakage Q_L of MM QP in the same units where the leakage is actually the difference between the sensor MF-OUT with MF-IN. The user has the ability to monitor in real time the value of the pressure sensor DM in V and mbar units. In addition, alarm enables the user to be notified whether the detector is over or within the leakage threshold as well as the pressure inside the detector set in accordance with the procedure described in previous sections. All sensor values listed are the average of 60 measurements per second recorded by FieldPoint.
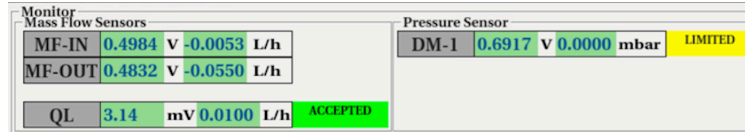
Figure 4.30: Checking the values of the sensors and the MM QP of each node with 1-Node Mode in the FRL method.

Plots

It enables the user to monitor the behavior of the various sensors over time through the plots frame, in particular it can monitor the inlet and outlet mass flow sensor, the gas leakage of the detector as well as the pressure inside of node, as shown in Fig. 4.31.
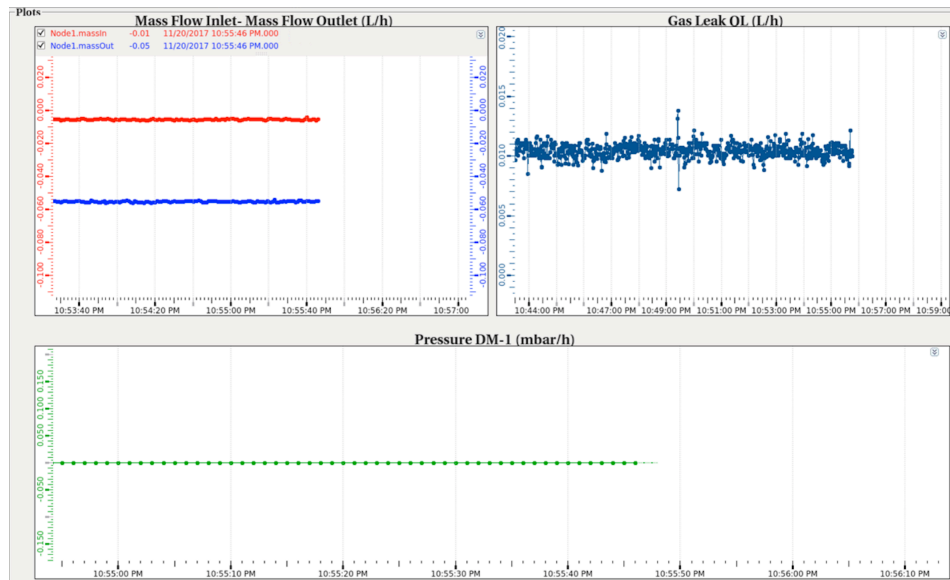
Figure 4.31: Check the sensors and MM QP of each node with 1-Node Mode in the FRL method.

Node Info
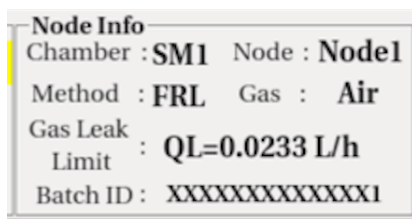
This box provides the user with information about the type, leakage limits and MTF Batch ID of the detector MM QP as well as what node is present and what gas or method is used to measure of the gas leak, as illustrated in the Figure.

Archive/Export

Through this frame, the user is able to store and export node's sensor data. As the user initiates the data logging process using the Start button, the Status box changes to Archiving mode while the circle shows the status of the logging system or not. With the Stop button,
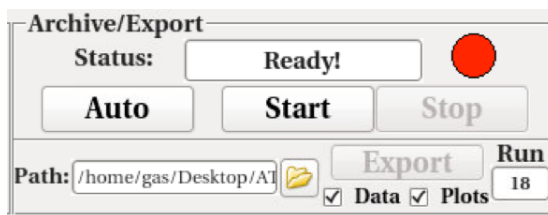
Figure 4.32: Frame for storing and extracting experimental data sensor data.

the user stops recording the data and the Export button becomes available to export the data. The Auto button is a user-defined time measurement that can be set by the user through the Tab Setting and the Auto Archive Time button where it sets the measurement time Auto in minutes, as shown in Fig. 4.33. After the specified time in Auto or when the user presses Stop, the data logging stops
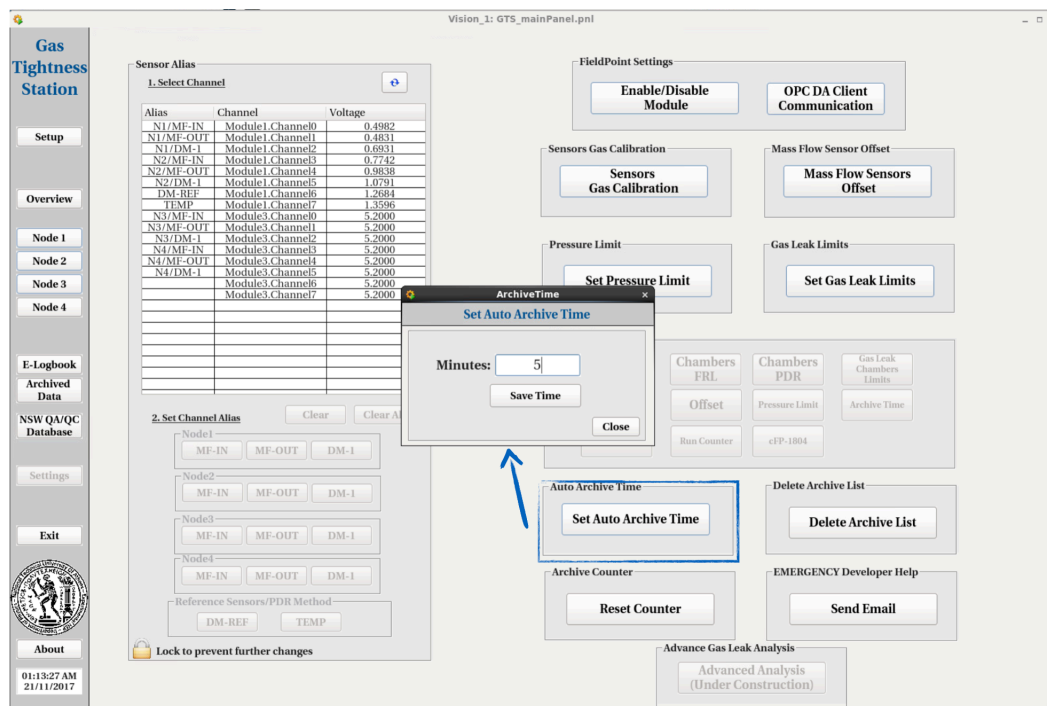
Figure 4.33: Setting the time for automated data logging.

and the Export button becomes available to the user. In the Path box via the folder icon it can specify the location on the computer where the data will be exported. GTS enables exporting data to data or plots either to 2. When the user selects the export format data, an ASCII file is exported named run_X.dat, where X is the number of measurement (Run) in the path specified. The ASCII file that is created has a specific structure and consists of a line that contains the information of node, the type of the detector, the method, the gas, the offset of the sensors as well as the Batch ID of the detector. It then includes a column of measurement time, the input and output mass flow sensor columns L/h, the gas leak in units L/h, and the pressure in units mbar. The second option for the user is to export the data in graphs for easier investigation of the results. The graphs were created using the ROOT Data Analysis Framework [48] of CERN where an algorithm can be run in the background via the shell script and generate the graphs from the data of the detectors. The export file is a png image named run x_plot.png, where X is the number of the measurement (Run), and stored in the path specified by the user. An example of the generated graph file is given below in Fig. 4.35. The graph of the inlet and outlet mass flow sensors, the inlet and outlet flow distribution histograms, the pressure graph and finally the gas leak are produced. In addition, all histograms give the measurement information (Entries), that is, how many seconds the measurement took and the mean of the measurements along with the standard deviation RMS in L/h. Finally, a table is provided that provides the measurement information, such as the type and Batch ID of MM QP, the gas used, the method, the date, the final leak of the detector as well and the measuring pressure.

Figure 4.34: The structure of the export file ASCII with the sensor data and node data measured by the FRL method.
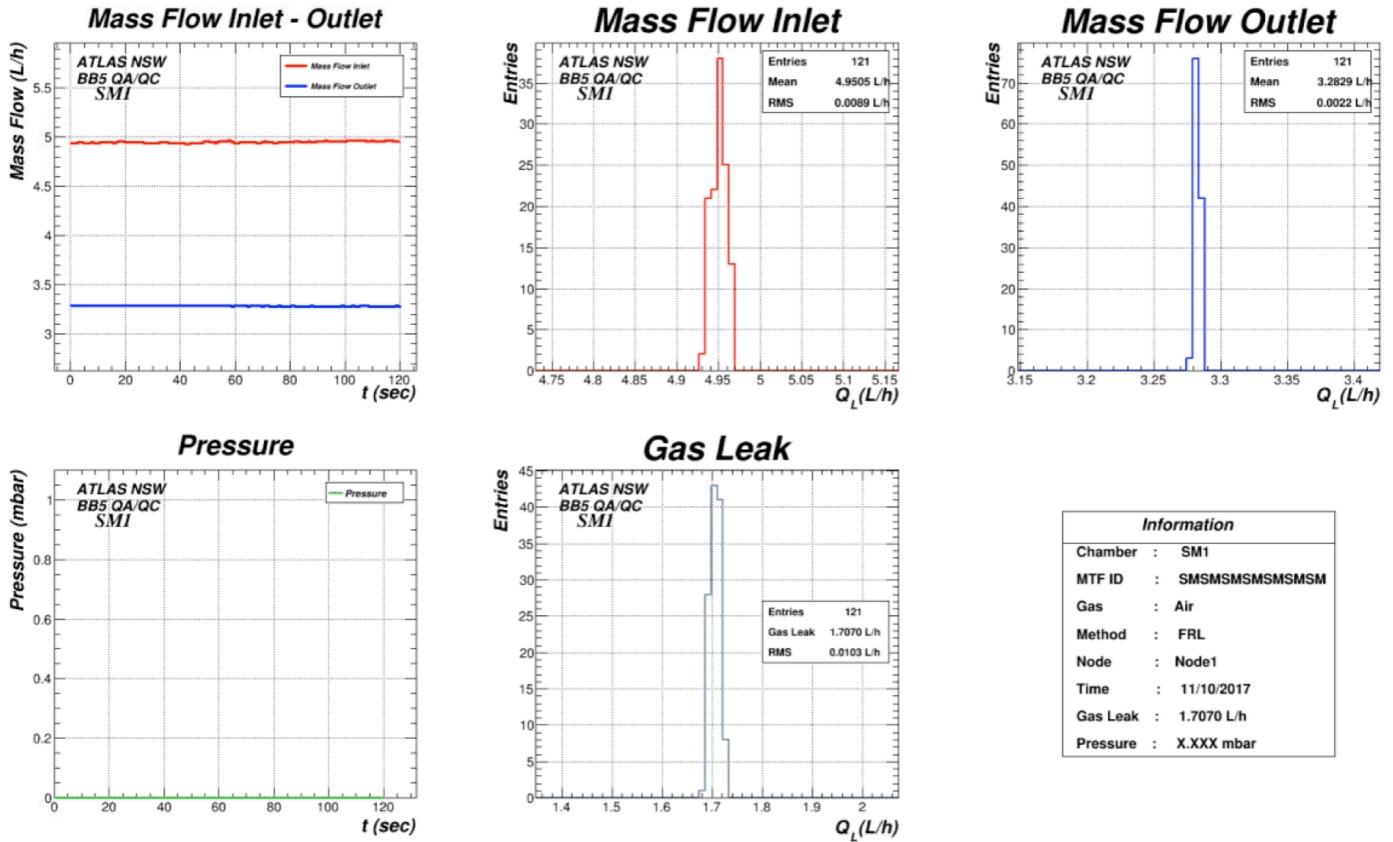
Figure 4.35: The exported plots using the ROOT Data Analysis Framework [48].

4.4.10   4-Node Mode

The user by selecting the Overview button on the left side of GTS has the ability to overview the experimental layout in a common graphical environment. This new environment, as shown in Fig. 4.36, enables the control of gas leakage in all nodes activated by the user. The user can control inlet/outlet flows, pressure and gas leakage simultaneously for all MM MPs available. In addition, a graphical representation of the gas leak is provided to control the leakage over time. The different colors of the detectors shown represent the alert (alarm) whether the detector is within or six of the leakage limits set. Additionally, there is Archiving indicating where the record is node when data is recorded through 1-Node Mode.

Export/Archive All

In the 4-Node Mode control, the user has the ability to archive the sensor's data of all MM QPs simultaneously by pressing the Start or Auto button, where the duration of the auto test is common with that one for the 1-Node Mode. By pressing the Stop button, user has the ability to finish the data acquisition. When, the data acquisition procedure is completed, the Export Data and Export Plots buttons are becoming available, and the user can export the data and plots accordingly. The structure of the ASCII file and the data plot which are produced has exactly the same form with that one that described in the 1-Node Mode, with the difference that the final data contains the 1-Node Mode file for every node, as shown in Fig. 4.34, and also different plot files are produced for the different
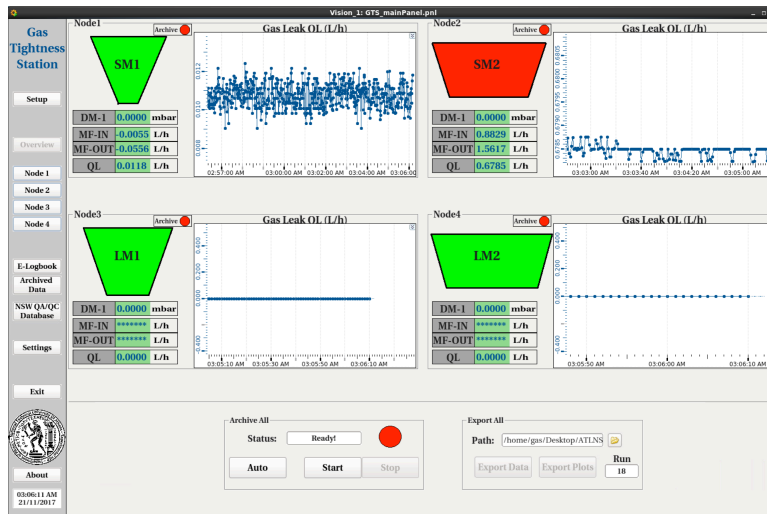
Figure 4.36: Check the sensors and MM QP of each node with 4-Node Mode in the FRL method.

nodes with the same structure of 1-Node Mode, as shown in Fig. 4.35.

4.4.11   Advanced Analysis

As mentioned above, the gas leakage rate is equal to the difference of the mass flow sensor (MFS) differential signal with the offset of these sensors. In the case of a very small gas leak of some mV, it is necessary to study the behavior of the sensors offset by recording the data in the branch offset. In the event of a minor leak, GTS provides detailed leak analysis using the Advanced Analysis button of Tab Settings. To perform the measurement, the user must collect two different sets of measurements with the value offset of the corresponding node equal to 0, one set will consist of the data of the two sensors for the offset of the sensors and a set of measurements by measuring the leakage of MM QP according to the procedure Selecting the two files will provide a detailed analysis of the leak and the end result will consist of a bar chart containing the offset and leak distributions along with the characteristics of the two partitions and the final leakage of the resulting from the difference between these two distributions, as shown in Fig. 4.37.
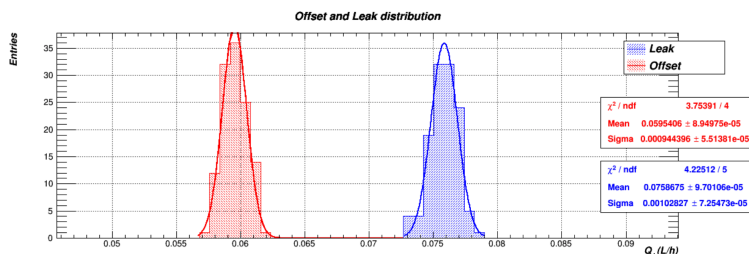
Figure 4.37: Use advanced analysis to determine the gas leakage of MM QP by additionally calculating the offset distribution of mass flow sensors in the FRL method.

4.5 Data storage

4.5.1 NSW QA/QC Database

In addition to storing the measurement data in the local disk of the computer, it is necessary to secure the measurement results in a central Database. For the purpose of validating the results of the QA/QC measurements, ie measuring the leakage of detectors MM QP, the central Logistics Database was built by the University of Freiburg ATLAS _MUON _NSW _MM _LOG. Includes ID (ID) and handling of all NSW equipment such as components and lots regardless of whether it is Micromegas, sTGC or electronic equipment as well as the history of various values that have been saved. Below the central Logistics Database ATLAS_MUON_NSW_MM_LOG are 3 sub databases containing detailed information about Micromegas, sTGC, Electronics and are ATLAS _MUON _NSW _MM _QAQC, ATLAS _MUON _NSW _STGC _QAQC and ATLAS _MUON _NSW _ELEC _QAQC, respectively. The databases include the saved settings as well as the type of measurements, as illustrated in Fig. 4.38 below. In addition, Fig. 4.39 depicts the structure of Database
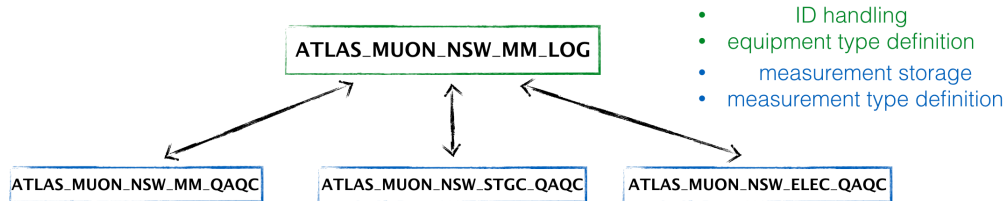
Figure 4.38: The structure of the NSW QA/QC Database.

Logistics (left) and the structure of MM QA/QC (right). The databases consist of several tables, for example MM QA QC consists of central CENTRALMEAS where it contains the list of metrics with result information, exact time and shifter, MEASCOMMENTS which includes the user's comments on the measurement they made, MEASDOCUMENTS which contains the metrics data files where the user can finally add MEASDOCLINK containing the metering link to the files the user added. The structure of the central
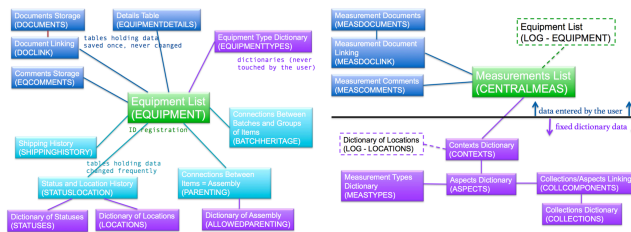
Figure 4.39: The structure of the NSW QA/QC Database.

table CENTRALMEAS is shown in Fig. 4.40 and consists of the column of the line added to the id assigned by Logistics Database, a word for information the measurement, the value of the measurement or the result in the case of QA/QC measurements, the user name and the date of the measurement. To add MM QP gas leakage measurement data, GTS enables the addition of this data through

Figure 4.40: The structure and content of the central table CENTRALMEAS.

the NSW QA / QC Database button, where you press the user enters a new environment designed by the University of Freiburg to connect to the central database, as shown in Fig. 4.41. The user then selects his name in the list of shifters and after pressing the Ok button, the Tab becomes available where by pressing the Load EQ key he typed MTF Batch ID of a MM QP and press Yes after typing
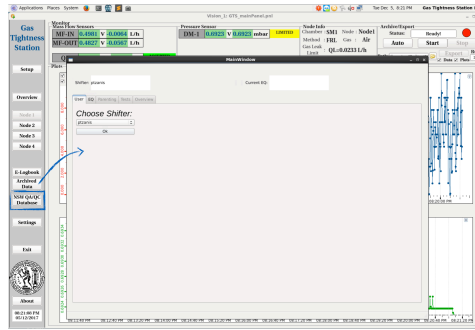
Figure 4.41: User login to Freiburg GUI to store metrics in NSW QA / QC Database.
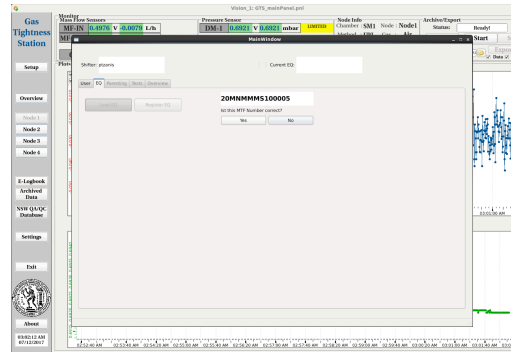
Figure 4.42: Introduction of Batch ID of MM QP to Freiburg GUI.

the correct Batch ID, as shown in Fig. 4.42. Subsequently, Tabs Parenting, Tests, Overview are made available to the user. where the user through Tests can enter measurement data Gas Leak by pressing the Start Test button. In the right box are various instructions for measuring or entering data, as well as the ability for the user to add comments and files to the data and graphs collected during the measurements. By filling in the data, the user, through the Commit Measurement option, validates the measurement in the central database, and it is displayed in the left-hand window of the window as depicted in Fig. 4.43. In addition, the user through the Tab Overview can see a general overview of the metrics he has assigned to the NSW QA/QC DB for the corresponding scanner MM QP and Batch ID .
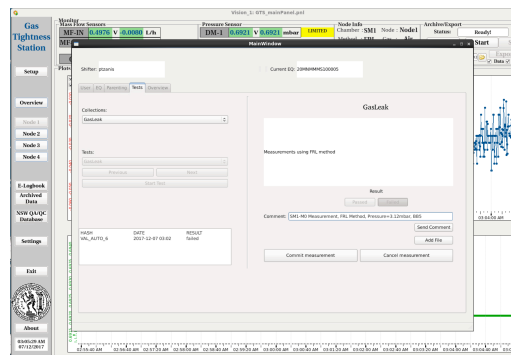
Figure 4.43: Validate data in NSW QA/QC DB via Freiburg GUI.

4.5.2 Data history

GTS makes it possible to search the data history on the local disk of the computer so that the user can refer to the measurements he has made in the past. Through the Archived Data button, the user enters a new graphical environment where he searches by MM QP type or Batch ID which is the identity of each chamber. By selecting both, the conditions of the measurement, such as the method used, the leakage measured, the gas, the measurement time, the offset of the sensors and the Batch, are made visible in the table. Id

of each cell, as shown in Fig. 4.44 below. The user selects the desired line of measurement and presses the Set Export Parameters button to display the measurement information in the various boxes, then the Export Data and Export Plots options are available. the user can store in ASCII and graphs the data collected during the measurement at the site specified through Path in exactly the same way as mentioned in the previous chapters on data extraction. The data being exported is located on the local disk of the computer, however alternative methods of storing and extracting data for data security are necessary.
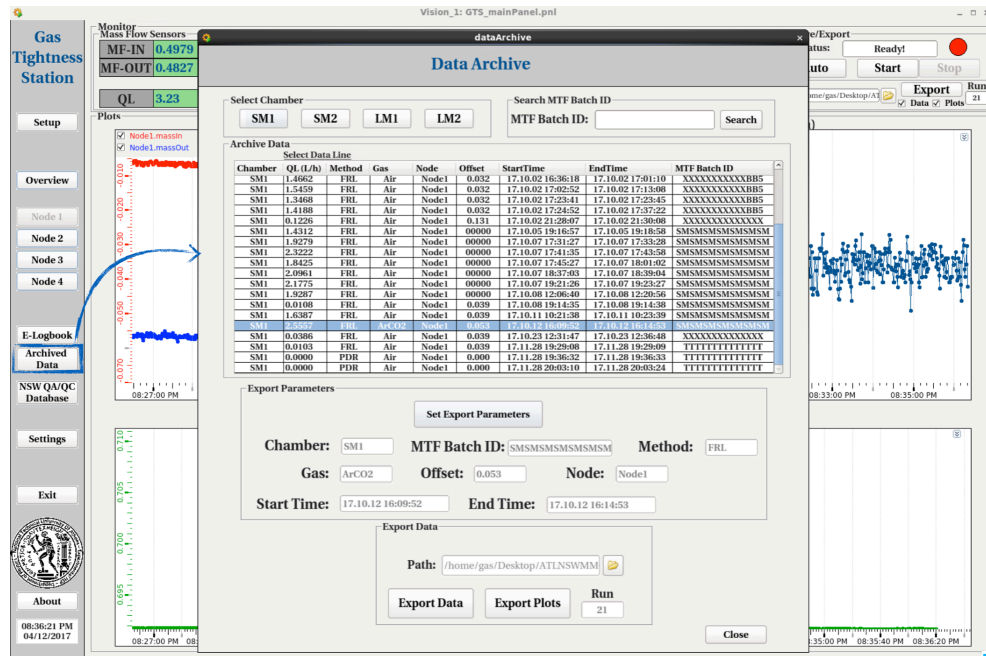
Figure 4.44: History of recording the measurements and extracting the data.

4.5.3 Online data storage

To secure the data of the gas leak detector measurements MM QP the site cern.ch/mmgtslogbookbb5 was developed to be the digital online log for recording and storing data. Through the website, the user will be able to save the measurement data he made in ASCII and graphs, and to add to the table the detailed measurement information as well as the log at the bottom Fig. 4.45. Therefore, it is possible to safely store data and access by users to monitor the results of detector quality control MM QP.

Figure 4.45: Digital calendar website to ensure the security of metrics data as well as accessibility by multiple users.

4.6 Emergency assistance

To ensure the correct operation of GTS and the correct detection of the leak detector threshold measurement MM QP, the user is allowed to contact the GTS operator if necessary to give him the appropriate instructions to continue his measurements. This feature is provided through the Tab Settings and the Send Email button, as shown in Fig. 4.46, where the user writes their name and email as and the comment he wishes to send to his manager GTS to immediately contact the user to resolve the situation he is facing.
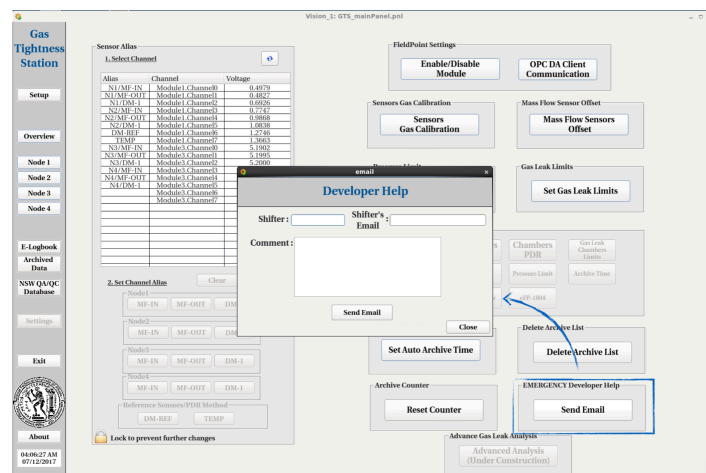
Figure 4.46: Digital calendar website to ensure the security of metrics data as well as accessibility by multiple users.

Chapter 5

High Voltage Station

This chapter describes the experimental setup and the software which developed for the high voltage validation of the Micromegas chambers prior to the installation to the New Small Wheels of the ATLAS experiment. The validation of the chamber is taking place at the BB5 and GIF++ irradiation area of CERN. The HV DCS software is using several common tools from the TestBeamSCS which developed by Paris Moschovakos.

5.1   Introduction

As we have described it the previous chapters, the New Small Wheel will consist of the Micromegas detectors. The operation principle of the Micromegas detectors is the ionization of the gas when a muon particle goes though it. After the production of the electrons due to the ionization, positive high voltage is applied in the cathode in order to collect them. These electrons in principal is the signal or the "pulse" that is producing thought the readout strips where the electronics boards are connected. Thus, for the operation of the Micromegas detector, we must ensure that gas tightness and high voltage operation is perfect in order to achieve 100% performance of the detector. As we have already describe, the gas tightness measurement is performed thought the Gas Tightness Software at BB5 and thus a experimental setup and software is needed to be developed in order to perform the high voltage validation in parallel with the gas tightness measurement. The general idea is to monitor the voltage and current that is applied to the different HV sections of the Micromegas detector thought the CAEN mainframe and the HV boards, an example of these devices is shown in Fig. 5.1.

Figure 5.1: The CAEN mainframe SY4527 and CAEN HV boards A7038 with 32 channels which are commonly used for the Micromegas HV validation.

A micromegas detector is divided into HV sections. and thus the validation procedure is the validation these HV sections. The HV sections number is specific for the type of the chamber. For the Micromegas detectors of the New Small Wheel, there are two types:

- Type 1: These are the SM1/LM1 modules which include 5 PCBs or 40 readout strips and 4 drift channels

63

- Type 2: These are the SM2/LM2 modules which include 3 PCBs or 24 readout strips and 4 drift channels

The 2 Micromegas detector types are shown in the Fig. 5.2. In the below figure, you can determine the different number of PCB per detector type and also the different HV sections with yellow colour and just for an example the L1L1 section is the HV section at the PCB 1, Layer 1 and Left side of a Micromegas detector of Type 1. Thus, the HV validation consists of the validation of all HV sections
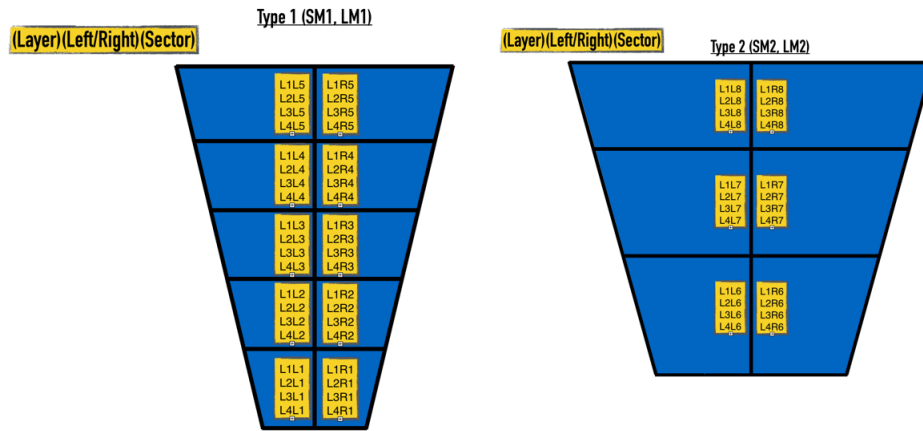
Figure 5.2: The Micromegas high voltage validation experimental setup at BB5.

per module and the experimental setups which developed will be described in the next section.

5.2   Experimental Setup

For the HV validation of the Micromegas (MM) modules, two separate setups developed in different places in order to test the high voltage under different circumstances. The setups are:

- BB5 setup: for the validation of the modules after the reception of the different construction sites
- GIF++ setup: for the validation of the modules under high radiation environment prior to the installation to the hazard ATLAS cavern

The different setups will be described in detail in the next subsections.

5.2.1   BB5

The experimental setup at the BB5 consists of 4 parallel nodes or test stands in order to perform the gas and high voltage validation of the Micromegas detectors in parallel. The experimental setup is shown in the below Fig. 5.3.

Figure 5.3: The Micromegas high voltage validation experimental setup at BB5.

As you can see in the above image, there are 4 parallel nodes and each of these nodes consists of independent HV and gas channels which can work in parallel. In general, the BB5 setup consists of 3 different sub-stations for the HV validation:

- HV Station: 2 CAEN SY4527 Mainframe supplied with 7 A7038STP CAEN boards or 224 HV channels in total
- Gas Station: Each station is supplied with an mass flow, humidity and pressure sensor connected to an Arduino and a Raspberry Pi for the gas monitoring
- Environmental Station: External environmental station for the monitor of the external pressure, humidity and temperature connected to an Arduino.

An overview schematic of the Micromegas high voltage validation experimental setup at BB5 is shown below in Fig 5.4.
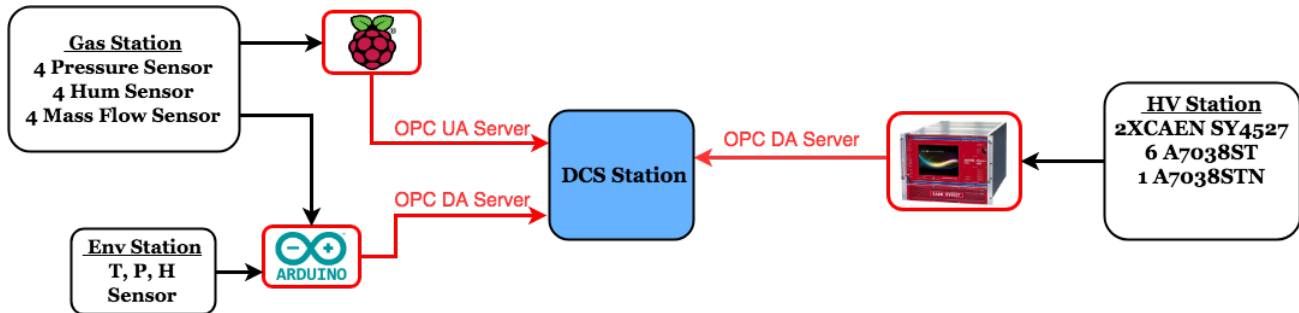
Figure 5.4: The overview schematic of the Micromegas high voltage validation experimental setup at BB5.

5.2.2 GIF++

The experimental setup at the GIF++ irradiation area consists of 4 parallel nodes or test stands in order to perform the high voltage validation of the Micromegas detectors in parallel under high irradiation environment as shown in Fig. 5.3. The GIF++ irradiation area contains a $14\,\mathrm{TBq}$ Cs^{137} source of $662\,\mathrm{keV}$ photons. The source will produce a background gamma field 30 times more intense than at GIF, allowing to accumulate doses equivalent to HL-LHC experimental conditions in a reasonable time. The $100\,\mathrm{m^2}$ GIF++ irradiation bunker has two independent irradiation zones making it possible to test real size detectors, of up to several m2 , as well as a broad range of smaller prototype detectors and electronic components. The photon flux of each irradiation zone will be tuned using a set of Lead filters. Flexible services and infrastructure including electronic racks, gas systems, radiation and environmental monitoring systems, and ample preparation area will allow time effective installation of detectors.
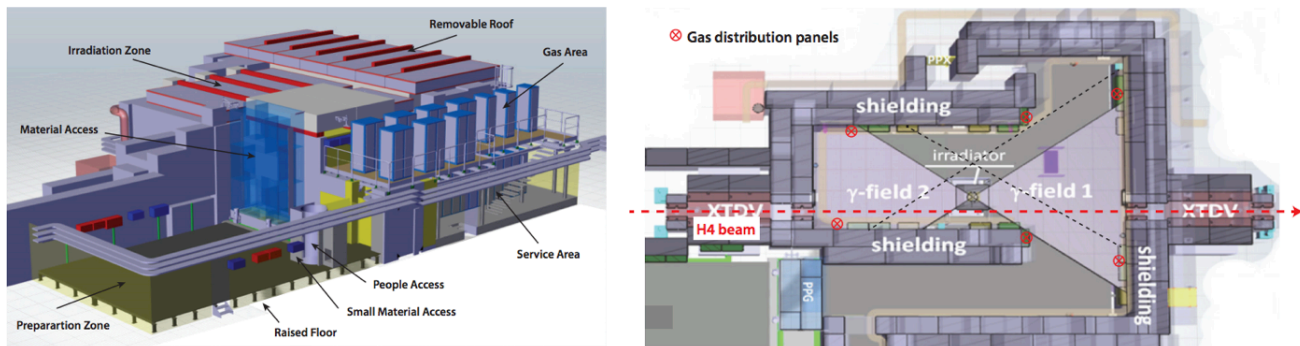
Figure 5.5: The Micromegas high voltage validation experimental setup at GIF++ irradiation setup.

The setup consists of 3 parallel nodes and each of these nodes consists of independent HV and gas channels which can work in parallel. In general, the GIF++ setup consists of 3 different sub-stations for the HV validation:

- HV Station: 1 CAEN SY4527 Mainframe supplied with 2 A1821P CAEN board, 7 A7030STP CAEN board, 1 A1821N CAEN board and 1 A7038STP CAEN Board
- Gas Station: Each station is supplied with an mass flow, humidity and pressure sensor connected to an Arduino for the gas monitoring
- GIF++ Station: External GIF++ station supplied with temperature, pressure, humidity, irradiator sensor connected via DIP protocol

An overview schematic of the Micromegas high voltage validation experimental setup at BB5 is shown below in Fig 5.6.
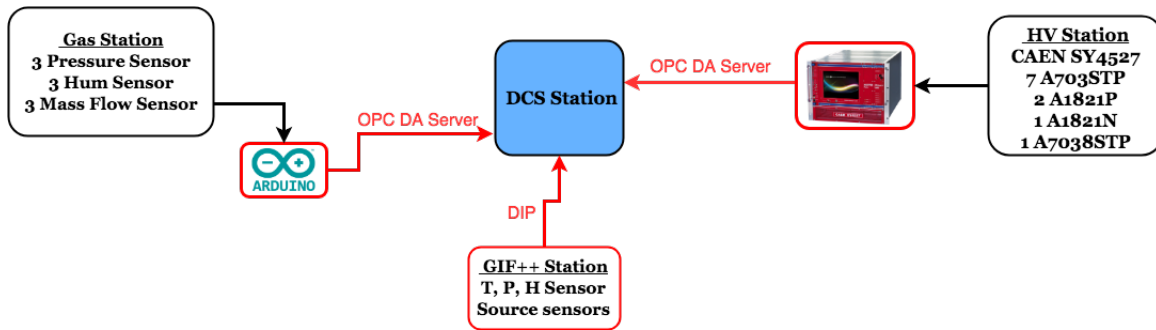
Figure 5.6: The overview schematic of the Micromegas high voltage validation experimental setup at BB5.

5.3   HV Station DCS

The HV Station DCS has been developed for the monitor and control of the Micromegas module's HV sections in order to validate the HV status. In the following subsection, the different user abilities of the software will be analyzed.

5.3.1   HV Mapping Setup

For the operation of the HV, the first step which is the HV mapping configuration or in other words the matching process between the Micromegas HV sections and the CAEN HV channels. This procedure can be done via the first tab "Setup" of the HV DCS as shown in the Fig. 5.7.
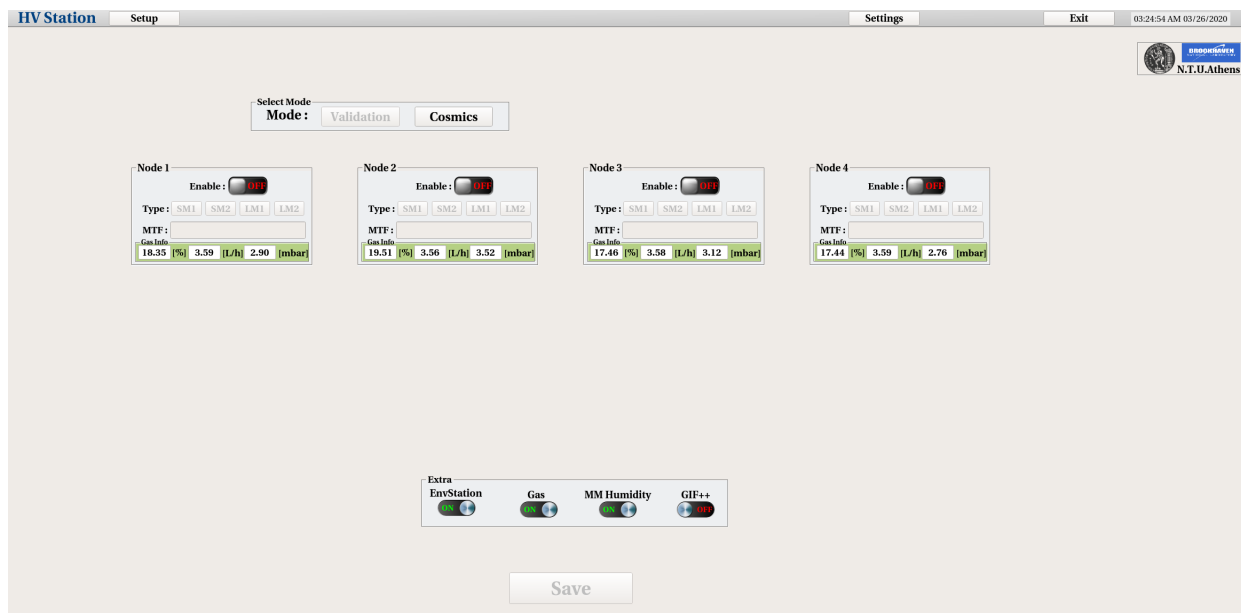
Figure 5.7: The "Setup" tab of the HV DCS where user can set the HV Mapping.

User via the button "Settings" is opening the Settings panel and via the "HV Setup" is opening the "HV Mapping setup" as shown in the Fig. 5.8. Inside this panel 5.7, user has the ability to choose between the mode ("Validation" for our case, "Cosmics" mode will be described in the next section), the node or MM module (4 parallel test stands/nodes), the type of the module ("Type 1" for SM1/LM1 or "Type 2" for SM2/LM2) and the Layer of the MM module. Then, when user is pressing "Set" and another windows is appearing in the bottom part. This window is a graphical widget of the selected Node, Type and Layer with the different HV sections shown. The green/red color indicates if there are HV channel settings for the corresponding HV section. In order to perform the HV mapping setup, user must select one section, as shown in Fig. 5.9, and the selection will appear near the "Selected Sector" textfield. In the "Set Channel Hardware" textfield user must insert the CAEN board and channel by selecting the channel of the channel list which will appear. After the selection of the HV channel, user must press the "green Tick" button and then the "Configure" button in order to save the settings for this specific HV section. Thus, user must do the same procedure for all the HV settings by setting the HV section
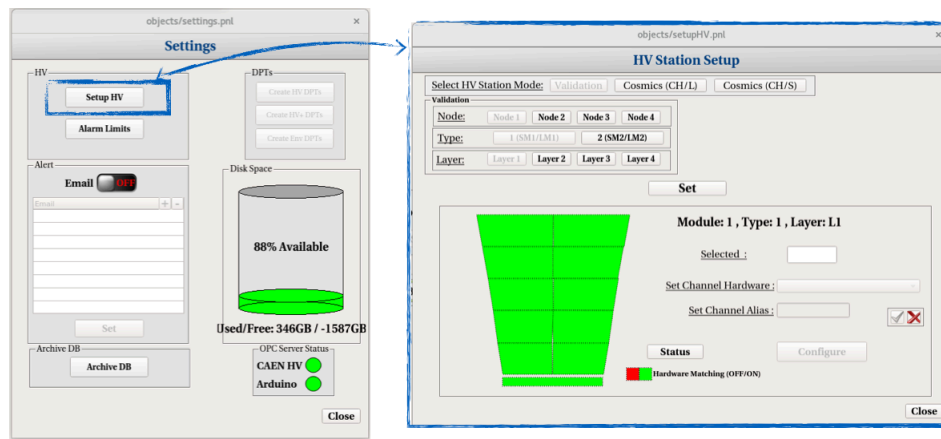
Figure 5.8: The panel for the HV Mapping setup via the "Settings" panel.

to the corresponding HV channel which he/she has connected.
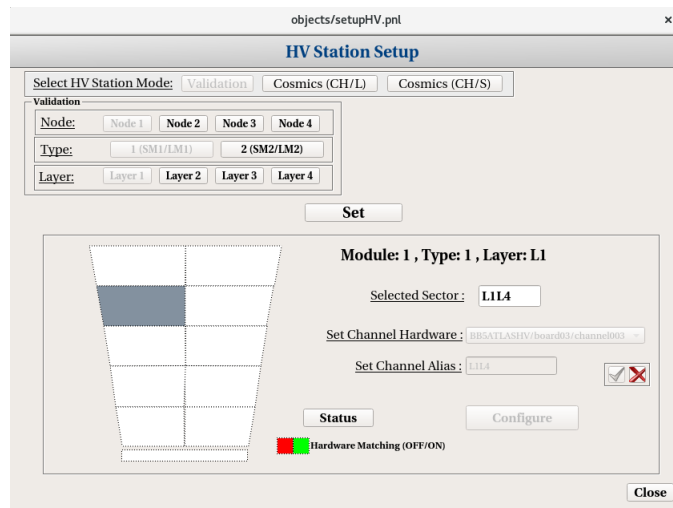
Figure 5.9: User sets the HV board and channel of the selected HV section.

When user has complete the HV mapping of the nodes that he/she will use he can press "Close" button and return to the first "Setup" tab as shown in 5.7.

5.3.2 Node Setup

The next step is the node setup. In the first "Setup" tab as shown in 5.10, user selects the "Mode" ("Validation" for our case, "Cosmics" mode will be described in the next section), and 4 windows, which are the corresponding modules under testing, will appear. The user should enable the corresponding node, select the type of the chamber between SM1/SM2/LM1/LM2, insert the 14-string MTF Batch ID of the module and select extra features in the "Extra" frame. Also, under each node user has the ability to monitor the pressure, mass flow and humidity value of the corresponding node's gas line in order to prepare it for the HV validation.
The "Extra" frame includes all the extra sensors of the experimental setup and these are:

- EnvStation: Environmental sensors for monitoring the temperature, pressure and humidity of the environment
- Gas: Mass flow and pressure sensors of the node gas lines
- MM Humidity: Humidity sensors of the node gas lines
- GIF++: Various sensors provided by GIF++ infrastructure via DIP protocol

When user inputs the information of the node's corresponding module under testing and also the extra feature that he want to monitor, he should press the "Save" button in order to save the node settings, as shown in 5.10.
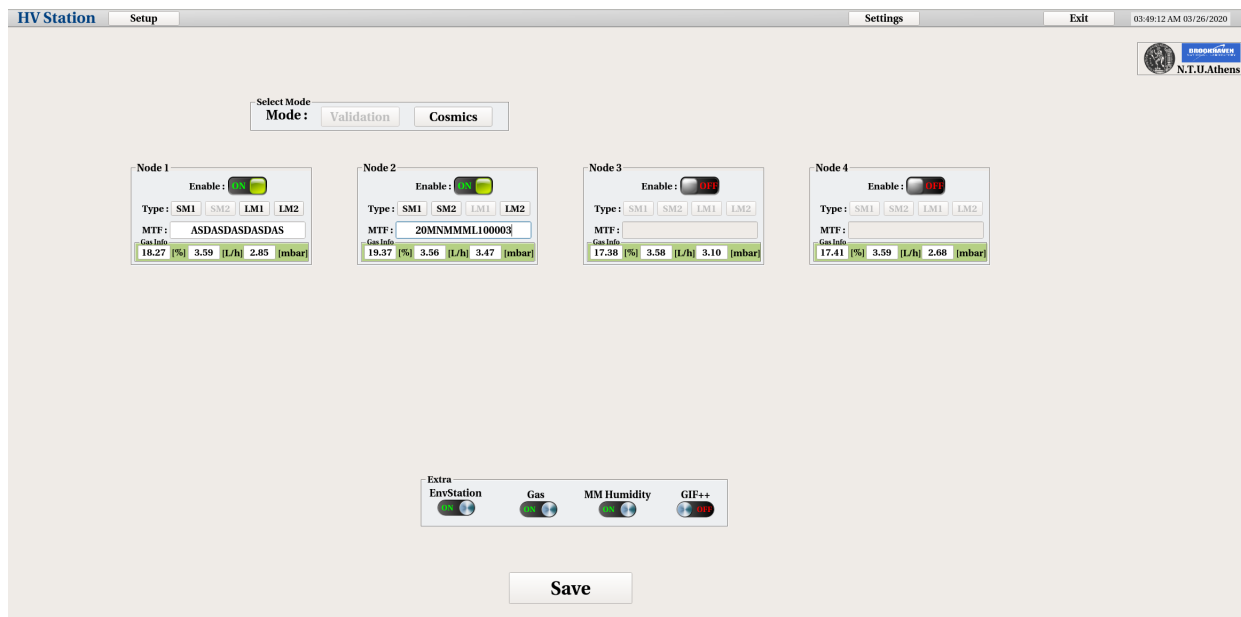
Figure 5.10: User sets the HV board and channel of the selected HV section.

And that's it, user can continue with the Micromegas HV validation.

5.3.3 Operation

As you already read in the previous section, user by pressing the "Save" button in the "Setup" tab saves the settings per node. By pressing the "Save" button, the software is automatically initializes the enabled nodes and the corresponding user enabled Nodes are appearing in the top bar of the HV DCS as buttons as you can see in Fig. 5.11 below.
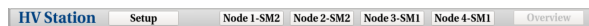
Figure 5.11: When user is pressing the "Save" button, the HV DCS is saving the node settings and the user enabled Nodes are appearing.

As you can see in the above Fig. 5.11, the "Node X-Type" button are appearing which correspond to the user-defined settings per node. Every Node button correspond to the specific module which is connected to this node. By pressing this "Node" button, user can navigate though the corresponding module for testing. Also, another "Overview" button is appearing in order to control/monitor all the nodes in parallel. So, the next step is the monitor and control of the nodes, things which be analyzed in details in the next subsections.

5.3.4 Monitor

When user presses the "Node X-Type" button, he/she is inserting to the main control/monitor window of the HV DCS software as shown in the below Fig.5.12, and as you can see there a lot of information that should be described in details.
Let's start analyzing the main panel Fig.5.12, it is divided in different purpose windows:

- **HV Channels:** User can monitor the all the individual HV sections, he/she can monitor the voltage value and the current value. The green color indication of the HV section label displays the current status of the channel. The different states of the channel are: "Green" for ON channel, "Grey" for OFF channel and "Red-Grey" blinking for Tripped channel. There is also an option, where user can right-click over the HV section label and a pop-up window will open with the corresponding HV section graph of the voltage/current versus time. User also can check the checkbox option in order to open the graph of the voltage/current versus time in the "HV Plots" window.

- **HV Plots:** This is the regions where the checkboxed HV sections of the "HV Channels" window graphs of the voltage/current versus time are displayed.

Figure 5.12: The main panel of HV DCS software for control and monitoring.

- **Extra Info:** This is the region where user can monitor the sensors that are defined in the "Extra" frame of the "Setup" tab. For example, user car monitor under the "MM Gas" frame, the mass flow, pressure and the humidity of the corresponding node. Also, under the "EnvStaion" frame, user can monitor the pressure, environment and humidity value of the environment. Via the "Env Plots" and "Gas" Plots, user can open the corresponding plots. For the GIF++ mode, inside this "Extra Info" window, the various GIF++'s sensors are displayed.

- **HV Alarm:** In this region, user can have a visually representation of the module under testing. The user has the option to select between two modes, voltage or current representation using the "switch" button. The limits are user-defined and user can set them up though the "Settings" button and the "Alarm Limits" button, procedure that will be described in the next subsections.Near the "switch" button, user can find the voltage or current limits and the color representation for this limits. Also, user has the ability to monitor the Layer's HV sections by left-clicking on the "Layer X" button and the individual HV section by left-clicking in the corresponding HV section in the graphical representation. In the bottom part, user can monitor the status of the HV sections that are in the user defined "green (OK)" area pear Layer and per full Module. By using the histogram, histogram can have a quick idea of the HV status of the module.

- **HV Efficiency:** User has the ability to monitor the HV efficiency per Layer and per Module in total, in order to estimate and validate quickly the HV status of the Micromegas module under testing. The HV efficiency is based on an experimental curve that collected during the testbeam of a SM2 Micromegas module during summer of 2018 at H8 area of North area at CERN. The experimental curve is the following:

$$\epsilon_{layer}(V) = \frac{\sum_{n=1}^{n} \frac{x_0}{1+e^{-x_1(V-x_2)}}}{n} \tag{5.1}$$

where n the number of the HV sections,V is the HV Section voltage and $x_0 = 96.7336$, , $x_1 = 0.0626969$, $x_2 = 521.418$

- **Archive/Export:** In this region, user can archive and export the all the data which are selected, will be described under details in the next sub-sections.

- **Auto-Trip recovery mechanism:** User can enable the auto-trip recovery mechanism and set the V_{sub} value. By enabling this, it means that when a HV section will trip and is powering off, the auto mechanism is powering on it and it sets the V_{set} of this value into $V_{set} - V_{sub}$.

- **Overview mode:** In order to insert this mode, user mist press the "Overview" button and then he is navigating in the Overview

mode display where he/she can monitor all the modes in parallel as shown in Fig.5.13 . In this mode, user can easily validate the module by monitoring the HV sections alarm-color limits, the histograms which show the sections are in the good region and the gas info per node.
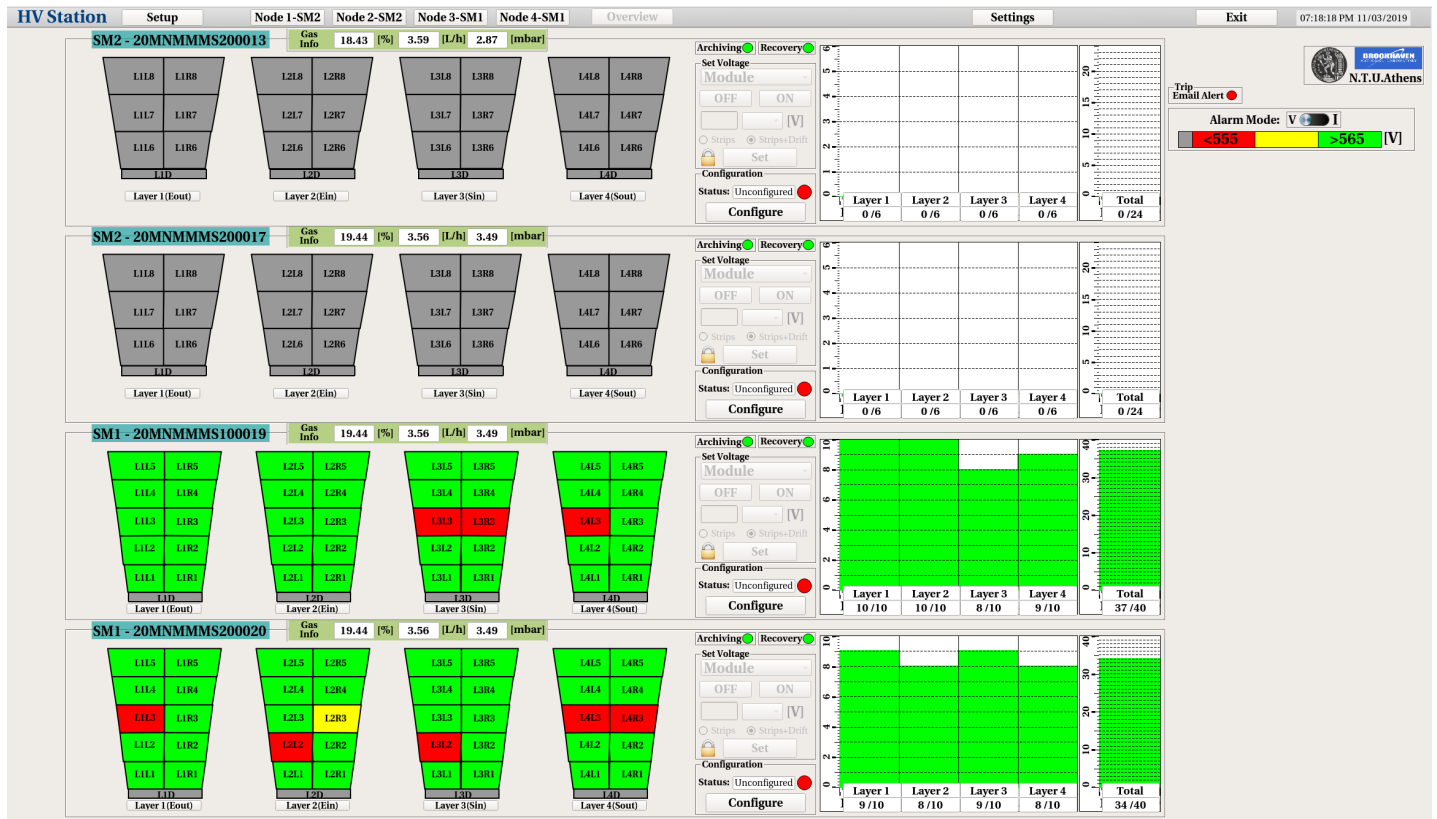
Figure 5.13: The overview panel of HV DCS software for control and monitoring all the nodes in parallel.

5.3.5 Control

User has several options to control the Micromegas's HV sections. In principal, via the HV DCS software user has the ability to control the following parameters of the CAEN boards hardware:

- **onOff:** This is the power on/off setting of the HV channel
- **vSet:** This is the voltage setting of the HV channel
- **i0:** This is the first current limit that the HV channel cannot exceed
- **i1:** This is the second current limit that the HV channel cannot exceed
- **tripTime:** This is the time limit which if a HV channel's current value is over i0/i1, it trips
- **vMax:** This is the max voltage setting that user can insert for safety reasons in order to not exceed it
- **rUp:** This is the voltage ramping up step of the HV channel, for example 10 V/s
- **rDown:** This is the voltage ramping down step of the HV channel, for example 10 V/s

In the following Fig. 5.14 the different ways of HV controlling is showing and described.
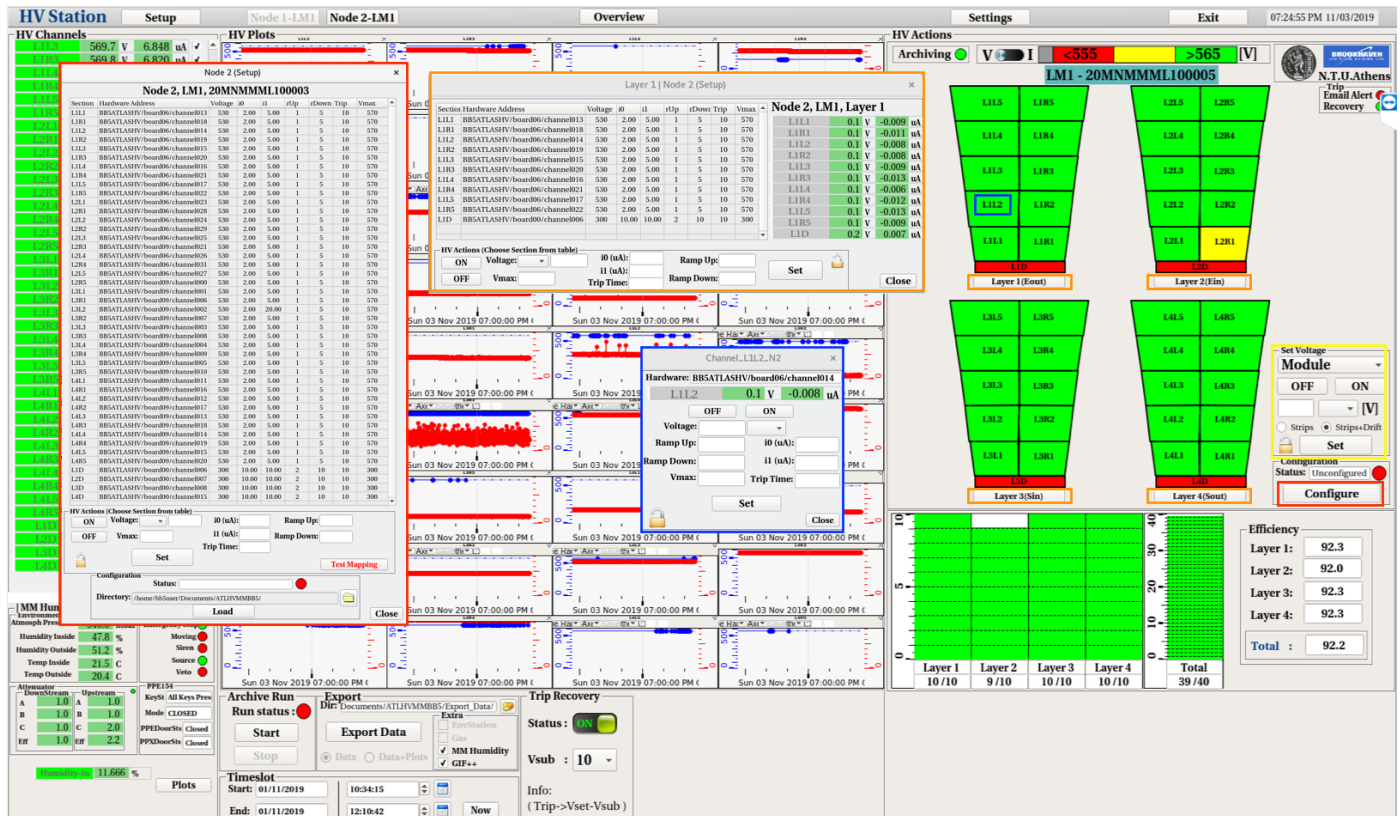
Figure 5.14: The HV control options of HV DCS software.

User has multiple ways to control the HV sections, from module up to individual channel control, and the ways are the following as shown also in Fig. 5.14:

- **Node Control:** User has the ability to control all the HV sections of the Micromegas module by pressing the "Configure". He/she has the ability to select all or individual channel and control all the settings.
- **Layer Control:** User has the ability to control all the HV sections of the Micromegas layer by pressing the "Layer X" button.
- **Channel Control:** User has the ability to control one individual HV section of the Micromegas module pressing a section object, "L1L2" for example.
- **Quick Control:** User has the ability to control the Module or Layer, strips or drift channel in a quick compact way.
- **Overview Control:** Via the "Overview" panel user has the ability to access all the control function. He/She can control the the Module, Layer and individual channels by accessing the Node, Layer, Channel and Quick Control "functions", as shown in Fig. 5.15.
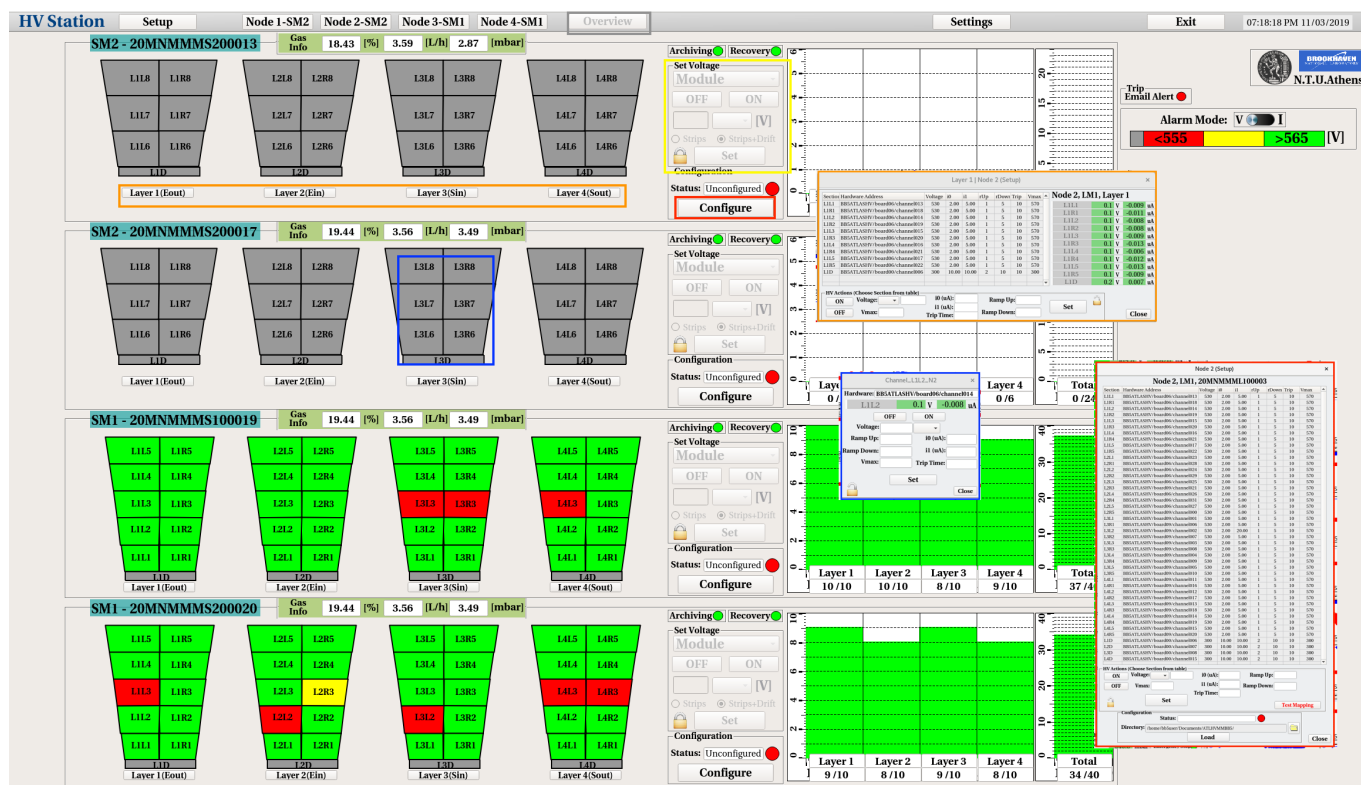
Figure 5.15: The Overview HV control options of HV DCS software.

5.3.6 Archive/Export

The monitor and control of the HV channels is the first step of the HV validation. The second step is the archiving, exporting and analyzing the data. The HV DCS software has the ability for unstoppable archiving of all the data. In other words, all the HV channel, gas, environment, and GIF++ parameters are archived during the operation of the Micromegas module. As shown in Fig. , user has the ability to start and stop a Run by clicking the corresponding button. By doing this, the time-slot between the start and the end of the run is autofilled and thus, user can press the "Export" button. By pressing the "Export" button, user is exporting the HV and the "Extra" data which are selected to a user-defined directory specified under the "Dir" text-field. Also, user has the ability to manually select the "Start" and "End" time of the data that he wants to export manually by filling the corresponding fields under the "Timeslot" frame.

Figure 5.16: The archive/export options of the HV DCS software.

5.3.7 Archive DB

Via the "Settings" button and the "Archive DB" button as shown in Fig.5.8, user has the ability to access the history of the HV measurements which he took using the "Start/Stop Run" mechanism which described in the previous subsection. As you can see in the Fig. 5.17, user has the ability to search by the type of the chamber or the MTF Batch ID, select the corresponding data time-slot that he/she prefers and export all the HV data plus the "Extra" data that he/she has already took during this run.

Figure 5.17: The Run Archive DB of the HV DCS software.

5.3.8 Alarm Limits

Via the "Settings" button and the "Alarm Limits" button as shown in Fig.5.8, user can set the voltage and current limits as shown in Fig. 5.18, which are used for the "HV Alarm" as described in section 1.4.1.

Figure 5.18: The Alarm Limit Settings of the HV DCS software.

5.3.9   Features

The HV DCS software gives the ability for email notification for HV channel Trip, CAEN hardware and Arduino lost communication. If something of the above cases is happened, user is notified via an email in order to investigate more the problem. The user can subscribe to this email notification list by enabling the "Email" switch, adding his/her email under the list and presses the "Set" button via the "Settings" panel as shown in the below Fig. 5.19.
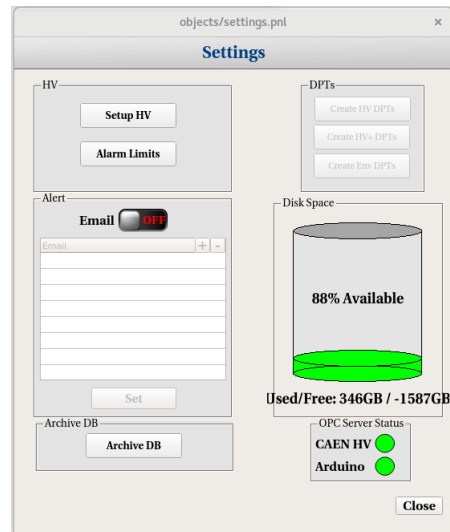
Figure 5.19: The Settings panel of the HV DCS software.

Also, user has the ability to monitor the hard disk space of the computer and also the CAEN and Arduino hardware connectivity status via the "Settings" panel as shown in the below Fig. 5.19.

Chapter 6

ArdEnvironment Station

This chapter includes information about the ArdEnvironment Station that have installed within Gas TIghtness Station, HV Validation and the Cosmics Test Stand at BB5.

6.1 Setup Wiring

The ArdEnvironment Station consists of an Arduino Mega 2560 Board, Wiznet W5500 Erthernet board and the Adafruit BME 280 sensor for pressure, temperature and humidity measurements. The below figure includes the Arduino-Wiznet setup, the BME280 sensor and also the wire labeling connection between the Arduino and the sensor. After the wire connection, user can check for the right connection between the Arduino and the sensor by power on the Arduino and check the flushing blue LED.

If blue LED doesn't flush, user must check the wire connection, press the white button for Arduino Soft Reset on the top right side of red Wiznet board and re-check the blue LED as shown below.

Figure 6.1: Left: The ArdEnvironment setup consists of the Arduino Mega 2560 and the Wiznet 5500 Ethernet Shield, Top Right: The BME280 sensor for pressure, humidity and temperature measurements, Bottom Right: The wire connection between Arduino and BME280 sensor

6.2   OPC DA Server Operation

If blue LED flushes, user can connect the Arduino to a computer via an ethernet cable. The IP of the Arduino is 10.0.0.10, so for the right connection with the computer user must set computer's static ip under the same subnet (10.0.0.X). Also, user can test the connection with Arduino by executing the following command via terminal and checking the output:

```
>   ping 10.0.0.10
```

If ping is successful, the steps which user must follow to establish the Arduino OPC DA Server operation are:

1. Open "OPC Server for Arduino/Genuino" program as administrator under Windows
2. Press "Arduino Ethernet" Tab and insert 10.0.0.10 in "Arduino IP" field and 80 in "Port" field
3. Press "Save Configuration" button and close the window by tapping "X" icon
4. Run "register.bat" file as administrator
5. Open "OPC Server for Arduino/Genuino" program as administrator under Windows

After the completion of these steps, the OPC DA server forwards the sensor's values to WinCC-OA software. Also, it is important to be mentioned that "OPC Server for Arduino/Genuino" program is initialized in minimized mode under the Notification area of Windows down right.

Figure 6.2: Configuration and start of Arduino OPC DA Server under Windows partition.

6.3   ArdEnvironment Station Software

The ArdEnvironment Station Software can be accessed from GTS Software by pressing "ArdEnvironment Station" button. The main panel consists of 3 plots and values which display the pressure, temperature and humidity values respectively as shown below.

Figure 6.3: ArdEnvironment Station main panel, user can monitor and archive/export the pressure, temperature and humidity.

User can archive pressure, temperature and humidity values simultaneously by pressing "Start" button under "Archive" area. The default sampling time is set to 1 mean value per 1 minute but user can adjust sampling time settings by pressing the "Settings" icon under "Archive" area. Under "Export" area, user can export the archived data for specific user-defined time slot, by selecting the start and end date/time. Software gives the ability to export the archived data as data file "ArdEnvStation_Start_TO_End.dat" or plots file "ArdEnvStation_Plots_Start_TO_End.png", where "Start" and "End" are the user-defined time slot, in the default output directory inside the project folder "ArdEnvStation_Data" or a user-defined directory by pressing "Folder" icon. The form of the exported data and plots are shown below. Finally, archive must be always ON (green indicator), otherwise user must press the "Start" button.

Figure 6.4: Form of exported data and plots using ArdEnvironment Station.

Chapter 7

SCA Electronics Station

This chapter describes the software which developed for the electronics validation of the New Small Wheel sectors prior to the installation to the New Small Wheels of the ATLAS experiment. The validation of the sectors are taking place at the BB5, 180 and 191 buildings at CERN.

7.1 NSW Electronics

The Fig. 7.1 represents the NSW Electronics and DAQ dataflow full chain. The reader can define 3 different window or regions:

- Front-End Boards: The FEBs are the electronics cards that are attached on the readout strips or pads of the NSW detector and collects the data and trigger information.

- On-chamber or on-Rim boards: The purpose of these cards is to drive the different data/trigger signals that are generated by the FEBs

- USA15: This is the area where a lot of services are running like the Trigger Processor, the calibration, configuration, DCS and ROC processes for example

Also, in the NSW electronics chain there are different configuration/monitor, trigger and readout paths.
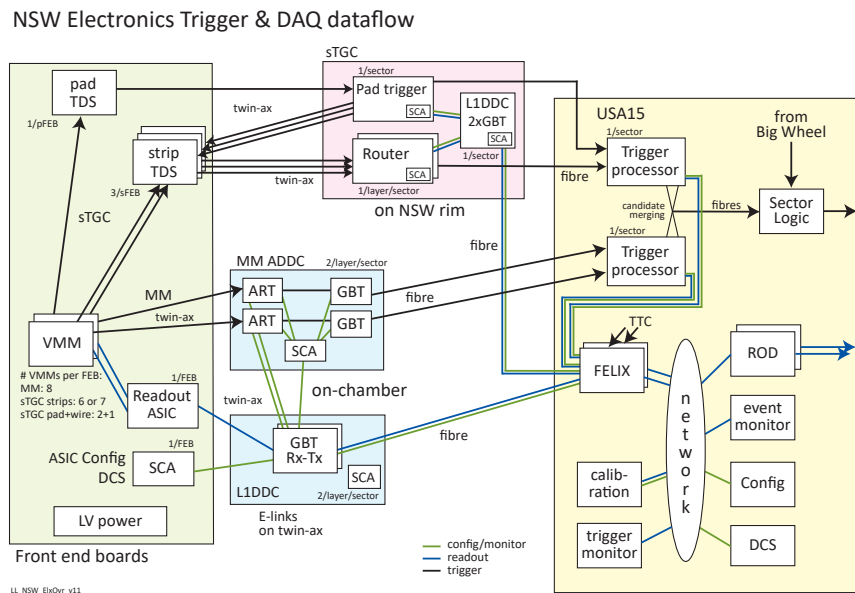
Figure 7.1: The NSW Electronics Trigger and DAQ dataflow.

79

7.2   Micromegas Electronics

Let's focus on the Micromegas electronics, a picture of a Micromegas sector is shown in Fig. 7.2.
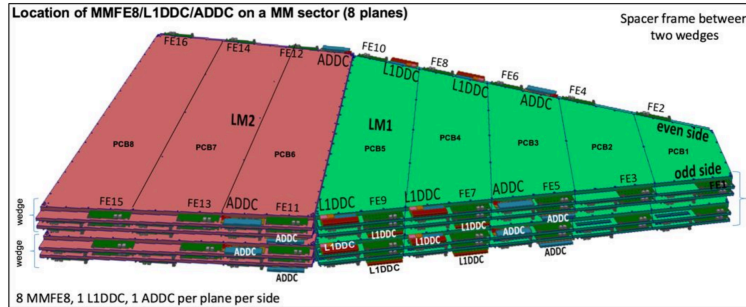
Figure 7.2: A Micromegas sector equipped with electronics.

Each MM sector combines:

- 128 Micromegas front-end board or MMFE8
- 16 Art Data driver card or ADDC
- 16 L1 data driver card or L1DDC
- 16 Low voltage distributor cards of LVDB

Every board has a different work which is described below:

- MMFE8: Houses 8 VMM chips that convert analog signal of the detector into digital, which includes the ART data.
- ADDC: Collect ART data from eight MMFE8s and relay it to the Trigger Processor.
- L1DDC: Interface of the MMFE8s and ADDCs to FELIX, passing along configuration data and clock source.
- LVDB: Provides low voltage power to MMFE8, L1DDC and ADDC boards
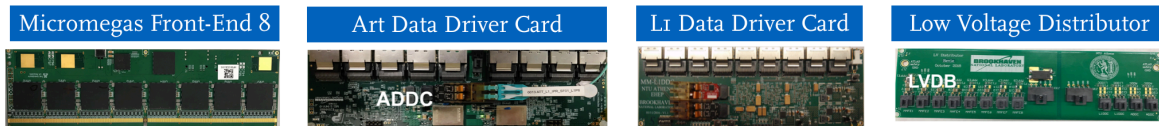
Figure 7.3: The MM electronics boards.
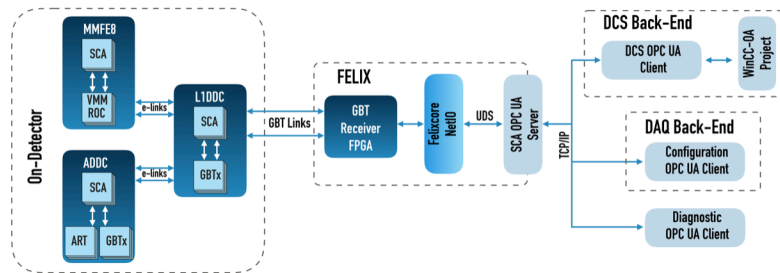
Figure 7.4: The MM electronics chain.

7.2.1 DAQ path

As for the DAQ path as shown in Fig. 7.5, we have again the on-detector electronics, in the MMFE8 we have the VMM chip which digitizes detector signals and send trigger primitives, then the ROC in the MMFE8 buffers and filters data from 8 VMMs to match ATLAS trigger selection, then the GBTx chip in the L1DDC pack up readout data and though the FELIX to the network infrastructure where we performing the data acquisition and the event monitor.
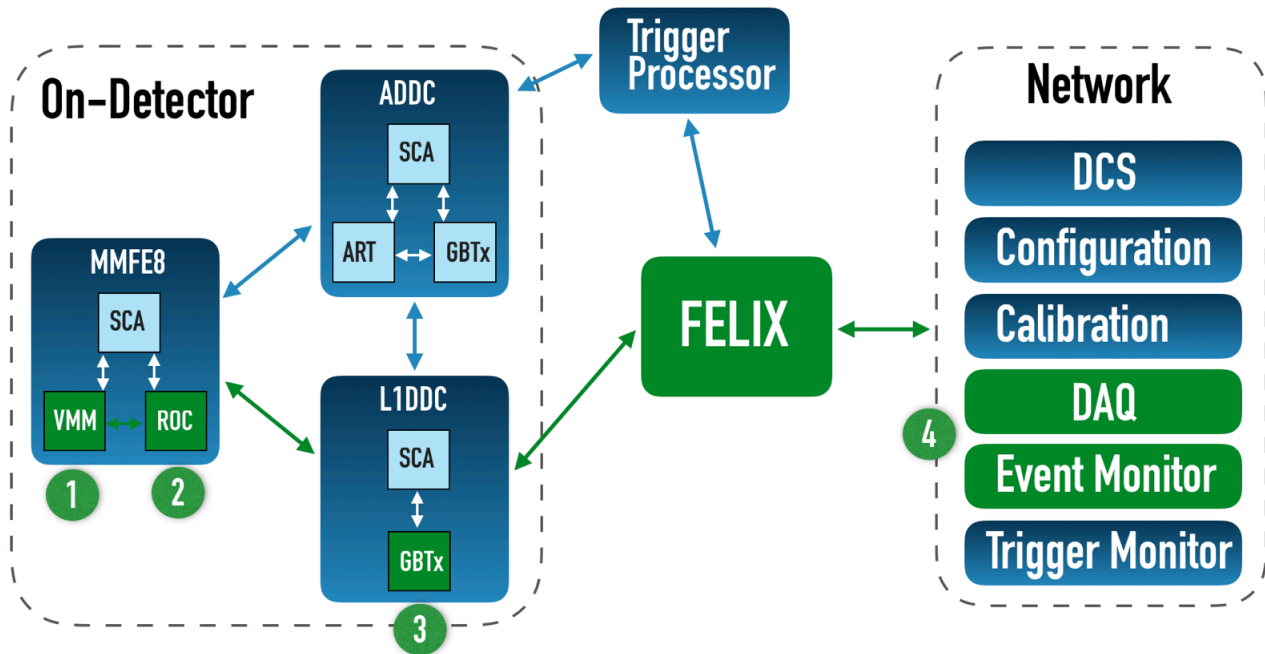
1   VMM: digitizes detector signals and send trigger primitives (64 channels)

2   ROC: buffers and filters data from 8 VMMs to match ATLAS trigger selection

3   GBTx: packs up readout data and sends to FELIX

4   DAQ and event monitor

Figure 7.5: The MM DAQ path.

7.2.2 Trigger path

As for the Trigger path as shown in Fig. 7.6, we have again the on-detector electronics, in the MMFE8 we have the VMM chip which digitizes detector signals and send trigger primitives, then the ART in the ADDC packages trigger primitives from 32 VMM and stamps with bunch crossing ID, then the GBTx chip in the L1DDC packs up trigger data and sends to the Trigger Processor. Then the Trigger Processor makes a candidate "track" from trigger primitives and and sends the data to the network, where finally we have the trigger and event monitor.

1 VMM: digitizes detector signals and send trigger primitives (64 channels)

2 ART: packages trigger primitives from 32 VMMs and stamps with bunch crossing ID

3 GBTx: packs up trigger data and sends to Trigger Processor

4 TP: makes a candidate "track" from trigger primitives

5 Trigger and event monitor
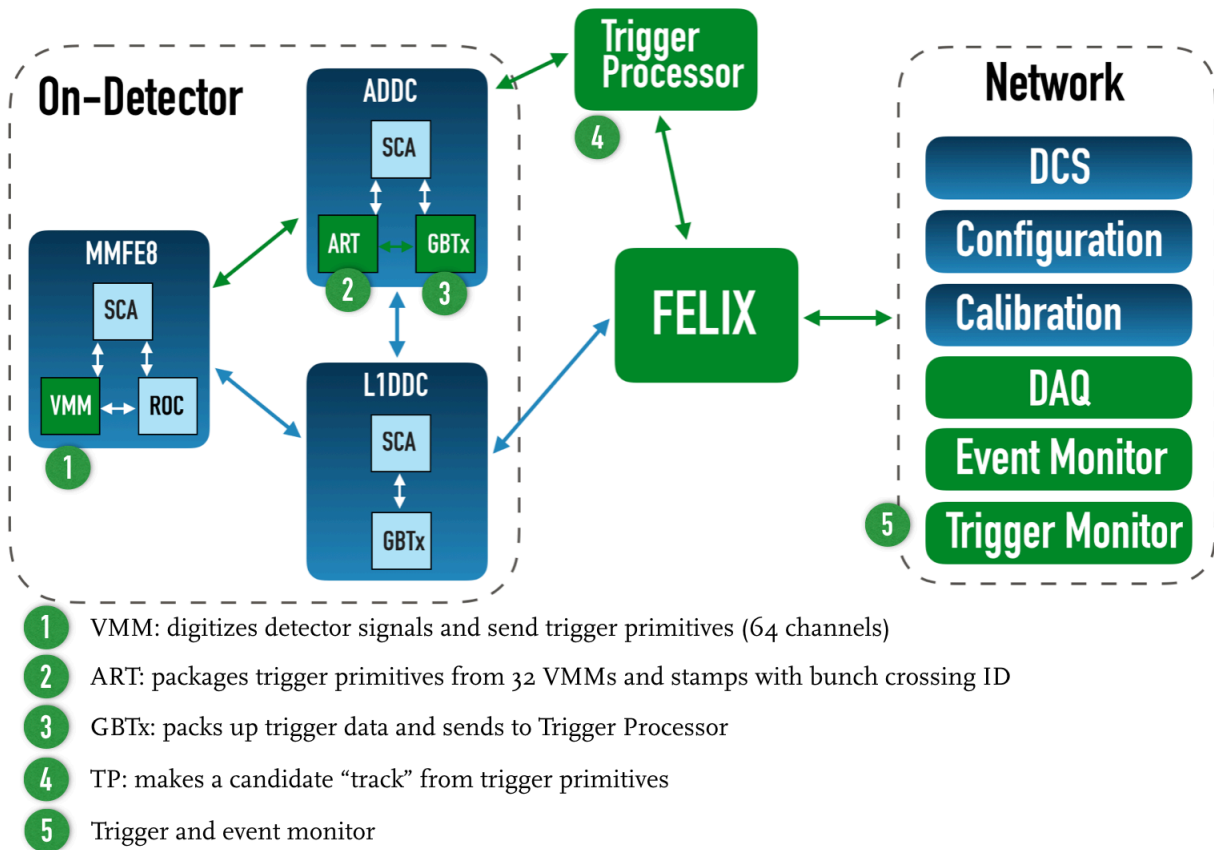
Figure 7.6: The MM Trigger path.

7.2.3 Configuration path

The GBT-SCA ASIC (Giga-Bit Transceiver - Slow Control Adapter) is the part of the GBT chip-set which purpose is to distribute control and monitoring signals to the front-end electronics embedded in the detectors. The user interface ports are:

- 1 SPI master
- 16 independent I2C masters
- 1 JTAG master
- 4 DAC (8-bit)
- 32 GPIO
- 31 ADC (12-bit) channels

In the bottom image, i am showing a more detailed schematic of the MM electronics schematic, we have the on-detector electronics, where SCA in installed in all the boards and is connected to the boards chips and sensor, thought the SCA we are performing the configuration, the monitoring and the calibration of these boards.
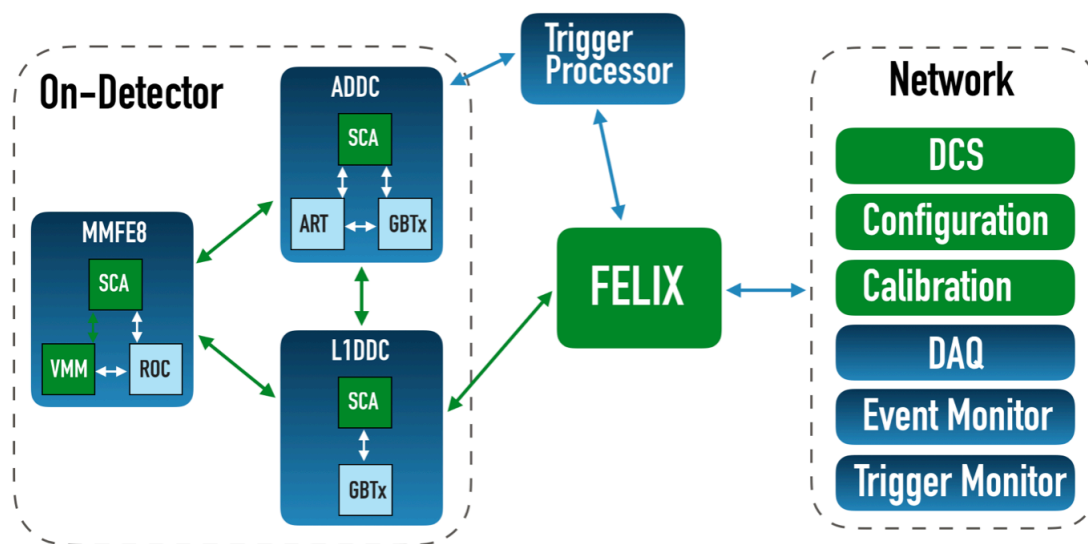
Figure 7.7: The MM Configuration/Monitoring path.

In summary, the SCA chip is giving us the ability to:

- Perform front end monitoring using the SCA to read Feast PW/temperature, board(NTC), VMM and SCA temperature
- Perform the configuration of VMM, ART, ROC and GBTx chips via I2C and SPI
- Perform the VMM calibration using the ADC channel

In total, 5120 SCAs for the Micromegas electronics we will have 100 thousand parameters like voltages, temperatures and GPIOs.

7.3   SCA DCS

In this section, the SCA DCS for the electronics monitoring will be described in details. The SCA DCS has been developed in a compact design and consists only by one window as shown in Fig. 7.8. The user can switch between all the layer of the sector and monitor all the temperature and power sensor values.
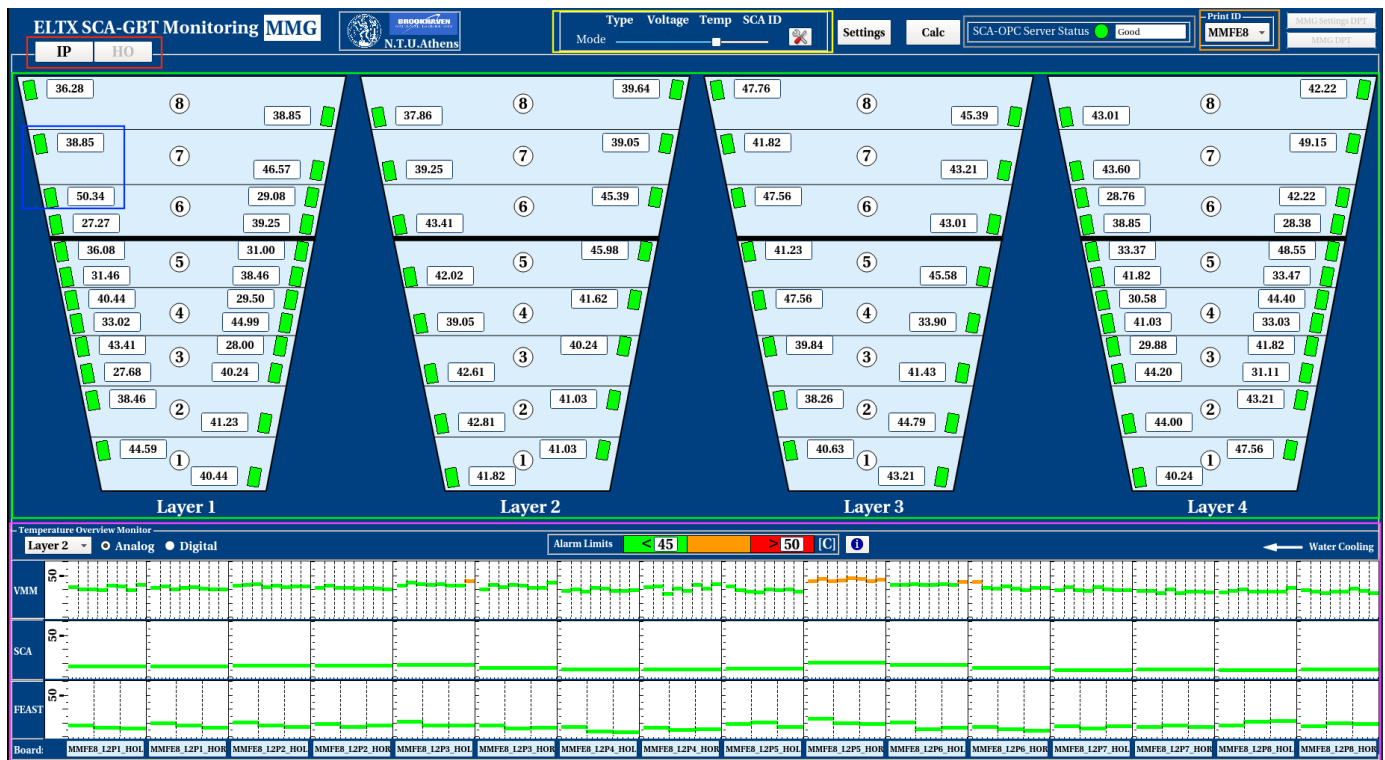
Figure 7.8: The main SCA DCS panel for Micromegas electronics monitoring.

The SCA DCS features the following:

- **Wedge Side Selection:** User has the ability to switch between the IP and HO wedge of the sector.

- **Quick Display:** User has the ability to monitor the SCA connectivity status and a board parameter. By left click, user is opening a pop-up plot of the parameter and by right-clicking it user opens the full board monitoring.

- **Layer Display:** User has the ability to monitor the all board SCA connectivity status and parameter of all layers.

- **Mode View Selection:** User has the ability to switch between board type, voltage, temperature and SCA ID value monitor. Via the "Settings" button, user can set the parameter for the quick display for every type of board.

- **SCA OPC UA Status:** User has the ability to display the SCA OPC UA connection status via the main panel.

- **SCA ID Print:** User has the ability to export the SCA ID list per board in the /Desktop area of his/her computer

- **Temperature Overview Monitor:** The user can display all the parameters of all boards of the sector and switch between the layers and the Analog (MMFE8) and Digital (ADDC, LɪDDC) boards. Also, color alarm is used for quick display if a value is in between the proper limits and user can change the limits by changes the values inside the text-fields.

7.3.1 Board Monitoring

The user via the "Quick Display" which described in the previous section, has the ability to monitor all the parameters of the board by right-clicking on the board. A window per board is opening, so user has the ability to monitor in details all the parameters as shown in Fig. 7.9. The monitoring parameters per board are:
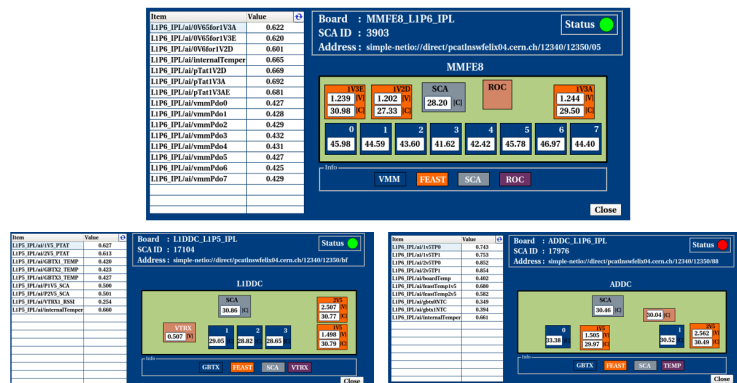
Figure 7.9: The board SCA DCS panel for Micromegas electronics monitoring.

- Temperature sensors
- Power sensors
- On-chip temperatures
- SCA online status
- SCA ID
- SCA OPC UA Server Board name
- FELIX e-link

7.3.2 sTGC SCA DCS

A DCS software created also for the sTGC electronics monitoring for use at building 180 and 191 at CERN, as shown in Fig. 7.10. Via the SCA DCS, user can monitor all the parameters of all the sTGC boards like sFEB, pFEB, LiDDC, Rim-LiDDC, PadTrigger and Router board.
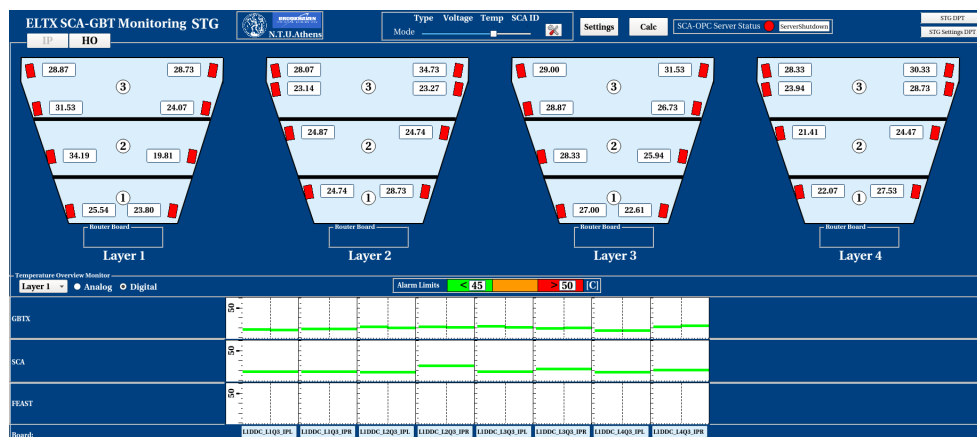
Figure 7.10: The SCA DCS panel for sTGC electronics monitoring.

7.4   Readout concept

An illustration of the Micromegas electronics overview is shown in Fig. 7.11. On the Micromegas detector, there are the on-detector electronics boards or MMFE8, L1DDC and ADDC boards. On the boards, there is the GBT-SCA chip which is connected to various sensors like temperature, power and on-chip temperature sensors. The first step is the creation of the SCA OPC UA Server XML file, which the various sensors connected to the SCA ADC channels are specified. Then, the second step is the initialization of the FELIXcore and the SCA OPC UA Server, services which are running into the FELIX machine. The third step, is the subscription to the SCA OPC UA Server via a WinCC-OA OPC UA Client. Then, another step is the creation of the SCA OPC UA Serve XML items into DPEs inside the WinCC-OA. And finally, the monitor of the board parameters via the SCA DCS.
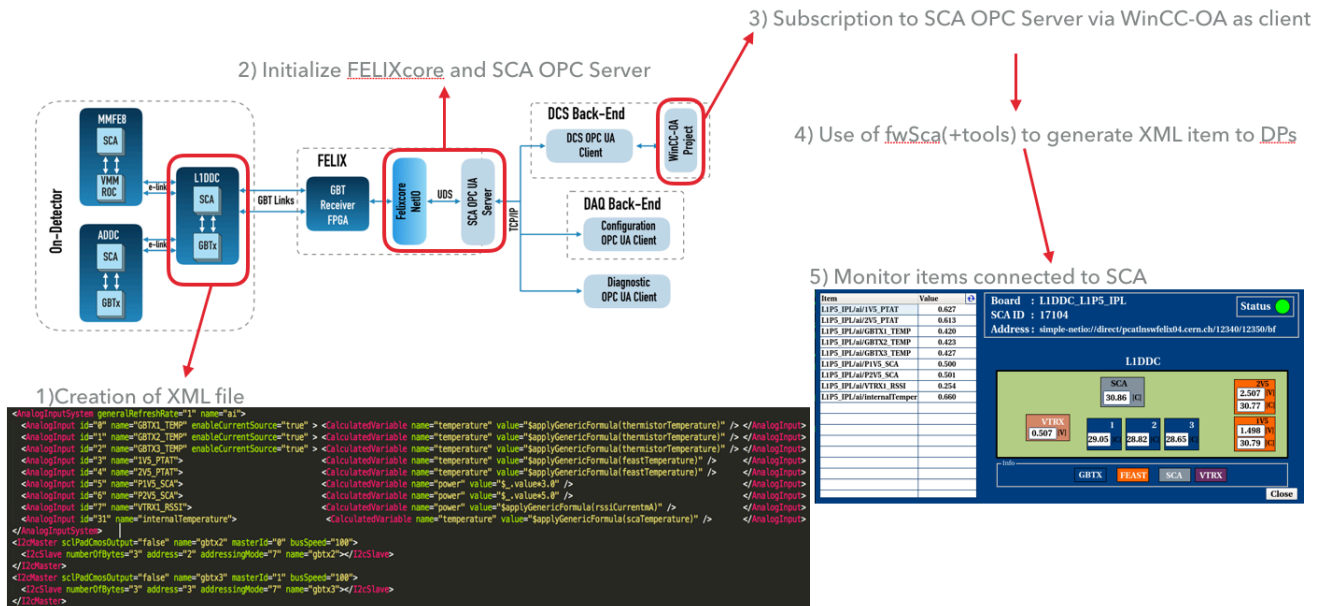
Figure 7.11: The readout concept of the SCA DCS.

Chapter 8

Cosmics Stand Station

This chapter describes the experimental setup and the software which developed for the cosmics validation of the Micromegas sectors prior to the installation to the New Small Wheels of the ATLAS experiment. The cosmics validation is the final step in the validation procedure of the Micromegas detector and thus is a combination of gas, HV and electronics validation.

8.1 Setup

The Cosmics Station setup is principal the Micromegas sector which is supplied with all the HV, gas, cooling, alignment and electronics services prior to the installation to the ATLAS cavern. The reader can understand that it's a really complicated system and each Micromegas sector needs several people with a lot of care and several weeks to be completed. An image of a real Micromegas sector at the Cosmics Stand setup at BB5 CERN is shown in Fig. 8.1.
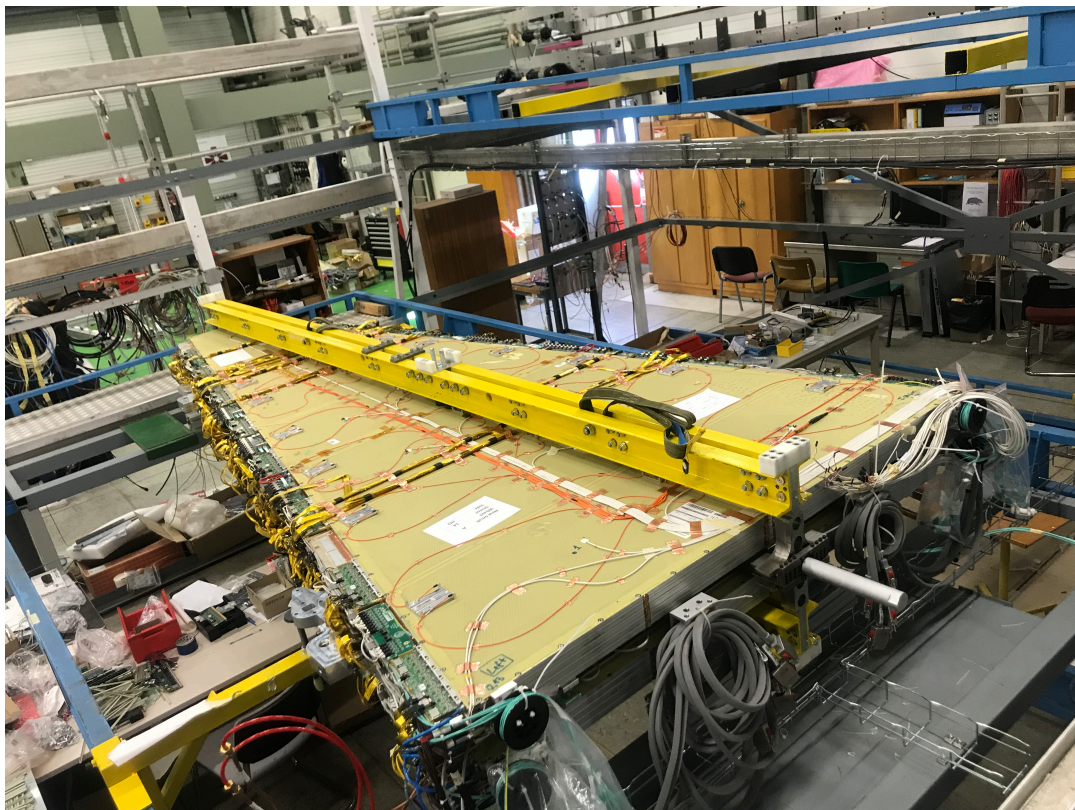
Figure 8.1: A real Micromegas sector at the Cosmics Stand setup at BB5 CERN.

8.2 Cosmics Stand DCS Station

8.2.1 Overview Schematic

Due to the complexity of the Micromegas sector, the Cosmics Stand Station is a combination of several sub-stations:

- HV Station: For the monitor and control of the HV channels
- LV Station: For control of the LV of the electronics boards installed on the sector
- SCA Station: For the monitor of the temperature and power levels of the electronics boards
- MDM Station: For the monitor of the temperature sensors installed on the surface of the sector
- Gas Station: For the monitor of the gas sensors of the sector
- Env Station: For the monitor of the environmental conditions during the cosmics runs
- Safety Station: For the safety mechanisms in case of incidents

An overview schematic is shown in the below Fig. 8.2.
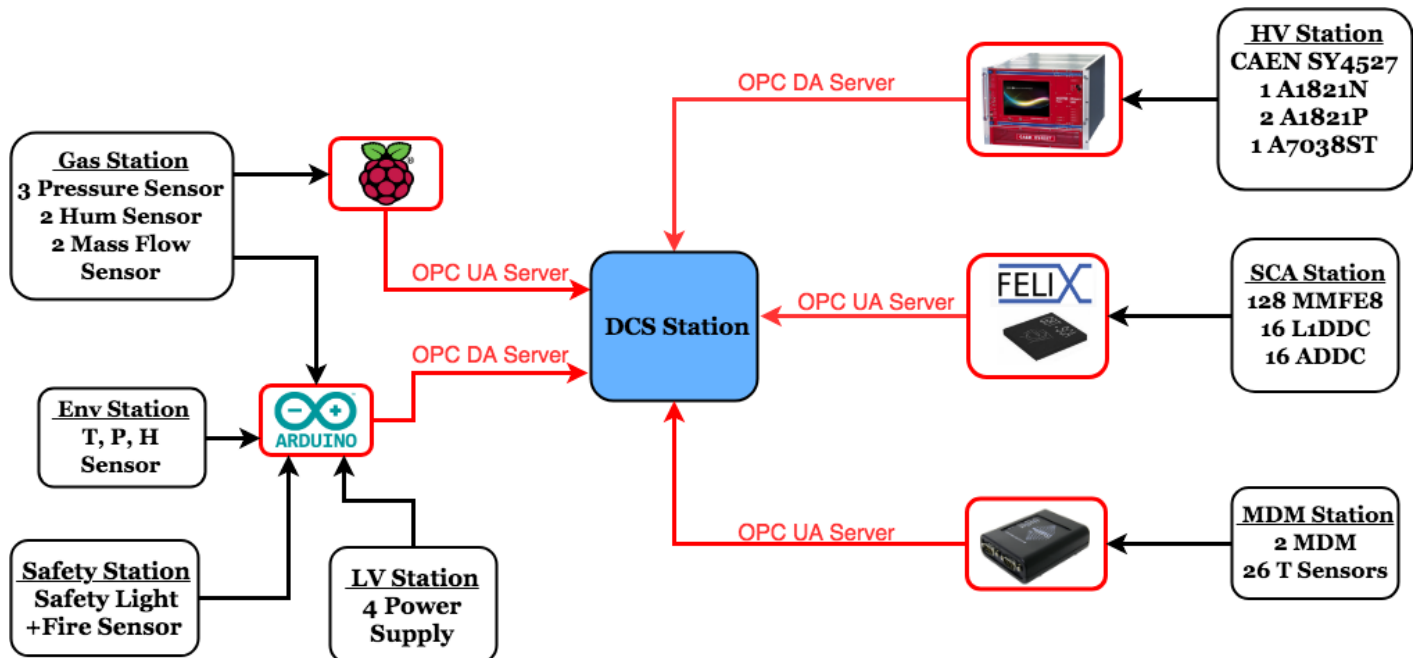
Figure 8.2: The overview schematic of the Cosmics Stand DCS Station

8.2.2   HV Station

When user presses the "Sector X" button, he/she is inserting to the main control/monitor window of the HV DCS software as shown in the below Fig.8.3, and as you can see there a lot of information that should be described in details. Let's start analyzing the main
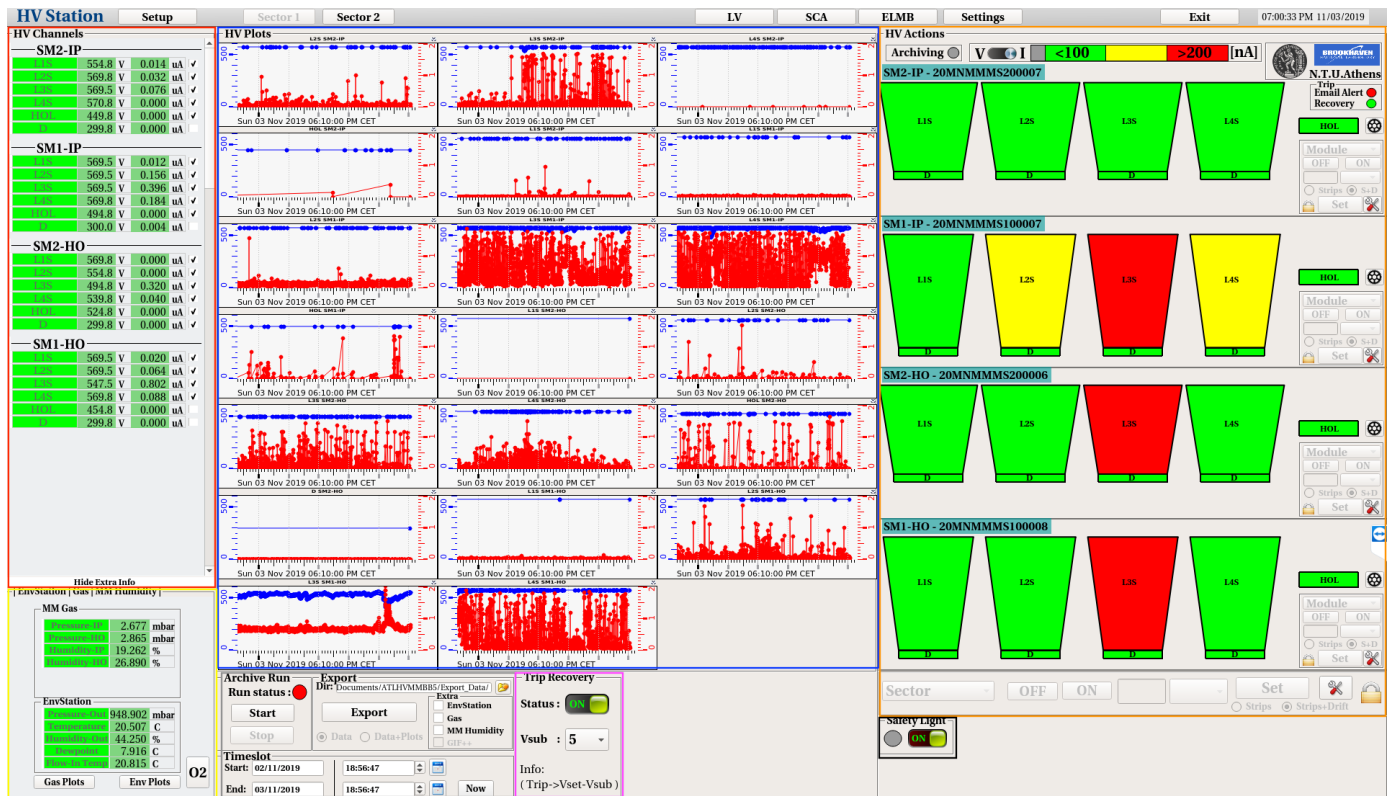
Figure 8.3: The main panel of HV DCS software for control and monitoring.

panel Fig.8.3, it is divided in different purpose windows:

- **HV Channels:** User can monitor the all the individual HV sections, he/she can monitor the voltage value and the current value. The green color indication of the HV section label displays the current status of the channel. The different states of the channel are: "Green" for ON channel, "Grey" for OFF channel and "Red-Grey" blinking for Tripped channel. There is also an option, where user can right-click over the HV section label and a pop-up window will open with the corresponding HV section graph of the voltage/current versus time. User also can check the checkbox option in order to open the graph of the voltage/current versus time in the "HV Plots" window.

- **HV Plots:** This is the regions where the checkboxed HV sections of the "HV Channels" window graphs of the voltage/current versus time are displayed.

- **Extra Info:** This is the region where user can monitor the sensors that are defined in the "Extra" frame of the "Setup" tab. For example, user car monitor under the "MM Gas" frame, the mass flow, pressure and the humidity of the IP and HO wedge. Also, under the "EnvStation" frame, user can monitor the pressure, environment and humidity value of the environment. Via the "Env Plots" and "Gas" Plots, user can open the corresponding plots.

- **HV Alarm:** In this region, user can have a visually representation of the module under testing. The user has the option to select between two modes, voltage or current representation using the "switch" button. The limits are user-defined and user can set them up though the "Settings" button and the "Alarm Limits" button, procedure that will be described in the next subsections.Near the "switch" button, user can find the voltage or current limits and the color representation for this limits. Also, user has the ability to monitor the Layer's HV sections by left-clicking on the "Layer X" button and the individual HV section by left-clicking in the corresponding HV section in the graphical representation. In the bottom part, user can monitor the status of the HV sections that are in the user defined "green (OK)" area pear Layer and per full Module. By using the histogram, histogram can have a quick idea of the HV status of the module.

- **Archive/Export:** In this region, user can archive and export the all the data which are selected, will be described under details in the next sub-sections.

- Auto-Trip recovery mechanism: User can enable the auto-trip recovery mechanism and set the V_{sub} value. By enabling this, it means that when a HV section will trip and is powering off, the auto mechanism is powering on it and it sets the V_{set} of this value into $V_{set} - V_{sub}$.
- Safety Light: User has the ability to power on-off the HV safety light indication in order to inform lab users that HV is enabled.

Control

User has several options to control the Micromegas's HV sections. In principal, via the HV DCS software user has the ability to control the following parameters of the CAEN boards hardware:

- onOff: This is the power on/off setting of the HV channel
- vSet: This is the voltage setting of the HV channel
- i0: This is the first current limit that the HV channel cannot exceed
- i1: This is the second current limit that the HV channel cannot exceed
- tripTime: This is the time limit which if a HV channel's current value is over i0/i1, it trips
- vMax: This is the max voltage setting that user can insert for safety reasons in order to not exceed it
- rUp: This is the voltage ramping up step of the HV channel, for example 10 V/s
- rDown: This is the voltage ramping down step of the HV channel, for example 10 V/s

User has multiple ways to control the HV sections, from module up to individual sector control, and the ways are the following:

- Sector Control: User has the ability to control all the HV sections of the Micromegas sector by pressing the "Configure". He/she has the ability to select all or individual channel and control all the settings.
- Layer Control: User has the ability to control one individual HV layer of the Micromegas sector pressing a section object, "L1S" for example.
- Quick Control: User has the ability to control the Module or Layer, strips or drift channel in a quick compact way.

Archive/Export

The monitor and control of the HV channels is the first step of the HV validation. The second step is the archiving,exporting and analyzing the data. The HV DCS software has the ability for unstoppable archiving of all the data. In other words, all the HV channel, gas, environment, and GIF++ parameters are archived during the operation of the Micromegas module. As shown in Fig. , user has the ability to start and stop a Run by clicking the corresponding button. By doing this, the time-slot between the start and the end of the run is auto-filled and thus, user can press the "Export" button. By pressing the "Export" button, user is exporting the HV and the "Extra" data which are selected to a user-defined directory specified under the "Dir" text-field. Also, user has the ability to manually select the "Start" and "End" time of the data that he wants to export manually by filling the corresponding fields under the "Timeslot" frame.

8.2.3 LV Station

Via the "LV" button through the HV DCS panel as shown in Fig. 8.3, user has the ability to access the LV Station as shown in Fig. 8.4. User has the ability to power on/off the Analog(MMFE8) and Digital(L1DDC,ADDC) boards via a trigger relay which is interconnected to power supplies and an Arduino.
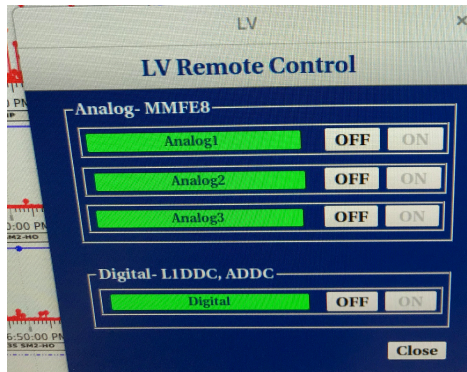
Figure 8.4: The LV Station of the Cosmics Test Stand Station.

8.2.4 SCA Station

Via the "SCA" button through the HV DCS panel as shown in Fig. 8.3, user has the ability to access the SCA Station as shown in Fig. 8.5 and monitor the temperature and power levels of all the electronics boards. The monitor options are described in details in the previous section.
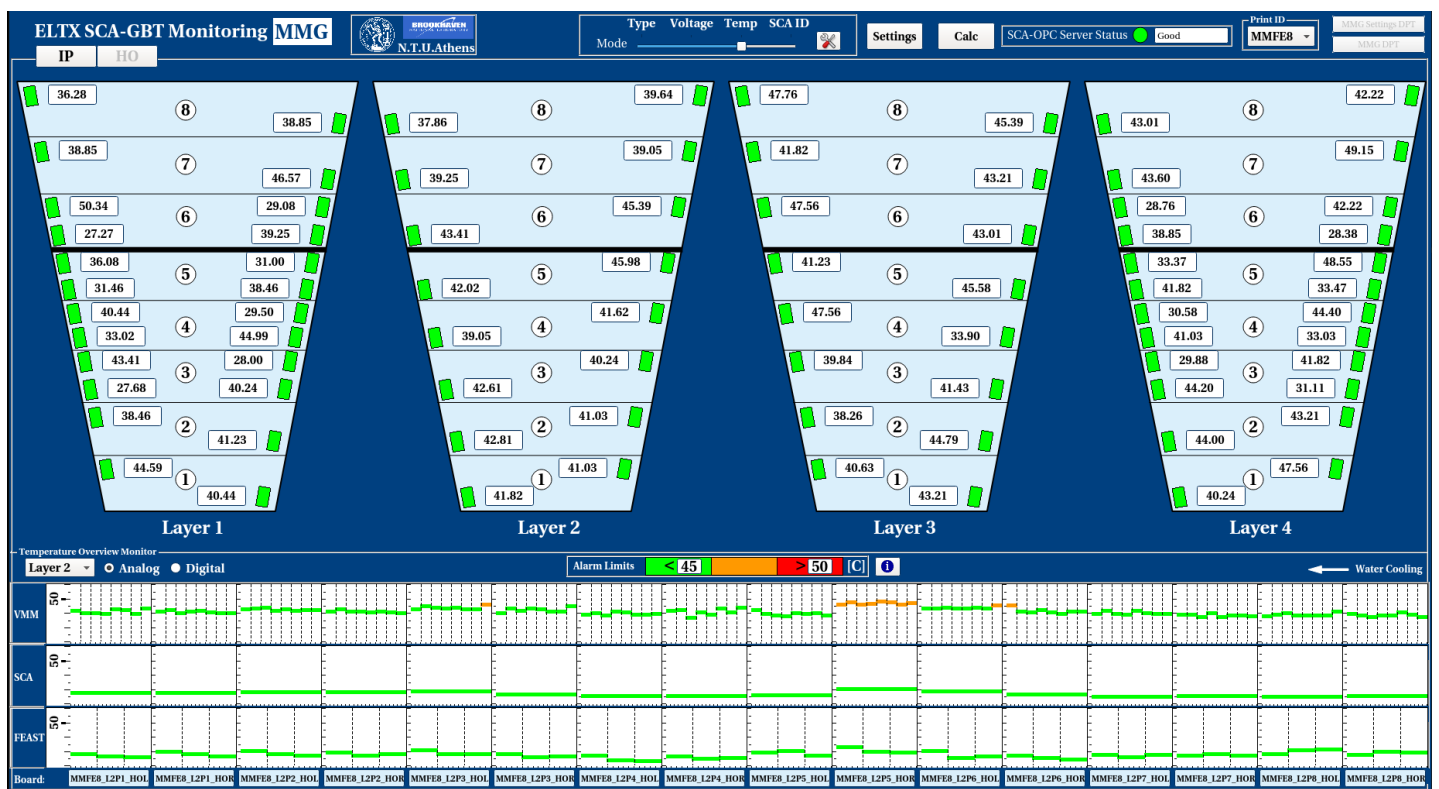
Figure 8.5: The SCA Station of the Cosmics Test Stand Station.

8.2.5 MDM Station

Via the "ELMB" button through the HV DCS panel as shown in Fig. 8.3, user has the ability to access the MDM Station as shown in Fig. 8.6 and monitor the temperature sensors which are installed on the surface of the sector. The MDM Station is designed by the colleague and friend Christos Paraskevopoulos.
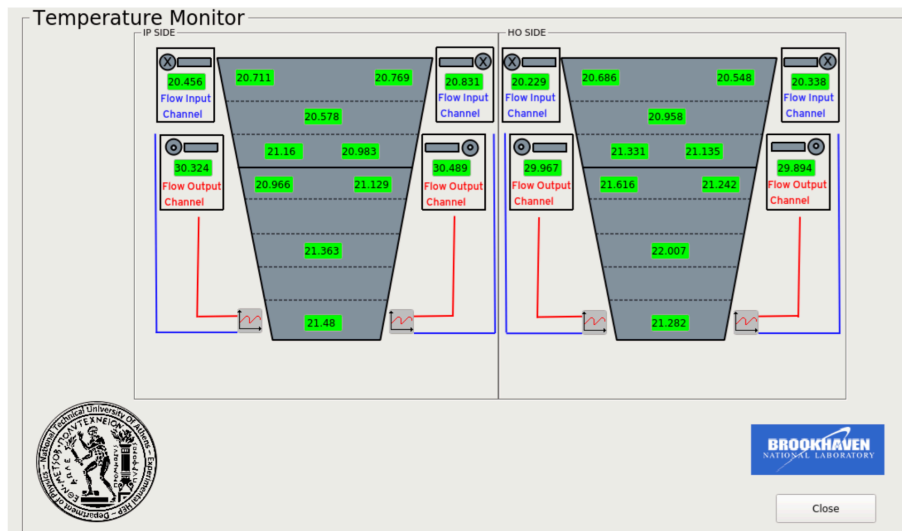
Figure 8.6: The MDM Station of the Cosmics Test Stand Station.

8.2.6 Gas Station

Via the "Gas plots" button through the HV DCS panel as shown in Fig. 8.3, user has the ability to access the Gas Station as shown in Fig. 8.7 and monitor the pressure and humidity sensors which are installed in the gas lines of the Micromegas sector. The pressure sensors system is designed by the colleague and friend Stamatios Tzanos.
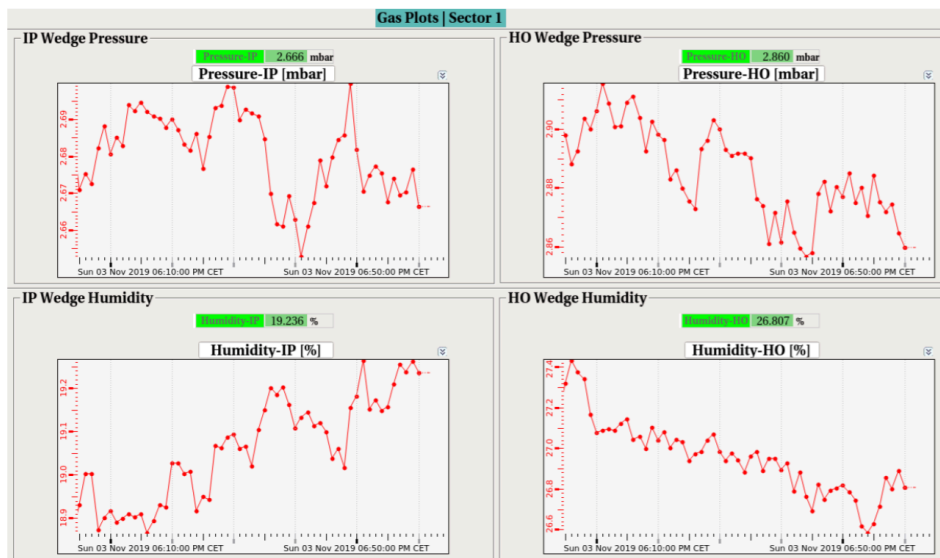
Figure 8.7: The Gas Station of the Cosmics Test Stand Station.

8.2.7 Env Station

Via the "Env plots" button through the HV DCS panel as shown in Fig. 8.3, user has the ability to access the Env Station as shown in Fig. 8.8 and monitor the environment, pressure, humidity and dewpoint levels of the laboratory. The monitor options are described in details in the previous section.
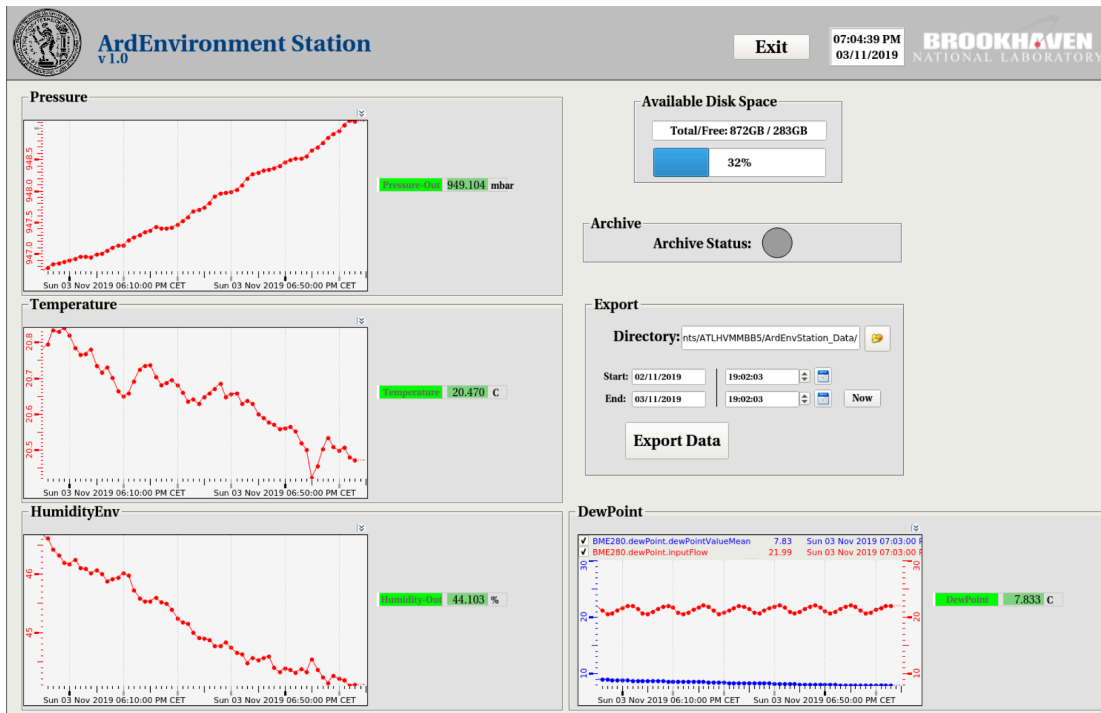
Figure 8.8: The Env Station of the Cosmics Test Stand Station.

8.2.8 Safety Station

The Safety station consists of automatic scripts which are running in the background in order to avoid incidents related to electronics, gas, cooling etc. The alarms which are enable 24h/7d are:

- If input/output flow temperature is over 30 C, the LV is automatically powered off and SMS and email are sent automatically to safety people
- If input/output flow temperature is over 27 C, SMS and email are sent automatically to safety people
- If sector's pressure is over 6 mbar, SMS and email are sent automatically to safety people
- If input flow $T - T_{dewpoint} < 2$ C, SMS and email are sent automatically to safety people

Appendix A

Gas Tightness Station User Manual

Chapter 1

Introduction

The purpose of this document is to constitute a User's Guide of the Gas Tightness Station at BB5 Building of CERN. The National Technical University of Athens has designed and implemented a gas tightness station setup for the Micromegas Quadruplets QA/QC Validation for the New Small Wheel Upgrade Project of ATLAS Experiment. The schematic of the setup and the constructed Gas Tightness Station located at BB5 Building are shown in the below figure.

User must follow the following chapters of the User's Guide step by step to accomplish successful gas leak measurements of the Micromegas Quadruplets.
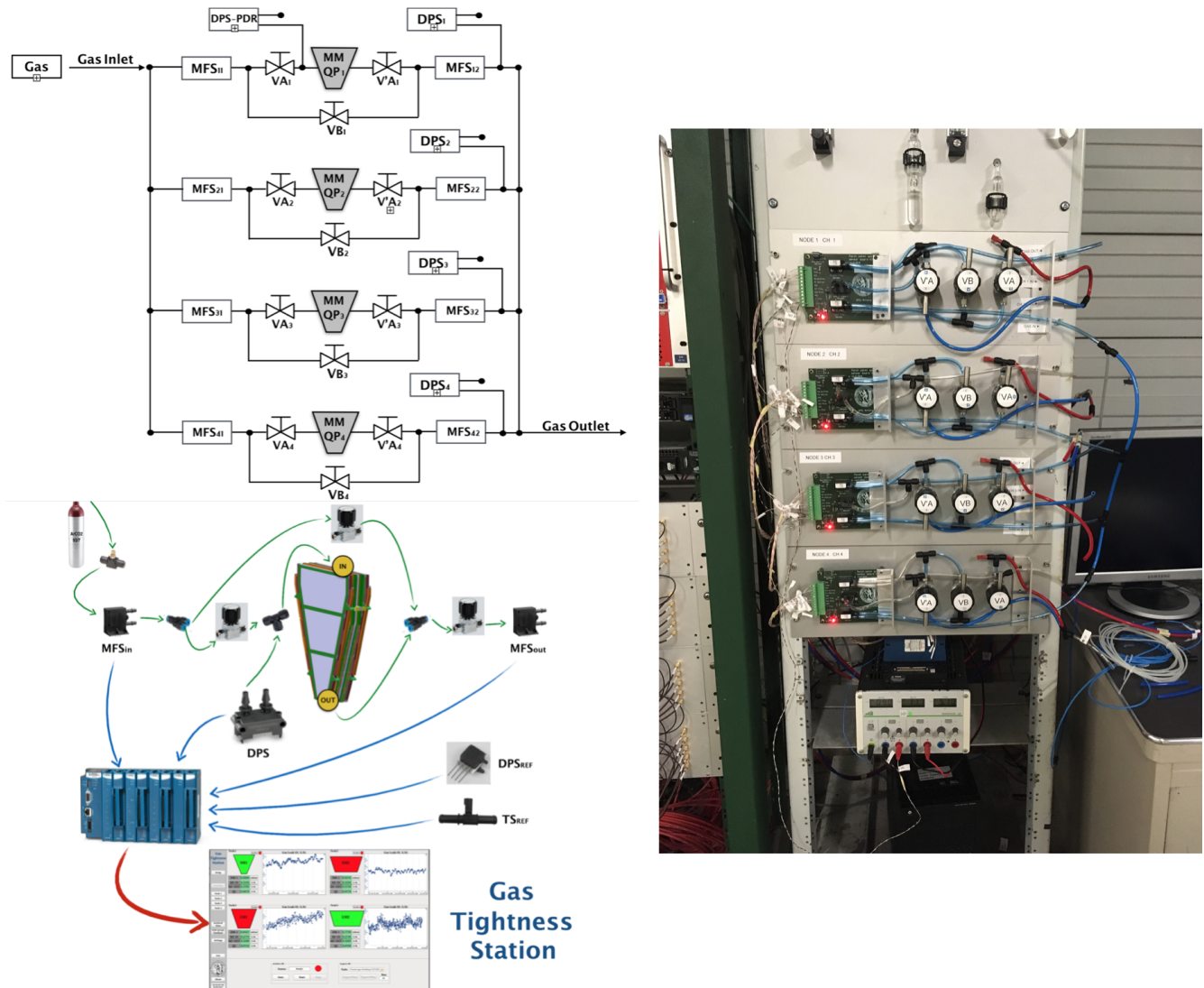
Figure 1.1: Gas Tighrness Station at BB5 Building for Micromegas Quadruplets gas leak measurements.

Chapter 2

Preliminary Procedure

This chapter includes the preliminary procedure that have to completed for the preparation of the Gas Tightness Station prior to Micromegas Quadruplets QA/QC measurements. User must follow step by step the preliminary tasks in order to measure the gas tightness of the MM QPs. Briefly, information about the Gas Tightness Station Software, the Experimental Setup, the Micromegas Quadruplets connection and the Gas Supply are given below. Be advised that these tasks has to be checked always before the start of the gas tightness measurements.

2.1 Gas Tightness Station Software Operation

The GTS software is a mandatory requirement for the MM QPs gas tightness measurements, as a result the software is always open in the Gas Station PC and user is inserted to the "Setup" Tab of the software (Figure 2.1). The "Setup" Tab consists the gas tightness station setup configuration settings for the measurements. In case of previous filled configuration settings, user should press the "Delete Settings" button to reset the setup configuration settings as shown below.
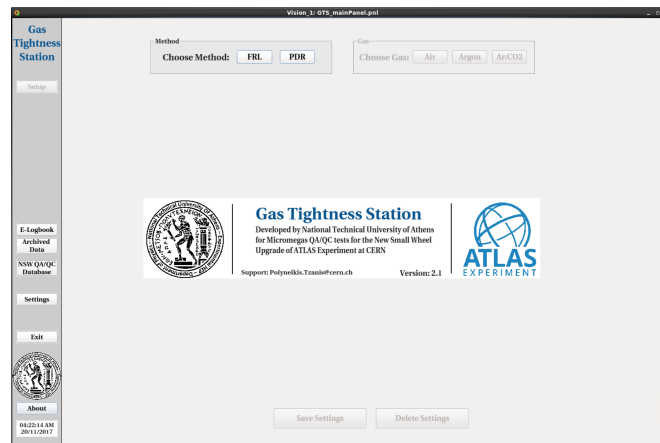
Figure 2.1: "Setup" Tab of GTS software.

> ⚠️ **Warning: If GTS software is closed due to PC shutdown or various reasons, user is forced to follow the steps provided in the Expert Chapter to re-open it.**

> ✅ **Checklist: Check Gas Tightness Software operation**

2.2 Electronic Sensor Boards Operation

The 4 Electronic Sensor Boards of the gas tightness station setup are crucial for the gas tightness measurement and the flushing LED indicator shows the board's power respectively. So, user must check the 4 LED indicators and in case of switched-off LEDs, user must power on the power supply of the boards as seen below with the blue rectangle.
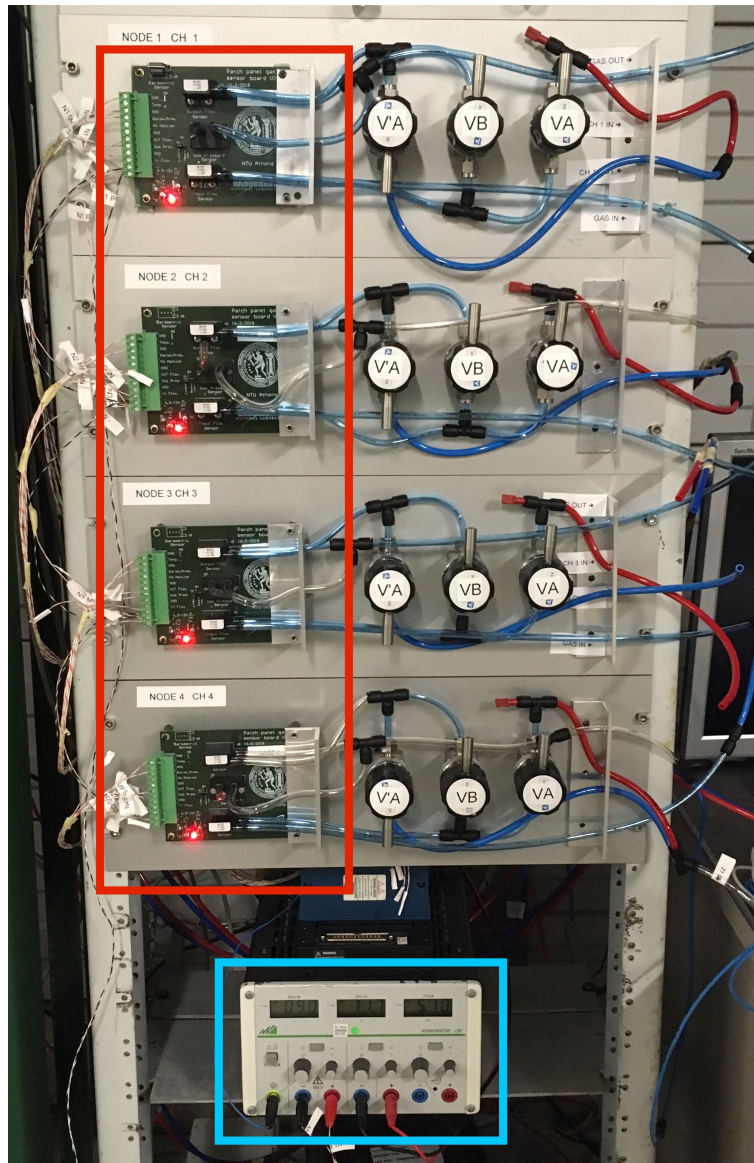
Figure 2.2: Red rectangle: The flushing LED indicator show the power of the electronic sensor board. Blue rectangle: Power supply of the boards.

Checklist: Check 4 Electronic Sensor Boards operation via flushing LED indicator

2.3 FieldPoint OPC Communication

The analog output voltages of the Electronic Sensor Boards are led up to the FieldPoint ADC. User can check the communication with the FieldPoint though the GTS software. Specifically, user can review the communication status by pressing the "OPC DA Client Communication" button under "Settings" Tab, the pop up window consists of 4 Modules of the FieldPoint. However, the current Gas Tightness Setup is operated by Module 1 and Module 3 and user can check the online voltage output of the 8 channels per module. The communication between the FieldPoint and the GTS Software has established when grey field "Disconnected" is disappearing of the Modules (1 and 3) and the channel's values are switching rapidly. It's important to note that in case of power supply reset, communication between the FieldPoint and the GTS Software demands ~ 5 minutes to be established.
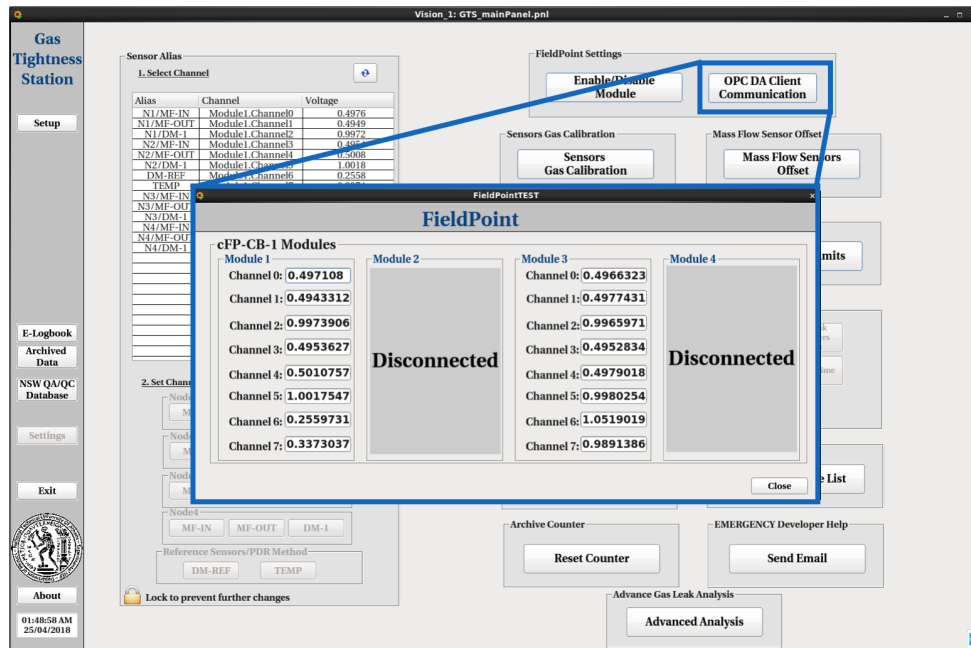
Figure 2.3: Panel for the FieldPoint OPC Communication status.

Warning: If Module 1 and Module 3 are disconnected for several minutes, user is forced to follow the steps provided in the Expert Chapter.

Checklist: Check FieldPoint OPC Communication

2.4   Gas Tightness Setup Preparation

At next step, user must turn the valves of all the 4 patch panels to by-pass mode, by opening VB valve and closing both V'A and VA valves of the 4 patch panels as shown below in the figure.
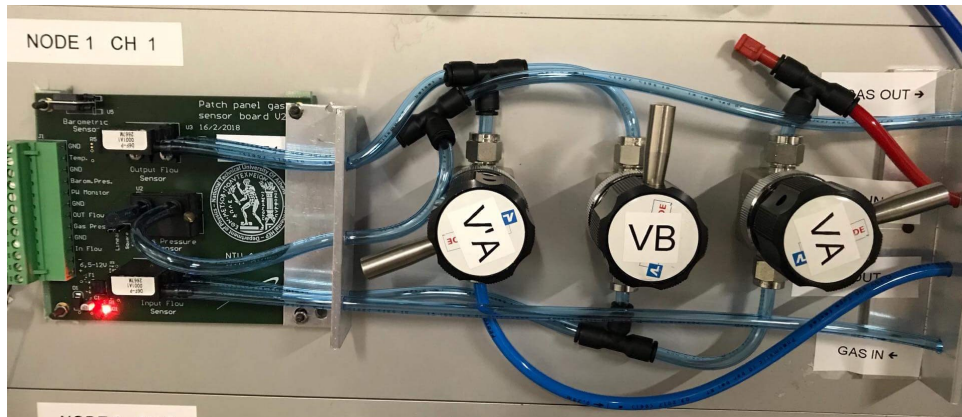
Figure 2.4: Patch panel into by-pass mode by rotating V'A, VA and VB valves.

Also, user must close the gas INPUT flow-meter at the local gas patch panel by rotating it (black rotor) to the right as shown below in the figure (blue rectangle).
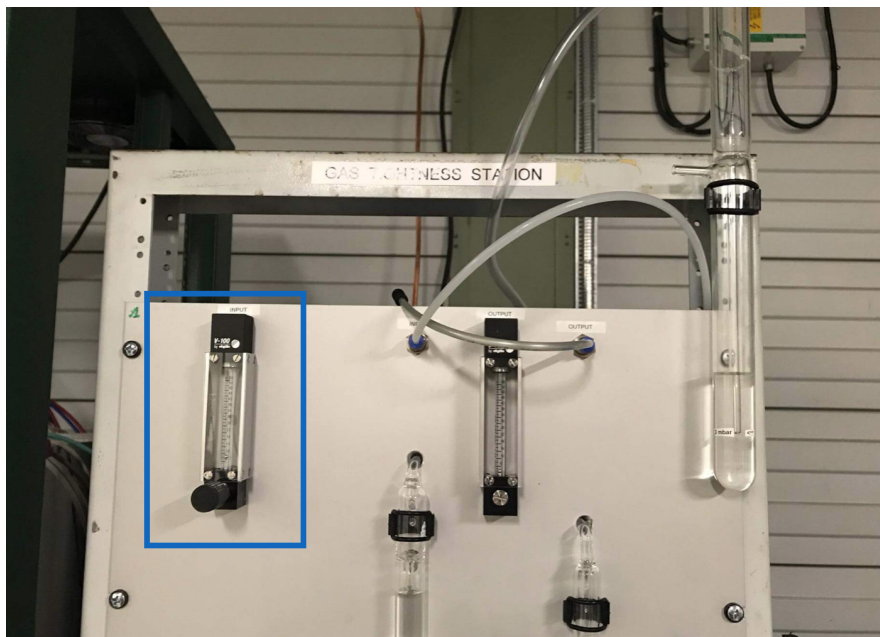
Figure 2.5: Local gas panel and input gas flow-meter (blue rectangle).

Checklist:
1) Turn all 4 patch panel to by-pass mode by opening VB valve and closing both VA and V'A valves
2) Close the INPUT flow-meter (rotating black valve to the right)

2.5   Gas Mixture Ar:CO2 Supply Preparation

For the gas tightness measurements at MM HV and Gas test area, user must open the central gas mixture Ar:CO2 supply which is placed at the Assembly area of BB5 building as shown below. The steps that user should follow are:

1. Turn on ARGON MDT (white valve) and CO2 (black valve) valves by turning them upwards, as shown in the lower picture.

2. Turn on the black valves by turning them upwards as shown below in the top picture.

3. Check the display for the gas mixture rates under the black valves as shown in the top picture.
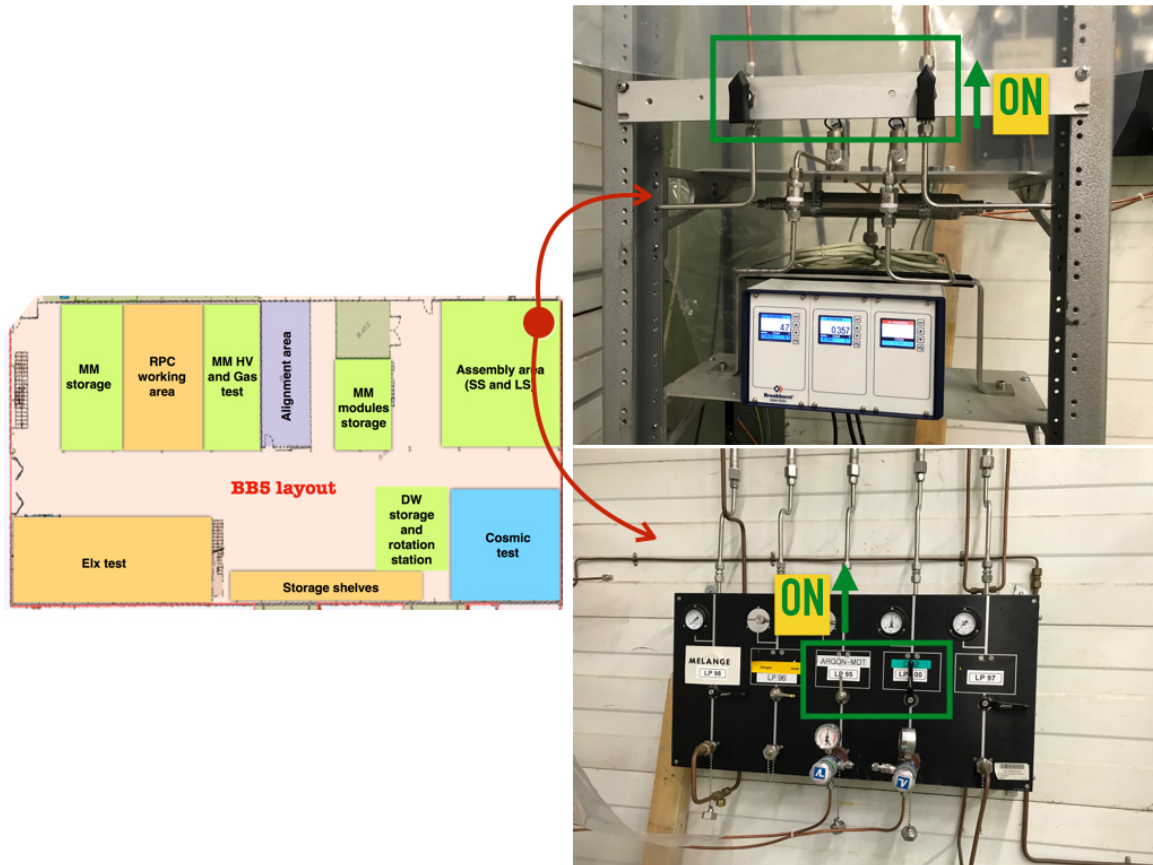
Figure 2.6: Panel for the FieldPoint OPC Communication status.

Checklist: Open Gas Mixture Ar:CO2 Supply valves

2.6 Gas Tightness Station Gas Flow Check

After opening the central gas mixture Ar:CO2 supply, user must return to gas tightness station area and turn left the gas INPUT flow-meter (green rectangle) until the gas bubble inside the pressure gas cylinder reach the black line of 3 mbar (blue rectangle), as shown below in the figure.

Figure 2.7: User turns left the gas INPUT flow-meter (green rectangle) until the gas bubble inside the pressure gas cylinder reach the black line of 3 mbar (blue rectangle).

Next step, user must check the gas supply pressure through all the 4 nodes (patch panels), using the "Check Gas" button under "Settings" Tab of GTS Software. The user must set up the pressure (DM-1) of all the 4 nodes to the nominal pressure of 3 ± 0.2 mbar by turning left the gas INPUT flow-meter (green rectangle). If the node's pressure reaches the nominal value the alarm box status will change to green "ACCEPTED", if it is over the nominal value the alarm box status will change to red "WARNING" where user must decrease the pressure by rotating the input flow-meter until it reaches the nominal pressure and if it is under the nominal value the alarm box status will change to yellow "LIMITED" where user must increase the pressure by rotating the input flow-meter until it reaches the nominal pressure. When all nodes have the nominal pressure (green "ACCEPTED" alarm) and have steady MF-IN values, user can continue with the MM QPs gas leak measurements.
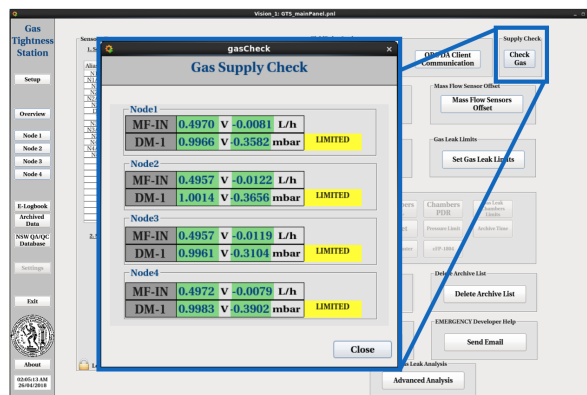
Figure 2.8: Panel for the FieldPoint OPC Communication status.

Warning: ALL Nodes must be set up to nominal pressure of 3 ± 0.2 mbar **(green "ACCEPTED" alarm) and have steady gas inlet flow (MF-IN) before the MM QPs gas leak measurements.**

Checklist: Rotate left the gas flow-meter until it reaches the nominal pressure value of 3 ± 0.2 mbar **using the gas cylinder pressure line and the "Check Gas" button**

Chapter 3

Micromegas QPs FRL Measurement Procedure

3.1 Micromegas QPs - Node Connection

After the successful preliminary procedure, gas tightness station is ready for MM QPs gas leak measurements. The first step that user must follow is to perform the right connection of Micromegas Quadruplets to patch panel Nodes. User must connect the MM QPs to the corresponding Node's inlet tube (red tube) and outlet tube (blue tube), as shown below in the figure. Also, the inlet and outlet tubes includes labeling (CHX IN or CHX OUT) which corresponds to the Node (patch panel) number.
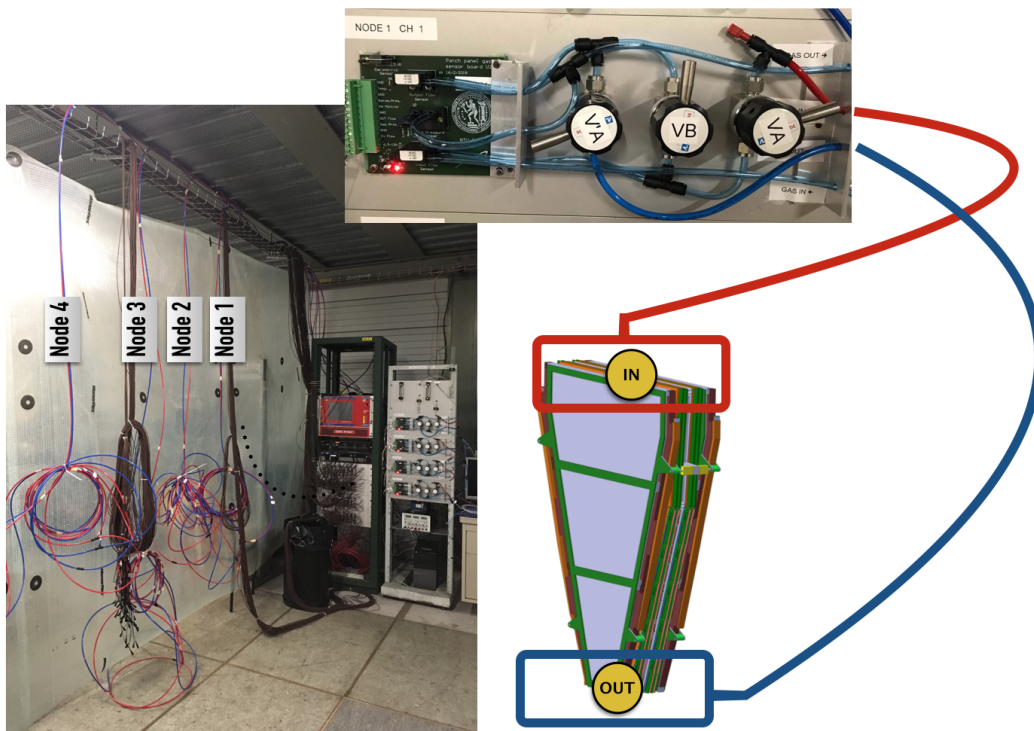
Figure 3.1: Gas inlet (red) and outlet (blue) tube connection layout for the gas flow though MM QPs.

Checklist: Connect the inlet (red tube) and outlet (blue tube) of Micromegas Quadruplet to the corresponding Node (patch panel)

3.2 GTS Software Configuration Setup

Thereafter the MM QPs connection to the nodes, user is ready to configure the gas tightness station through "Setup" Tab in GTS Software and must complete the following steps:

1. Choose the method, Flow Rate Loss (FRL) as baseline method

2. Choose the gas, Ar:CO2 gas mixture

3. Enable the Nodes that corresponds to the connected Micromegas Quadruplets position (see Figure 3.1)

4. Set the type of the Node's corresponding Micromegas Quadruplet

5. Set the 14-digit MTF Batch ID of the Node's corresponding Micromegas Quadruplet

6. Press "Save Settings" button

In case of previous setup configuration, user should press the "Delete Settings" button to set new configuration.
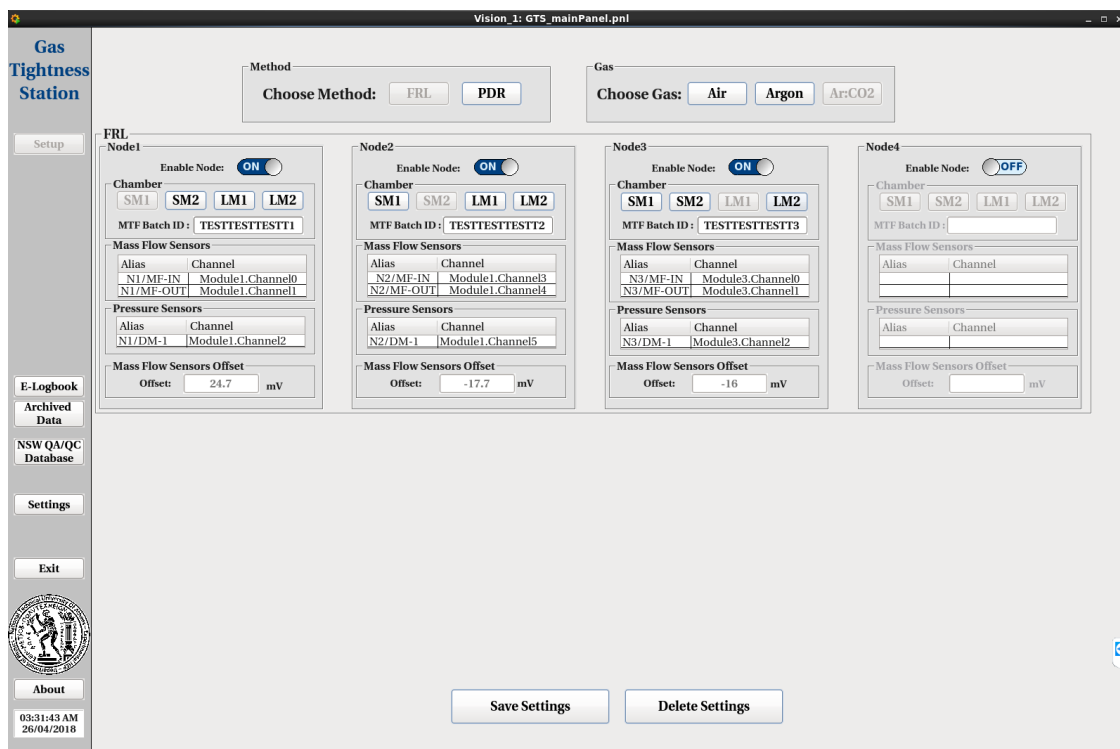
Figure 3.2: Gas Tightness Station Setup Configuration panel through GTS Software.

Checklist: Set the Setup Configuration through Setup Tab of GTS Software by selecting the gas tightness method, the Ar:CO2 gas mixture, enabling and set up the type and MTF Batch ID of Nodes which correspond to the connected Micromegas Quadruplets

After the completion of the setup configuration, 2 monitor modes will become available to user:

1. 1-Node Mode Monitor

2. 4-Node (Overview) Mode Monitor

These monitor modes will be available for switching using the corresponding "Node-X" button for 1-Node Mode Monitor and "Overview" button for 4-Node (Overview) Mode Monitor (detailed description in next page).

3.2.1 1-Node Mode Monitor

The 1-Node Mode Monitor gives user the ability to monitor in real time the values of the mass flow and pressure sensors. The MF-IN displays the Inlet Mass Flow, MF-OUT displays the Outlet Mass Flow, QL displays the Gas Leak, DM-1 displays the pressure of the corresponding connected to the Node MM QP. Also, there is an area which conclude the Node Configuration Information and an area for data Export/Archive of the corresponding Node. The top left plot represents the MF-IN (red line) and the MF-OUT (blue line), the top right plot represent the Gas Leak QL and the down plot represents the pressure of the corresponding MM QP. Furthermore, the alarm box next to QL value displays if the under measurement MM QP is under the nominal limit, "NOT ACCEPTED" for over limit values and "ACCEPTED" for under limit values. Also, the alarm box next to pressure DM-1 value displays if the pressure is close to nominal pressure value of 3 ± 0.2 mbar and warnings are same as described at Chapter 2.6.
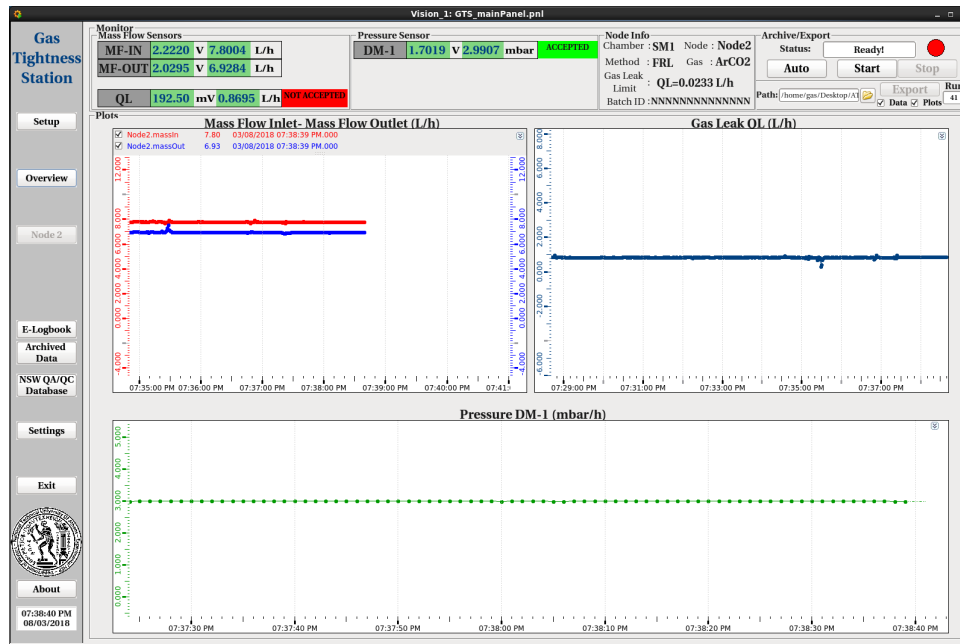
Figure 3.3: Gas Tightness Station 1-Node Mode Monitor.

3.2.2 4-Node (Overview) Mode Monitor
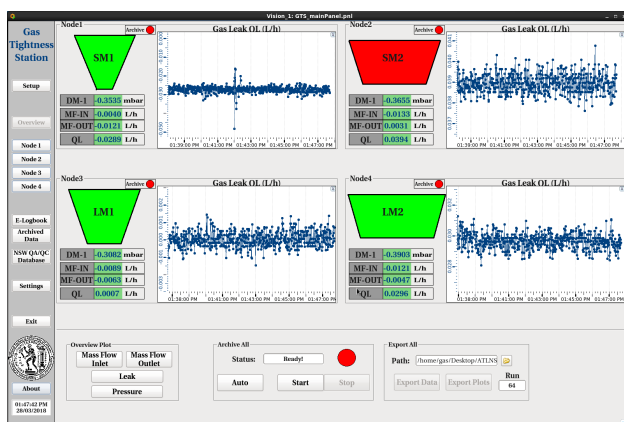
The 4-Node (Overview) Mode Monitor gives user the ability to monitor in real time the values of the mass flow and pressure sensors and gas leak acceptance of all the MM QPs that has been connected to the gas tightness setup. The MF-IN displays the Inlet Mass Flow, MF-OUT displays the Outlet Mass Flow, QL displays the Gas Leak, DM-1 displays the pressure of the corresponding connected to the Node MM QP. Also, the color of the MM QP frame represents if the corresponding gas leak of the Chamber is under the acceptance limit, red for over limit or green for under limit. The "Archive" box over the chamber frame displays the archiving status of the corresponding Node. The plot next to the chamber frame displays the MM QP's gas leak. Additionally, user can display overview plots of all the connected MM QPs by selecting the sensor's corresponding button under the "Overview Plots" area. Finally, there are the areas of "Archive All" and "Export All" for simultaneously archiving/exporting of all connected MM QPs.

3.3 Micromegas QPs Flushing Procedure

Before the MM QPs flushing procedure, user must re-check if Node's pressure DM-1 is at the nominal value of 3 ± 0.2 mbar using the alarm box near DM-1 and if the gas flow MF-IN and MF-OUT are steady by viewing the Mass Flow Inlet-Mass Flow Outlet Plot in 1-Node Mode or the "Mass Flow Inlet" button under "Overview Plots" frame in 4-Node Mode.
After re-checking pressure and mass flow inlet of the connected to Node MM QP, user is ready to switch the patch panel valves to leak mode by rotating the V'A, VA and VB valves of the corresponding Node's patch panel to MM QP as shown below in the figure.
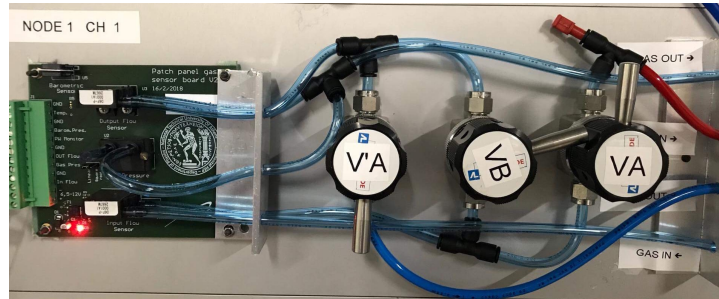
Figure 3.4: Patch panel into leak mode by rotating V'A, VA and VB valves.

After rotating the Node's corresponding valves into leak mode, the MM QP flushing procedure begins. User can monitor the flushing of the Node by checking the top left plot of Mass Flow Inlet-Mass Flow Outlet and the top right plot of Gas Leak. User can observe an steady mass flow inlet MF-IN (red line) and a slight increase of mass flow outlet MF-OUT (blue) or a decreasing of the gas leak in the top right plot. The MM QP's flushing procedure is completed until MF-IN and MF-OUT lines, in the top left plot, approaching steady state (parallel lines) or the QL line in the top right plot approaching steady state (straight line). Important to be mentioned that flushing procedure depends on the corresponding MM QP volume and demands ~ 30 minutes. When flushing procedure of current Node or all the connected Nodes is ready, user can continue to gas leak measurement (see next Chapter).
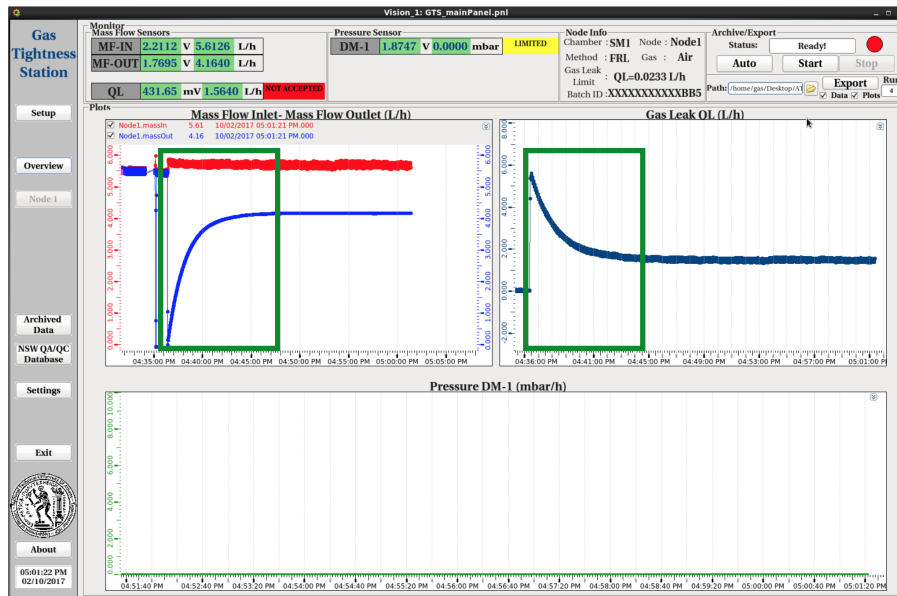
Figure 3.5: MM QP's flushing procedure (green rectangle).

⚠ **Warning: 1) Configure steady Mass Flow Inlet and nominal Pressure before flushing!**
2) Flushing depends on the corresponding MM QP volume and demands ~ 30 minutes!

✅ **Checklist: Set Node's valves to leak mode and monitor flushing procedure through GTS Software**

3.4 MM QPs Gas Leak Measurement (Baseline)

After the successful flushing procedure, until MF-IN and MF-OUT line in the top left plot approaching steady state (parallel lines) (black rectangle) or the QL line in the top right plot approaching steady state (straight line) (black rectangle), user can continue to MM QPs gas leak measurement.

When Node is in steady status as shown with black rectangle in the figure below, user can start the gas leak measurement and the archiving of data by pressing the "Auto" button under "Archive/Export area" in 1-Node Mode Monitor which lasts 5 minutes (default value). After 5 minutes of measurement the circle's alert status turn to red and a yellow pop-up box is displayed to inform user that the measurement has finished. At the same time "Export" button becomes available and user can export data and plots to default directory (/Gas_Exported_Data inside project folder) or in a predefined directory by pressing the "folder" icon.

In summary the steps of MM QPs gas leak measurement are:

1. Wait for the flushing procedure to be completed and MM QP transits to steady status (MF-IN, MF-OUT, DM-1, QL)

2. Archive data for 5 minutes by pressing "Auto"

3. Yellow Pop-up windows is displayed for the Node's corresponding end archiving procedure after 5 minutes

4. Press "Export" button to export plots and data to default directory or predefined directory by tapping "folder" icon

The exported data or plots are saved under the directory with filenames "run_X.dat" and "run_X_plot.png" where X is the number which is displayed near "Export" button.
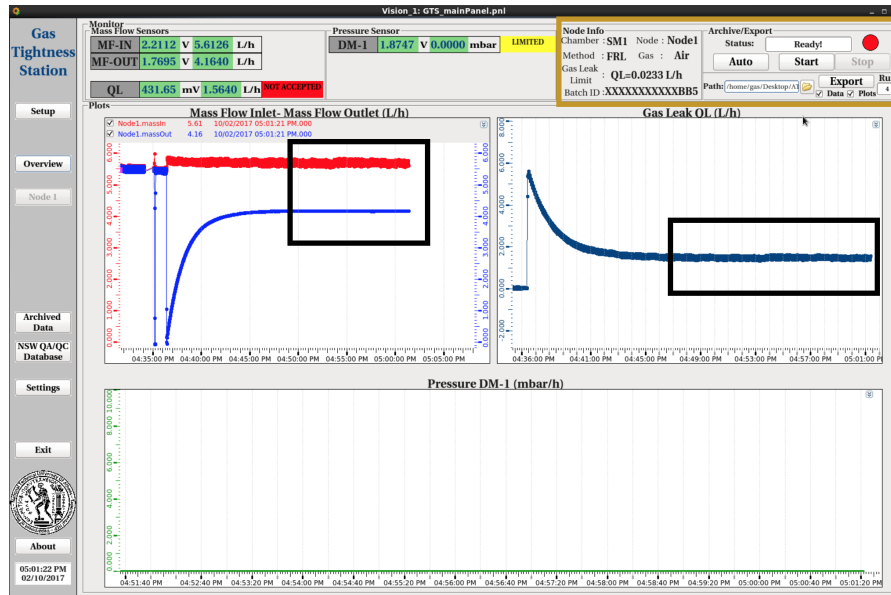
Figure 3.6: MM QP's gas leak measurement area (black rectangle) and archive/export area (yellow rectangle).

Figure 3.7: Archive/Export of all connected Nodes simultaneously

Also, GTS software gives the ability to archive the data of all the connected Nodes by tapping "Auto" button under "Archive All" frame. When the archiving of all Nodes is ready after 5 minutes a yellow pop-up window is displayed and "Export Data/Plots" buttons become available. By tapping "Export Data" button user exports the data with the filename "run_X.dat" and by tapping "Export Plots" button exports the plots with the filename "run_X_plot_K.png", where X is the number which is displayed near "Export Data/Plots" button and K is the corresponding Node number, to default directory (/Gas_Exported_Data inside project folder) or in a predefined directory by pressing the "folder" icon.

3.4.1 Results Review

User can review the gas leak measurements results by accessing the exported data or plots which are saved under the directory with filenames "run_X.dat" and "run_X_plot.png" where X is the number which is displayed near "Export" button. The form of data file is shown in below figure.

Figure 3.8: Exported data file form.

The form of exported plot is show in below figure.
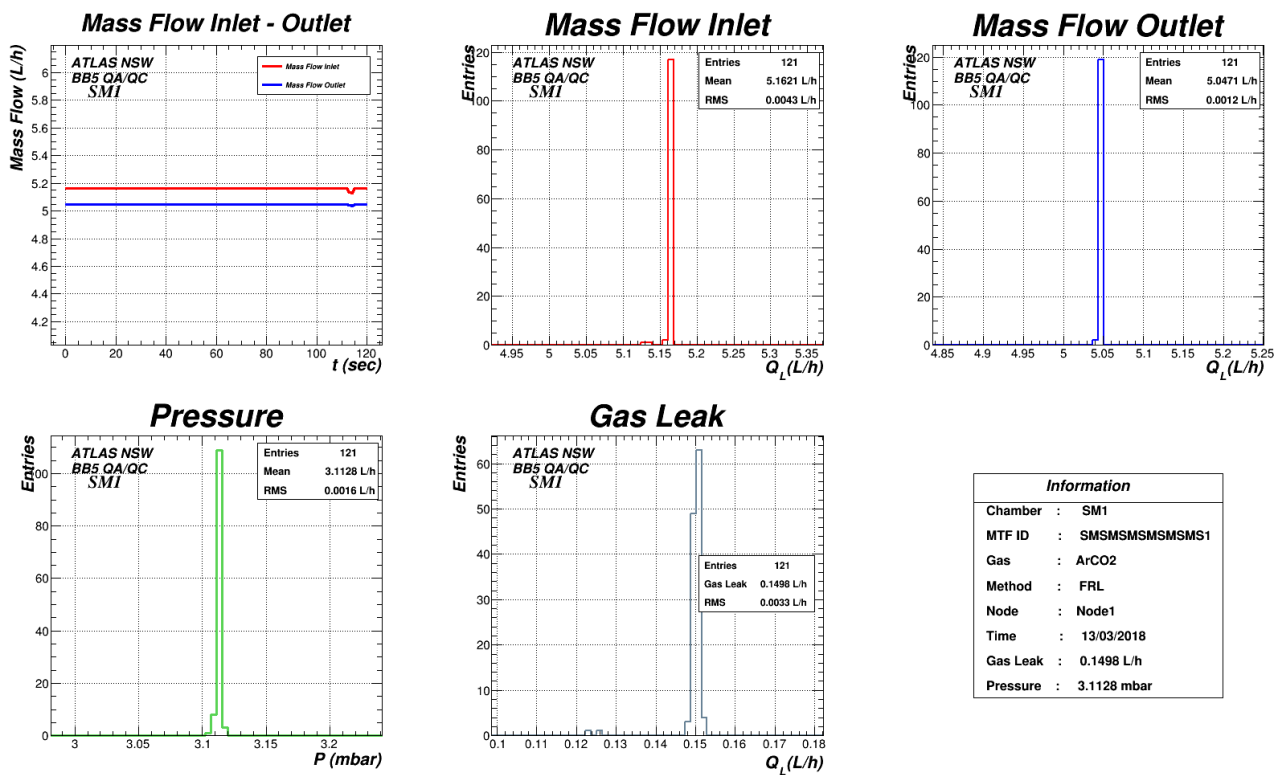
Figure 3.9: Exported plot file form.

Checklist: Wait for the flushing procedure to be completed and transition to steady status, archive and export the data of the corresponding Node or all Nodes by pressing the "Auto" and "Export" buttons

Warning: User can now move to Chapter 4 for data storing, otherwise in difficult gas leak measurements with very low leak rates ($Q_L \leq 0.0200 \, \text{L/h}$), user must follow the Advanced Analysis Procedure described in the next section.

3.5 Advanced Analysis Procedure

⚠️ **Warning: This procedure must implemented in difficult gas leak measurements with very low leak rates** ($Q_L \leq 0.0200\,\mathrm{L/h}$)

The advanced analysis procedure demands two different measurements at the same MM QP, the offset and the leak distribution measurement. The steps for advanced analysis procedure are:

1. Switch Node's patch panel valves into by-pass mode (see Figure 2.4)

2. Archive and Export data by tapping "Auto" and "Export" (Offset File)

3. Switch Node's patch panel valves into leak mode (see Figure 3.4)

4. Archive and Export data by tapping "Auto" and "Export" (Gas Leak File)

Then, user must move to "Settings" tab of GTS software and tap the "Advanced Analysis" button. In the pop-up windows, as shown below, user must choose the "Gas Leak File" and the "Offset File" by tapping the "folder" icon. When user have selected the two files the "Analysis" button becomes available and user choosing between "Basic or Basic+Fit" option exports the advanced analysis plot under the default directory (/Gas_Exported_Data inside project folder).
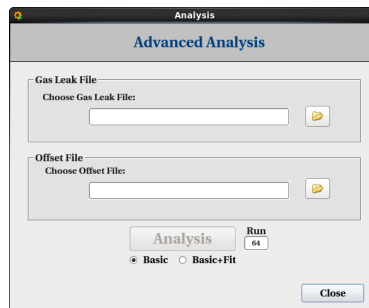
Figure 3.10: Advanced Analysis Panel via tapping "Advanced Analysis" button through "Settings" tab of GTS Software.

The exported plot is saved with file name "advancedAnalysis_X.png" where X is the run number which is displayed next to "Analysis" button.

3.5.1 Advanced Results Review

The form of the advanced analysis plot is shown in the below figure.
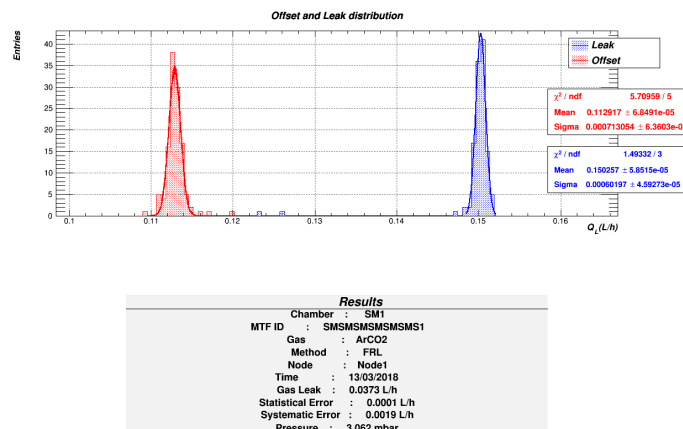
Figure 3.11: Exported advanced analysis plot file form.

Chapter 4

Data Access and Storing

4.1 Access Archived Data History

The GTS software provides a local database where user has the ability to access old archive data by tapping "Archived Data" button which is placed in the left side of software. The pop-up window, as shown in the below figure, user can search old data by MM QP type or the MTF Batch ID. The steps to retrieve old data are the following:

1. Search by MM QP type of MTF Batch ID

2. Select the covetable line of the measurement by tapping the line

3. Pressing "Set Export Parameters"

4. Export Data/Plots

User exports data and plots to default directory (/Gas_Exported_Data inside project folder) or in a predefined directory by pressing the "folder" icon.
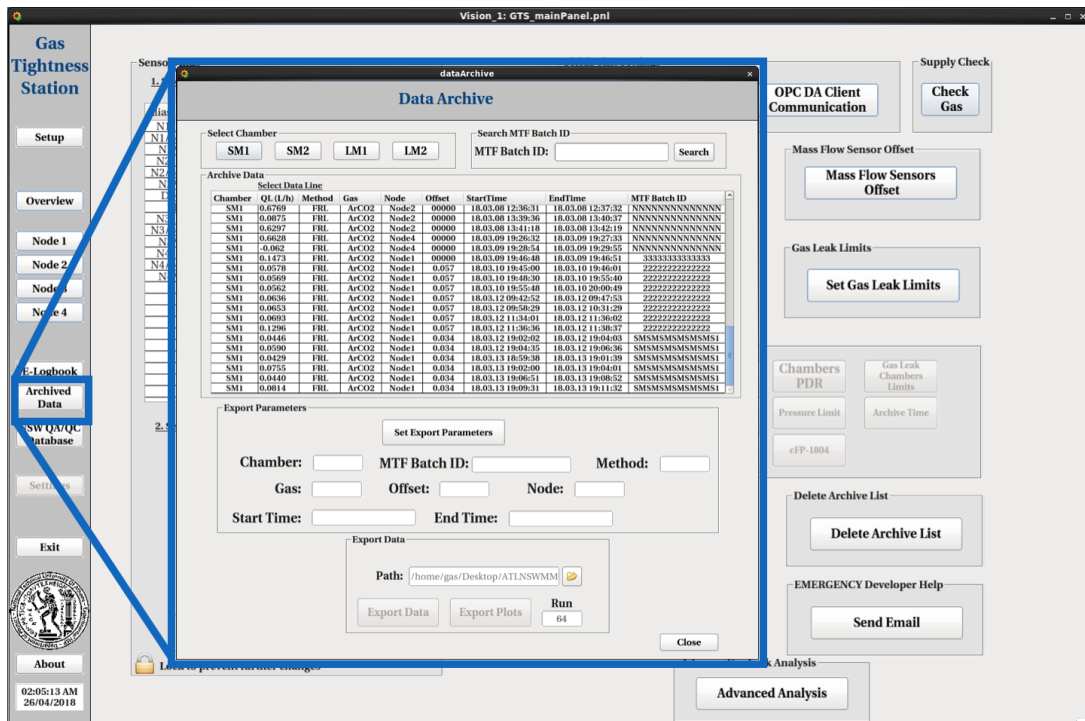
Figure 4.1: GTS Software panel to access old archived data by MM QP type or MTF Batch ID.

4.1.1 NSW QA/QC Database Data Store

The GTS Software provides user the ability to store data directly to the NSW QA/QC Database by tapping "NSW QA/QC Database" button which is placed in the left side of software. The steps to store data to NSW DB are:

1. Open NSW QA/QC Database by tapping "NSW QA/QC Database"

2. Choose Shifter and press "OK" button

3. Select "EQ" tab, press "Load EQ" button and type the MM QP's MTF Batch ID and press "Yes" button

4. Select "Test" tab, press "Start Test" button, select the QA/QC result according to the acceptance limit of the measured MM QP, comment the gas leak and pressure or any other comments of the measurement and press "Send Comment"

5. Press "Add File" and select the measurement plot

6. Press "Commit Measurement" button
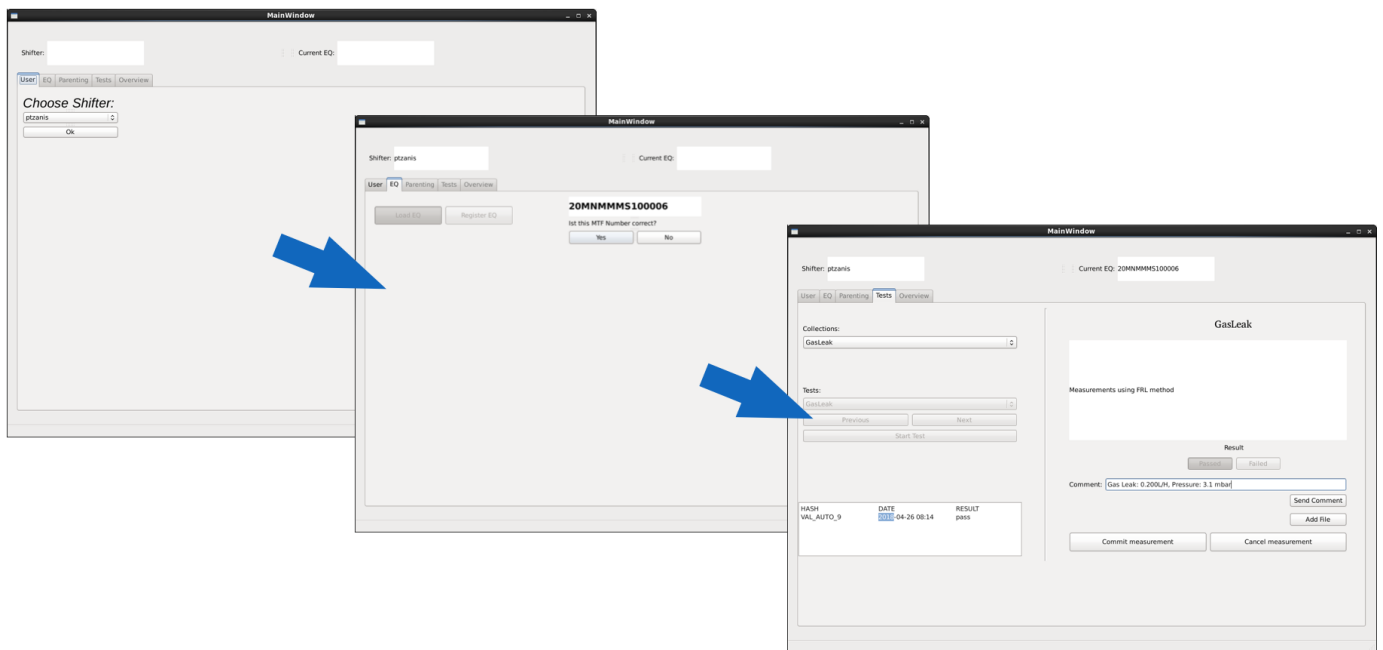
Figure 4.2: Freiburg UI within GTS software for sotring data directly to NSW QA/QC Database

Checklist: Store the gas leak results to NSW QA/QC Database

Warning:
1) QA/QC results (Passed/Failed) depends on the comparison between MM QP's gas leak measurement and MM QP's acceptance limits
(MM QPs acceptance limits: $SM1 = 0.0233\,\text{L/h}, SM2 = 0.0259\,\text{L/h}, LM1 = 0.0384\,\text{L/h}, LM2 = 0.0370\,\text{L/h}$**)**
2) Storing data to the NSW QA/QC DB is very crucial and user must be careful, as a result user stores one by one the MM QP's measurement

4.2 Online Data Store

The GTS Software gives user the ability to store data to the online Micromegas Gas Tightness Station E-Logbook by tapping "E-Logbook" button which is placed in the left side of software. The steps to store data to e-logbook are:

1. Press "E-Logbook", at the new window press "Edit in Browser" and fill the columns (orange lines)

2. Pressure "Documents", at the new window press "Upload" to store data and plot files (green lines)

Figure 4.3: Online Micromegas Gas Tightness Station E-Logbook to store data and plots within GTS Software.

Checklist: Store the gas leak results to Micromegas Gas Tightness Station E-Logbook

Chapter 5

Quick Step by Step Quide for FRL Measurement

The summary MM QP Measurement Procedure steps that user must follow before the measurements are:

Preliminary Tasks

1. Check Gas Tightness Software operation

2. Check 4 Electronic Sensor Boards operation via flushing LED indicator

3. Check FieldPoint OPC Communication

4. Turn all 4 patch panel to by-pass mode by rotating the V'A, VA and VB valves and close the gas input flow meter by rotating the black rotor

5. Open Gas Mixture Ar:CO2 Supply valves

6. Rotate the gas flow-meter until it reaches the nominal pressure value of 3 ± 0.2 mbar using the gas cylinder pressure line and the "Check Gas" button

Micromegas QPs FRL Measurement Procedure

7. Connect the inlet (red tube) and outlet (blue tube) of Micromegas Quadruplets to the corresponding Node (patch panel)

8. Set the Setup Configuration through Setup Tab of GTS Software by selecting the gas tightness method, the Ar:CO2 gas mixture, enabling and set up the type and MTF Batch ID of Nodes which correspond to the connected Micromegas Quadruplets

9. Set Node's valves to leak mode and monitor flushing procedure through GTS Software

10. Wait for the flushing procedure to be completed and transition to steady status, archive and export the data of the corresponding Node or all Nodes pressing the "Auto" and "Export" buttons

11. Perform advanced analysis procedure in difficult gas leak measurements with very low leak rates ($Q_L \leq 0.0100$ L/h)

Data Access and Storing

12. Access old archived data history

13. Store the gas leak results to NSW QA/QC Database

14. Store the gas leak results to Micromegas Gas Tightness Station E-Logbook

Chapter 6

ArdEnvironment Station

This chapter includes information about the ArdEnvironment Station that have installed within Gas TIghtness Station and Muon Test Stand at BB5.

6.1 Setup Wiring

The ArdEnvironment Station consists of an Arduino Mega 2560 Board, Wiznet W5500 Erthernet board and the Adafruit BME 280 sensor for pressure, temperature and humidity measurements. The below figure includes the Arduino-Wiznet setup, the BME280 sensor and also the wire labeling connection between the Arduino and the sensor. After the wire connection, user can check for the right connection between the Arduino and the sensor by power on the Arduino and check the flushing blue LED.

If blue LED doesn't flush, user must check the wire connection, **press the white button** for Arduino Soft Reset on the top right side of red Wiznet board and re-check the blue LED as shown below.

Figure 6.1: **Left:** The ArdEnvironment setup consists of the Arduino Mega 2560 and the Wiznet 5500 Ethernet Shield, **Top Right:** The BME280 sensor for pressure, humidity and temperature measurements, **Bottom Right:** The wire connection between Arduino and BME280 sensor

> ✅ **Checklist: Perform the right connection between the Arduino and the BME280 sensor by checking the blue LED**

6.2   OPC DA Server Operation

If blue LED flushes, user can connect the Arduino to a computer via an ethernet cable. The IP of the Arduino is **10.0.0.10**, so for the right connection with the computer user must set computer's static ip under the same subnet (10.0.0.X). Also, user can test the connection with Arduino by executing the following command via terminal and checking the output:

```
>   ping 10.0.0.10
```

If ping is successful, the steps which user must follow to establish the Arduino OPC DA Server operation are:

1. Open "OPC Server for Arduino/Genuino" program as administrator under Windows

2. Press "Arduino Ethernet" Tab and insert 10.0.0.10 in "Arduino IP" field and 80 in "Port" field

3. Press "Save Configuration" button and close the window by tapping "X" icon

4. Run "register.bat" file as administrator

5. Open "OPC Server for Arduino/Genuino" program as administrator under Windows

After the completion of these steps, the OPC DA server forwards the sensor's values to WinCC-OA software. Also, it is important to be mentioned that "OPC Server for Arduino/Genuino" program is initialized in minimized mode under the Notification area of Windows down right.

Figure 6.2: Configuration and start of Arduino OPC DA Server under Windows partition.

Checklist: Start of Arduino OPC DA Server

Warning: In case of Arduino power off or Ethernet cable switch off, user must follow the following steps to re-establish the OPC DA Server operation:

1. **Re-open "OPC Server for Arduino/Genuino" running program**

2. **Press "Delete Configuration" button and close the window by tapping "X" icon**

3. **Run "unregister.bat" file as administrator**

4. **Repeat the initially steps 1-5 for the establishment of the Arduino OPC DA Server operation**

6.3   ArdEnvironment Station Software

The ArdEnvironment Station Software can be accessed from GTS Software by pressing "ArdEnvironment Station" button. The main panel consists of 3 plots and values which display the pressure, temperature and humidity values respectively as shown below.

Figure 6.3: ArdEnvironment Station main panel, user can monitor and archive/export the pressure, temperature and humidity.

User can archive pressure, temperature and humidity values simultaneously by pressing "Start" button under "Archive" area. The default sampling time is set to 1 mean value per 1 minute but user can adjust sampling time settings by pressing the "Settings" icon under "Archive" area. Under "Export" area, user can export the archived data for specific user-defined time slot, by selecting the start and end date/time. Software gives the ability to export the archived data as data file "ArdEnvStation_Start_TO_End.dat" or plots file "ArdEnvStation_Plots_Start_TO_End.png", where "Start" and "End" are the user-defined time slot, in the default output directory inside the project folder "ArdEnvStation_Data" or a user-defined directory by pressing "Folder" icon. The form of the exported data and plots are shown below. Finally, archive must be always ON (green indicator), otherwise user must press the "Start" button.

Figure 6.4: Form of exported data and plots using ArdEnvironment Station.

**Warning: 1) If sensor's values don't change for several minutes, user must restart OPC Server by closing the "OPC Server for Arduino/Genuino" running program, then it restarts automatically. In case of computer power off, user must follow the steps given in Expert chapter.
2) Archive must be always "ON" (green indicator), otherwise user must press the "Start" button**

Checklist: Operation of sensor by checking values and confirmation of the "ON" Archive status

Chapter 7

Expert

7.1 Computer Shut Down

In the case of computer shut down of Gas Tightness Station's computer, user must accomplished the following steps for the reinstatement of the station.

Step 1 - Start of GTS Software

User must open the project (ATLNSWMMGTSBB5) via WinCC-OA Project Administration. The WinCC-OA Project Administration icon can be accessed by tapping the icon (blue rectangle), next user click on the ATLNSWMMGTSBB5 project and pressure the "green" button (green rectangle) and after some seconds the GTS Software will be automatically opened.
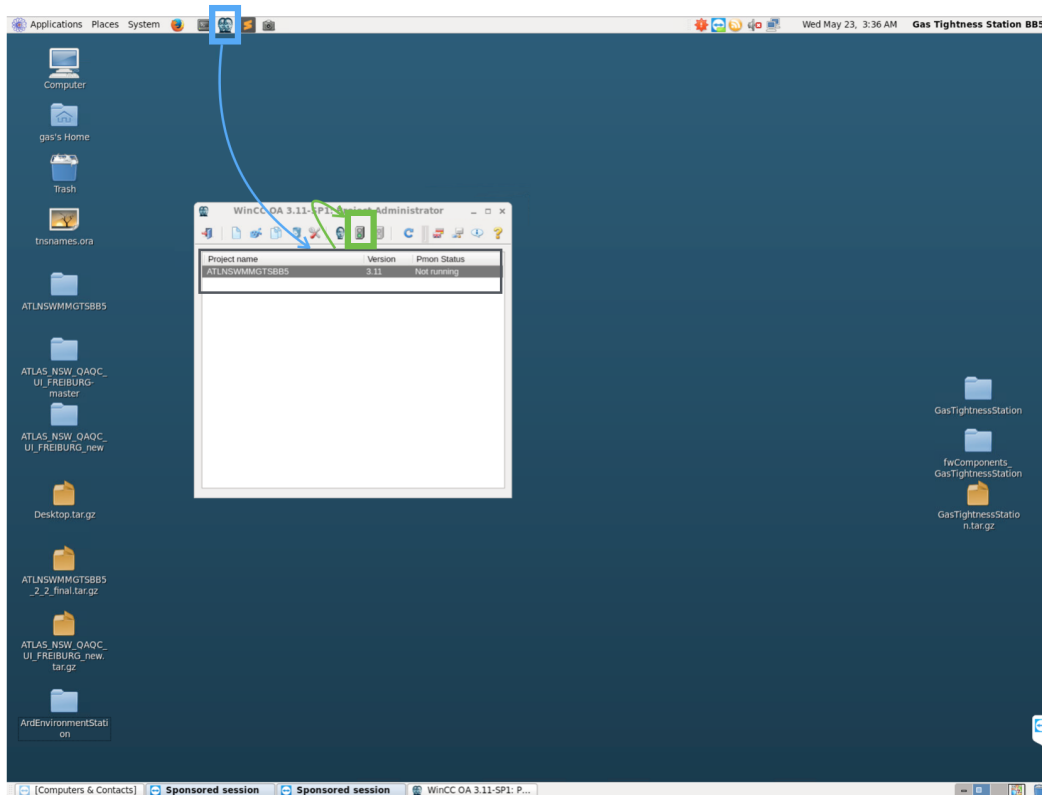
Step 2 - Start of Windows Virtual Machine

User executes the following command in Linux terminal to open Virtualbox program:

```
>    sudo virtualbox
```

After, under the opened "Oracle VM VirtualBox Manager" user chooses the "win7opc" option and presses the "Start" button to start the Windows VM as shown below.
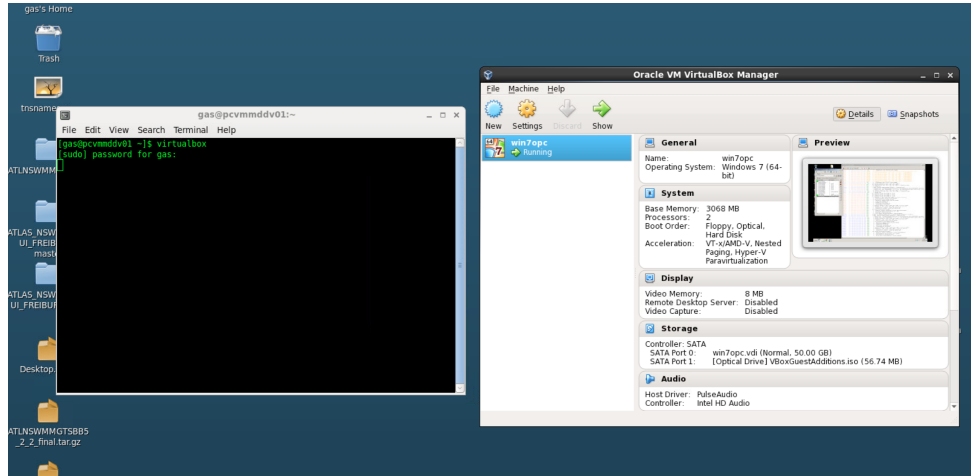
Step 3 - Start of WinCC-OA inside Windows

Inside Windows VM, user opens the WinCC-OA Project Administration by tapping the icon (blue rectangle), next user click on the OPCFIELDPOINT project and pressure the "green" button (green rectangle) to start the OPC DA Servers of FieldPoint and Arduino.
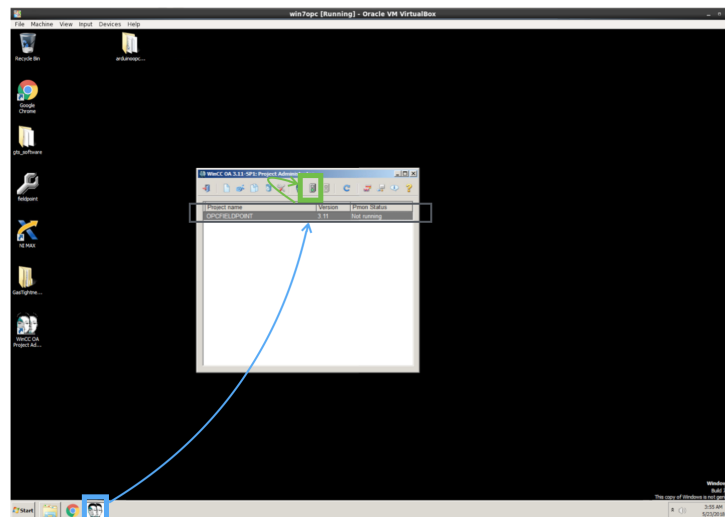
Step 4 - Check

After 2-3 minutes, user can check for the successful operation of the GTS software and FieldPoint and Arduino hardware by checking the values by tapping "OPC DA Communication" button under "Settings" Tab of GTS Software. In the case of not changing values, user must re-check all the above steps.

> ⚠ **Warning: User must have check the main power supply's status which is placed under the gas patch panels which supplies GTS Electronic Boards, FieldPoint and Arduino.**

7.2 Emergency Help

The GTS software gives user the ability to request help from the software's developer by sending email directly of GTS Software by tapping "Send Email" under "Settings" Tab. The user fills his name and email and also the comment/problem. By pressing "Send Email", a mail is been sending to the developer and user will get a reply in his email.
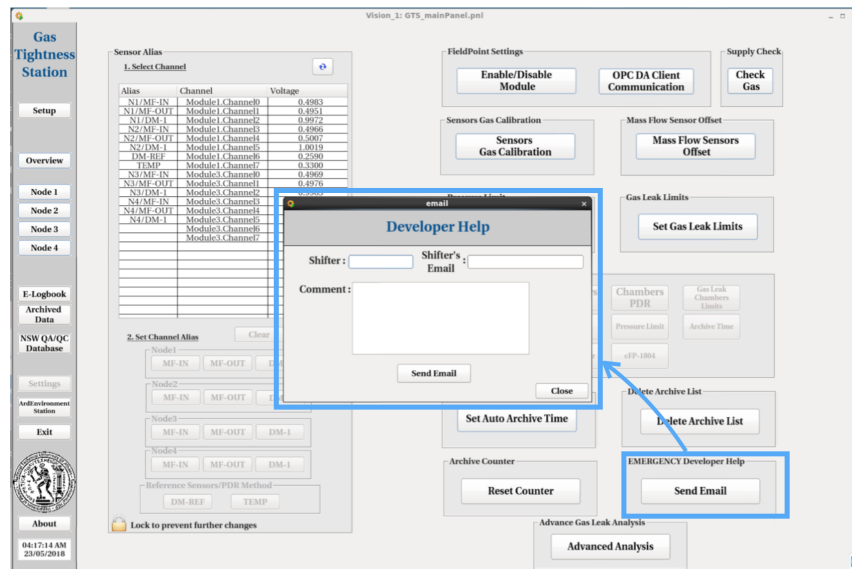
7.3 Software Requirements

Gas Tightness Station

1. WinCC-OA 3.11/3.15 (Linux & Windows)

2. OPC Core Components Redistributable x64 106.0 (Windows)

3. National Instruments Measurement and Automation Explorer 16.0.1 (Windows)

4. National Instruments FieldPoint (Windows)

ArdEnvironment Station

1. WinCC-OA 3.11/3.15 (Linux & Windows)

2. OPC Core Components Redistributable x64 106.0 (Windows)

3. OPC DA Server for Arduino/Genuino (Windows)

List of Figures

Bibliography

[1] Oliver Sim Bruning, Paul Collier, P Lebrun, Stephen Myers, Ranko Ostojic, John Poole, and Paul Proudlock. LHC Design book. CERN Yellow Reports: Monographs. CERN, Geneva, 2004.

[2] Carlo Wyss. LEP design book, v.3: LEP2. CERN, Geneva, 1996. Vol. 1-2 publ. in 1983-84.

[3] ATLAS Collaboration. ATLAS detector and physics performance: Technical Design book, 1. Technical Design book ATLAS. CERN, Geneva, 1999.

[4] CMS Collaboration. CMS Physics: Technical Design book Volume 2: Physics Performance, volume 34. 2007.

[5] ALICE Collaboration. ALICE: Physics Performance book. ALICE physics performance : Technical Design book, volume 32 of Technical Design book ALICE. CERN, Geneva, 2005.

[6] LHCb Collaboration. LHCb : Technical Proposal. Tech. Proposal. CERN, Geneva, 1998.

[7] Stefan Mättig. The Online Luminosity Calculator of ATLAS. Journal of Physics: Conference Series, 331(2):022035, 2011.

[8] Cheuk-Yin Wong. Introduction to high-energy heavy-ion collisions. World Scientific, Singapore, 1994.

[9] ATLAS central solenoid: Technical Design book. Technical Design book ATLAS. CERN, Geneva, 1997.

[10] J P Badiou, J Beltramelli, J M Baze, and J Belorgey. ATLAS barrel toroid: Technical Design book. Technical Design book ATLAS. CERN, Geneva, 1997.

[11] ATLAS end-cap toroids: Technical Design book. Technical Design book ATLAS. CERN, Geneva, 1997.

[12] S Haywood, L Rossi, R Nickerson, and A Romaniouk. ATLAS inner detector: Technical Design book, 2. Technical Design book ATLAS. CERN, Geneva, 1997.

[13] Alignment of the ATLAS Inner Detector and its Performance in 2012. Number ATLAS-CONF-2014-047. Geneva, Jul 2014.

[14] ATLAS calorimeter performance: Technical Design book. Technical Design book ATLAS. CERN, Geneva, 1996.

[15] ATLAS liquid-argon calorimeter: Technical Design book. Technical Design book ATLAS. CERN, Geneva, 1996.

[16] ATLAS tile calorimeter: Technical Design book. Technical Design book ATLAS. CERN, Geneva, 1996.

[17] ATLAS muon spectrometer: Technical Design book. Technical Design book ATLAS. CERN, Geneva, 1997.

[18] Peter Jenni, Marzio Nessi, Markus Nordberg, and Kenway Smith. ATLAS high-level trigger, data-acquisition and controls: Technical Design book. Technical Design book ATLAS. CERN, Geneva, 2003.

[19] M Sutton, N P Konstantinidis, J T M Baines, D Emeliyanov, P Parodi, C Schiavi, and H Drevermann. A Fast Tracking Algorithm for the ATLAS Level 2 Trigger. Number ATL-DAQ-CONF-2006-018. ATL-COM-DAQ-2006-039. Geneva, Jan 2006.

[20] ATLAS Collaboration. Search for exclusive Higgs and Z boson decays to $\phi\gamma$ and $\rho\gamma$ with the ATLAS detector. Search for exclusive Higgs and Z boson decays to $\phi\gamma$ and $\rho\gamma$ with the ATLAS detector. Number CERN-EP-2017-273. Geneva, Dec 2017.

[21] Collaboration ATLAS. Plot of invariant mass distribution of diphoton candidates after all selections of the inclusive analysis for the combined 7 TeV and 8 TeV data. Jul 2013.

[22] Ariel Schwartzman. Jet energy calibration at the LHC. Int. J. Mod. Phys., A30(31):1546002, 2015.

[23] Lucio Rossi and Oliver Brüning. The High Luminosity Large Hadron Collider: the new machine for illuminating the mysteries of Universe. Advanced series on directions in high energy physics. World Scientific, Hackensack, NJ, 2015.

[24] Letter of Intent for the Phase-I Upgrade of the ATLAS Experiment. Number CERN-LHCC-2011-012. LHCC-I-020. Geneva, Nov 2011.

[25] T Kawamoto, S Vlachos, L Pontecorvo, J Dubbert, G Mikenberg, P Iengo, C Dallapiccola, C Amelung, L Levinson, R Richter, and D Lellouch. New Small Wheel Technical Design book. Number CERN-LHCC-2013-006. ATLAS-TDR-020. Jun 2013. ATLAS New Small Wheel Technical Design book.

[26] ATLAS Collaboration. Technical Design book for the Phase-I Upgrade of the ATLAS TDAQ System. Number CERN-LHCC-2013-018. ATLAS-TDR-023. Sep 2013. Final version presented to December 2013 LHCC.

[27] Collaboration ATLAS. Letter of Intent for the Phase-II Upgrade of the ATLAS Experiment. Number CERN-LHCC-2012-022. LHCC-I-023. Geneva, Dec 2012.

[28] A. Abusleme et al. Performance of a Full-Size Small-Strip Thin Gap Chamber Prototype for the ATLAS New Small Wheel Muon Upgrade. Nucl. Instrum. Meth., A817:85–92, 2016.

[29] Georgios Iakovidis and Theodoros Alexopoulos. Research and Development in Micromegas Detector for the ATLAS Upgrade. Oct 2014.

[30] Panagiotis Gkountoumis. Electronics Design and System Integration of the ATLAS New Small Wheels. Number ATL-MUON-PROC-2016-012. Geneva, Nov 2016.

[31] K. Golshan. Physical Design Essentials: An ASIC Design Implementation Perspective. Springer US, 2007.

[32] Georgios Iakovidis, Venetios Polychronakos, and Gianluigi De Geronimo. VMM - An ASIC for Micropattern Detectors. Number ATL-MUON-PROC-2015-015. Geneva, Nov 2015.

[33] A Gabrielli, S Bonacini, K Kloukinas, A Marchioro, P Moreira, A Ranieri, and D De Robertis. The GBT-SCA, a radiation tolerant ASIC for detector control applications in SLHC experiments. 2009.

[34] Radu Mihai Coliban, Stefan Popa, Traian Tiberiu Tulbure, Victor Sorin Martoiu, Lorne Levinson, and Jos Vermeulen. The Read Out Controller for the ATLAS New Small Wheel. Jan 2016.

[35] Steve Kilts. Advanced FPGA design: architecture, implementation, and optimization. John Wiley & Sons, 2007.

[36] Panagiotis Gkountoumis. Level-1 Data Driver Card of the ATLAS New Small Wheel Upgrade Compatible with the Phase II 1 MHz Readout Scheme. Number ATL-MUON-PROC-2016-010. Geneva, Nov 2016.

[37] Kevin Thomas Bauer. FELIX: the new detector readout system for the ATLAS experiment. Number ATL-DAQ-PROC-2017-042. Geneva, Nov 2017.

[38] L Yao, V Polychronakos, H Chen, K Chen, H Xu, S Martoiu, N Felt, and T Lazovich. The address in real time data driver card for the MicroMegas detector of the ATLAS muon upgrade, volume 12. 2017.

[39] De Geronimo G. Polychronakos V., IakovidisG. ATLAS NSW Electronics Specifications: Component VMM3a. Geneva, 2017.

[40] Christos Bakalis. Guide Learning of VHDL Language and Application in the Firmware Development for the MMFE8 Boards for the Upgrade of ATLAS Experiment at CERN. Athens, 2017.

[41] H J Burckhart, J Cook, V Filiminov, T Franz, O Gutzwiller, V Khomutnikov, and S Schlenker. The Common Infrastructure Control of the ATLAS experiment. 2008.

[42] A Barriuso Poy, H Boterenbrood, H J Burckhart, J Cook, V Filimonov, S Franz, O Gutzwiller, B Hallgren, V Khomutnikov, S Schlenker, and F Varela. The detector control system of the ATLAS experiment, volume 3. 2008.

[43] Oliver Holme, Manuel Gonzalez-Berges, Piotr Golonka, and Sascha Schmeling. The JCOP Framework. Number CERN-OPEN-2005-027. Geneva, Sep 2005.

[44] Siemens. WinCC-OA.

[45] Konstantinos Ntekas and Theodoros Alexopoulos. Performance characterization of the Micromegas detector for the New Small Wheel upgrade and Development and improvement of the Muon Spectrometer Detector Control System in the ATLAS experiment. 2016.

[46] P P Nikiel, B Farnham, S Franz, S Schlenker, H Boterenbrood, and V Filimonov. OPC Unified Architecture within the Control System of the ATLAS Experiment. Mar 2014.

[47] Theodoros Alexopoulos, Stavros Maltezos, and Evangelos Gazis. Investigation of Gas Leak Test Methods for the NSW Micromegas Multiplet's Mass Production. Number ATL-COM-MUON-2015-054. Geneva, Oct 2015.

[48] CERN. Root data analysis framework. https://root.cern.ch/, 2017.